UNIVERSITY OF Southampton

FACULTY OF ENGINEERING AND THE ENVIRONMENT

Research group: Bio-Engineering

Podiatric skin health sensing in the diabetic foot

by

James Martin Coates

Thesis for the degree of Doctor of Philosophy

September 2016

Abstract

In this thesis a new approach to sensing soft tissue damage in the diabetic foot is presented and multiple sensor modalities including linear and rotational accelerometers, temperature, humidity and galvanic skin response (GSR), pressure/-force, blood oxygen heart rate and fore foot flexure will be investigated with the aim of using multi modal sensing to improve understanding the diabetic foot. Bioimpedance is proposed and investigated as a novel measurement modality that directly observes the response of the tissue under test as a means of estimating tissue condition. The new sensing system and data collection with critical assessment is presented complimenting the existing metric of assessment.

Diabetes is currently one of the greatest health risks facing the developed world where typically 6% of the population is diabetic and an estimated 1 in 3 people are currently in a pre-diabetic state. The condition adversely affects the body's glycaemic control mechanisms leading to macro vascular stiffening alongside the possible onset of peripheral neuropathy thus increasing the risk of secondary pathologies such as retinopathy, kidney failure and diabetic foot disorder. For those living with diabetes the loss of a foot due to diabetic foot disorder is one of the most debilitating and feared side effects of diabetes. The national health service (NHS) in the United Kingdom (UK) currently amputates circa 100 lower legs a week due to diabetic complications of which about 85% are avoidable. As amputation leads to increased morbidity and mortality (68% at five years post 1st amputation) as well as a marked reduction in quality of life, this concern is well founded. Many metrics have been investigated as indicators of diabetic foot disorder, though none have shown sensitivity and specificity that would enable their use as a reliable diagnostic or predictor of ulceration.

The following contributions to the body of knowledge will be presented:

1. Novel associations of sensors for monitoring the diabetic foot see Table 6.6.
2. The development of a novel bioimpedance measuring device.
3. The development of a novel wearable extensible multimodal sensing system
4. Demonstrate direct current (DC) through textile GSR measurement.
5. Demonstrate the effect of caffeine on GSR coherence for the first time.

Contents

List of Tables

List of Figures

Glossary

AC alternating current.

ADC analogue to digital converter.

ANS autonomic nervous system.

CG10 Clinical Guidance 10: Type 2 diabetes foot problems: Prevention and management of foot problems.

CNA Charcot neuro arthropathy.

CRC cyclic redundancy check.

DAC digital to analogue converter.

DC direct current.

DF the diabetic foot.

DPN diabetic peripheral neuropathy.

ECF extracellular fluid.

EDR electro dermal response.

EMG electromyography.

FEA finite element analysis.

FPC flexible printed circuit.

FR fore foot - rear foot loading ratio.

GSR galvanic skin response.

HbA1c glycated haemoglobin.

HF high frequency.

I^2C inter intergrated circuit serial buss.

ICF intracellular fluid.

IMU inertial measuring unit.

IQR inter quartile range.

LDF laser doppler flowmetry.

LEA lower extremity amputation.

LF low frequency.

NAN not a number.

NG19 Nice Guideline:Diabetic foot problems: prevention and management.

NHS national health service.

NICE The National Institute for Health and Care Excellence.

PAOD peripheral arterial occlusive disease.

PCB printed circuit board.

PG photoplethysmography.

PID proportional integral derivative control.

PP peak pressure.

PPG peak pressure gradient.

PPP peak plantar pressure.

PTI pressure time integral.

PVD peripheral vascular disease.

PWM pulse width modulation.

RC resistor capacitor.

SBC single board computer.

SPI serial peripheral interface.

SPO2 peripheral capillary oxygen saturation.

TCP transmission control protocol.

UK United Kingdom.

USA United States of America.

USB universal serial buss.

WHO World Health Organisation.

List of symbols

g Acceleration due to gravity.

R Electrical resistance.

Ω Ohm, unit of resistance.

$R.H.$ Relative humidity

N Newton, unit of force

kg Kilogram, unit of mass

f Frequency

Hz Hertz, unit of frequency. Number of cycles per second.

C Capacitance

F Farad, unit of capacitance

V Volt, unit of electrical potential

T Temperature

$^{\circ}\mathrm{C}$ Degree centigrade, unit of temperature

t Time

s Second, unit of time

D Distance

A Area

K Relative dielectric permittivity

E_o permittivity of free space

DECLARATION OF AUTHORSHIP

I, James Martin Coates declare that this thesis *Podiatric skin health sensing in the diabetic foot* and the work presented in it are my own and has been generated by me as the result of my own original research.

I confirm that:

1. This work was done wholly or mainly while in candidature for a research degree at this University;

2. Where any part of this thesis has previously been submitted for a degree or any other qualification at this University or any other institution, this has been clearly stated;
3. Where I have consulted the published work of others, this is always clearly attributed;

4. Where I have quoted from the work of others, the source is always given. With the exception of such quotations, this thesis is entirely my own work;

5. I have acknowledged all main sources of help;

6. Where the thesis is based on work done by myself jointly with others, I have made clear exactly what was done by others and what I have contributed myself;

7. Parts of this work have been published as:
   Paper: Wearable Multimodal Skin Sensing for the Diabetic Foot.
   Associated data for paper: http://dx.doi.org/10.5258/SOTON/386374
   Associated data for thesis: http://dx.doi.org/10.5258/SOTON/401515

Signed: .....

Date: .....

Acknowledgements

I would like to take this opportunity to thank and acknowledge my supervisory team Dr. Andy Chipperfield and Prof. Geraldine F. Clough for their invaluable support and insightful guidance throughout this project together with the Gerald Kerkut Charitable Trust, the Institute for Life Sciences (IfLS) UOS & EPSRC, (EP/K503150/) for their generous sponsorship of this project.

I would also like to thank the following people for their specialist help and advice:

Mr. Graham Allathan for his invaluable help and guidance developing code and data handling protocols without which it would have been difficult to complete the project.

Dr. Mark Scott for his guidance on data management, Unix and Latex which enabled the gathering and management of complex data.

Dr. Steven Johnston for his help in the management of embedded linux, associated hardware and discussions on technology and hardware.

and last but not least my parents Alan and Angela Coates for reading drafts of this document and finding many grammatical and spelling mistakes that I made along with their support through the whole project.

This project would not have been possible without your guidance and friendship.

Chapter 1

Introduction

Diabetes is a chronic endocrine condition that can develop at any stage of life and affects either the body's production or utilisation of insulin. Approximately 10% of the diabetic population has type I diabetes where an autoimmune reaction destroys the pancreatic production of insulin necessitating lifelong use of subcutaneous insulin. The remaining 90% of the diabetic population is almost entirely made up of those with type II diabetes which is related to lifestyle. Lack of exercise and obesity conspire to reduce insulin production and sensitivity leading to elevated blood sugar and consequently further diabetic complications. Other rare pathologies are noted in the literature, where lifestyle factors lead some to become resistant to, or deficient in the production of insulin. All diabetes leads too increased blood glucose that unless well controlled causes vascular disease and neuropathy throughout the body leading to serious co-morbidities, the most feared and debilitating of which are neuropathy, diabetic foot disorder, and renal failure [1].

The specific complication of tissue damage in the foot, the diabetic foot (DF) , can become sufficiently severe as to require amputation and is classified as a medical emergency. Alongside blindness it is one of the most feared secondary conditions for those living with diabetes. "Every 30 seconds a lower limb is lost somewhere in the world as a consequence of Diabetes" [2] of which 85 could be saved with early detection [3]. The cost to the patient's quality of life and the financial impact on the health provider is unacceptably high and in many cases avoidable.

For those living with diabetic foot disorder there is an ever present danger of ulceration developing in the soft tissue leading to partial or complete limb amputation. Where diabetic peripheral neuropathy (DPN) and peripheral vascular disease (PVD) are present lack of protective pain sensation and restricted immune response allow ulceration to rapidly reach a critical level prior to detection. Where ulceration is diagnosed and interventions implemented expediently, limbs can be saved retaining quality of life, mobility while reducing social and financial burdens. The mortality rates post first amputation are up to 68% at 5 years [4] so it is clearly desirable to avoid such a procedure if at all possible.

1.1 Motivation for research

The fight to cure diabetes is on-going, but unfortunately it is unlikely to be achievable in the short term due to the complexity of the disease. Diabetes is a chronic condition that is burdensome for those living with and managing it. On a daily basis this ranges from controlling food intake and exercising to monitoring blood glucose and administering subcutaneous insulin with periodic medical checkups. However, the onset of long-term complications have by far the greatest impact on quality of life. These may include visual impairment, kidney damage or failure, diabetic foot disorder/amputation, oedema, weight gain, heart attack to name a few, requiring management of the underlying diabetic condition, plus the co morbidities. This is costly to both those living with the condition and society as managing the disease becomes more challenging as it progresses.

In the interim it is necessary to enable the mitigation of the worst side effects of the disease to ensure that those living with diabetes have an acceptable quality of life. This research investigates the development of wearable multimodal sensing technology to better monitor the DF with the longer term aim of improving DF management, understanding the conditions experienced at the foot, determining tissue health and breakdown.

1.2 Research Hypothesis

This research aims to investigate the incorporation of multiple sensors into a single device to yield interpretable and relevant signals. This will in turn be used to investigate how multifactorial data from an ensemble of sensors at the foot could better inform the care team of changes in skin health. These will include existing sensing modalities and techniques novel to the area of research. By utilising multiple externally placed sensors we aim to ultimately enable better understanding of the pathogenesis of disease with the long term intent of utilising complex data to provide a simple traffic light indicator of tissue health as feedback to the wearer and a comprehensive data set to the clinician.

Thus this research has the following objectives:

- Develop multi sensory insole technology.
- Investigate the use of sensors printed or assembled directly on a film substrate to enable the implementation of cheap single or multi use sensing elements.
- To investigate the viability of using daily worn devices for monitoring foot health.
- To investigate novel associations of sensing technology that may offer new insights in podiatric skin health.

- To investigate the viability of using bioimpedance as a new method of monitoring skin health as either a wearable or daily use scanner.
- To investigate the use of GSR for monitoring autonomic nervous system (ANS) /sweat response in the foot.
- Determine a set of new sensing modalities.
- Determine a new system architecture.
- Demonstrate architecture and system capabilities.
- Perform a volunteer study to gather pilot data.
- Critically appraise the system and data.

1.3 Proposed research

In this thesis we will investigate the viability of gathering and examining data from multiple sensing modalities in an integrated wearable device. Some of the metrics such as temperature, force or pressure, pulse monitoring, peripheral capillary oxygen saturation (SpO2), GSR, acceleration and rotation have been examined by others individually and found to be useful in the identification of particular diabetic co-morbidities but none are individually capable of predicting or diagnosing ulceration. Alongside these metrics we propose the addition of in shoe monitoring of bioimpedance, flexure, environmental temperature and humidity. By analysing these in concert we aim to supplement the current techniques available for monitoring the diabetic foot with the intention of informing the design of a wearable or daily use device that can measure changes in the soft tissues in the foot to predict or diagnose ulceration.

1.4 Contributions

This thesis investigates novel systems of measuring and monitoring podiatric soft tissue condition. The combination of multiple measuring modalities into a single data gathering system allows the gathering and analysis of hither too unseen correlations between different metrics. This methodology enables new methods of investigating the diabetic foot that have not been practicable until now.

1. Novel associations of sensors for monitoring external factors experienced by the foot.
2. Novel sensor combinations for monitoring the diabetic foot see Table 6.6.

3. The design of a novel bioimpedance measuring device.

4. The development of a novel wearable extensible multimodal sensing platform as published in *electronics* [5].

5. Demonstrated through textile DC GSR measurement.

The correlations investigated here include linear/rotational accelerations, skin temperature, contact force, galvanic skin response, and bio-impedance alongside environmental factors such as temperature, humidity and time of day in a single device. This toolset will give access to new data that will enable the investigation of the interplay of factors that cause tissue breakdown in the diabetic foot.

The investigation of bioimpedance utilising alternating current (AC) for examining the foot is a novel adaptation of a technology already utilised in other areas of medicine. The use of capacitive coupling to ameliorate the risk of polarisation associated with galvanic coupling of the electrodes is also novel. Capacitive coupling also allows tissue measurement through dry skin with high DC resistance.

Publications

- J. Coates, A. J. Chipperfield and G. F. Clough "Wearable multimodal skin sensing for the diabetic foot" Electronics - *Raspberry Pi Technology*, vol. 5, no.3, p. 45, 2016 *(published)*

1.5 Report overview

In this chapter an introduction to diabetes and the associated co-morbidities has been presented together with an outline of the research undertaken. This is followed in chapter 2 by a literature review of the current understanding of the underlying pathologies pertinent to the diabetic foot, factors that stimulate and exacerbate ulceration with a review of the technologies that are suitable for monitoring the condition. Chapter 3 discusses the choice and specification of sensors that will be used in this investigation, laying out the justification for the sensor choices. Chapter 4 investigates the viability of using GSR as one metric in a multi sensory array for podiatric skin health sensing. This defines the development of a typical single measurement mode used in the overall system. Chapter 5 details the design and characterisation of the full multimodal sensing system with example data from a limited volunteer test set. Chapter 6 investigates the analysis of the data gathered. Finally in chapter 7 The output of this project is summarised alongside the recommendations for further work that would expand this field of research.

Chapter 2

Background and review

Introduction

This chapter provides an overview of the current research pertinent to the diabetic foot including the physiology, mechanistic physics and measurement techniques where novel approaches can be taken that apply to the diabetic foot. Section 2.1 investigates the pathology and current management of the diabetic foot. Section 2.2 investigates the mechanisms of injury and the available monitoring methodologies at our disposal. Section 2.3 reviews potential approaches to modelling the diabetic foot as a system. Section 2.4 suggests the use of haptic feedback as a means of addressing some of the sensory feedback problems associated with DPN. The final section 2.5 reviews the material discussed in this chapter.

In 1989 the St. Vincent Declaration under the aegis of the World Health Organisation (WHO) set out to improve the care of those living with type II diabetes. The declaration aimed to improve detection, management, education, research, promote patient independence and reduce diabetic side effects to improve patient quality of life and life expectancy [1].

Specific stated aims of the declaration include:

1. Elaborate, initiate and evaluate comprehensive programs for detection and control of diabetes and of its complications with self-care and community support as major components.

2. Promote independence, equity and self-sufficiency for all people with diabetes, children, adolescents, those in the working years of life and the elderly.

3. Remove hindrances to the fullest possible integration of people with diabetes into society

4. Reduce by one half the rate of limb amputations.

5. Establish monitoring and control systems using state-of-the-art information technology for quality assurance of diabetes, healthcare provision and for

laboratory and technical procedures in diabetes diagnosis, treatment and self-management.

The National Institute for Health and Care Excellence (NICE) stated in Clinical Guidance 10: Type 2 diabetes foot problems: Prevention and management of foot problems (CG10) (now superseded by Nice Guideline:Diabetic foot problems: prevention and management (NG19)) that 'Further research is required to identify the appropriate level and combination of risk factors at which patients should be categorised as at high risk of ulceration and be offered attendance on a protection program'. Despite these initiatives "The provision of healthcare for people with diabetes remains far from ideal" [6]. Other than the scoping study of [7] conducted for the Southampton Skin Health Sensing Initiative there have been few reviews of the current and imminent technologies applicable to sensing skin health. This chapter therefore aims to critically evaluate the current state of the art in this area.

2.1 The pathology and management of the diabetic foot

2.1.1 Diabetes

Diabetes is a chronic endocrine condition that can affect all age groups disturbing either the production or sensitivity to insulin [8]. People with diabetes usually fall into one of two separate classifications though other rare pathologies are acknowledged in the literature. The first of these is type 1 diabetes where an auto-immune reaction destroys the pancreatic production of insulin and will necessitate the life-long administration of insulin. This usually happens in childhood and accounts for approximately 10% of the diabetic population [9]. The second is type 2 diabetes which is a resistance to, or inadequate production of insulin. This is generally linked to poor diet and obesity and accounts for nearly 90% of diabetes cases. Management of type 2 diabetes ranges from controlling diet to full insulin therapy. In both type 1 and type 2 blood glucose is inadequately controlled causing secondary pathologies such as PVD and DPN. PVD reduces vascular compliance and alongside a reduction in the density of capillaries in the tissues that transport oxygen and metabolites to and from individual cells compromising tissue integrity. Reduced blood flow to the nerves causes DPN reducing the protective pain sensation. This often leads to organ damage, usually in the eyes, kidneys, digestive system and the extremities, particularly the feet. A specific complication of tissue damage in the foot, DF, can become sufficiently severe as to require amputation and is one of the most feared secondary conditions after blindness, by people with diabetes. Currently 6% people in the UK are receiving treatment for diabetes and this figure is rising steadily over time. The disease is a global problem with an expected growth from 120 million in 2011 to 333 million by 2025 [10], though prevalence is higher in developed economies. It should also be noted that although type 2 dia-

betes was traditionally associated with the middle and elderly population it is now being diagnosed in ever younger people including children with obesity as young as 6 years old [11].

The successful management of diabetes requires the restoration of glycaemic control involving the patient monitoring their blood glucose and either controlling diet and/or administering medications. There are two measures of glycaemic control in common usage at present, the most common blood glucose that is the current level of sugar in the blood. The second is glycated haemoglobin (HBA1C) the level of haemoglobin permanently bound to sugar. This is an effective indicator of average sugar levels over the past 2-3 months. Good control of diabetes is achieved at a normo-glycaemic level of HBA1C 48 to 58 $\mathrm{mmol/mol}$ (6.5-7.5%) [12]. Micro-vascular risk is deemed to be low with an HBA1C level of 7.0 8.0% while arterial risk reduces until a level between 6.0 – 7.0% is reached [13]. Control may be achieved through a number of independent or interdependent strategies including diet control, exercise, oral drugs, manual or automatic insulin injection. Management strategy is usually tailored to the patient, based on the pathogenesis, life style and history.

Hyperglycaemia causes long-term damage to the body's tissue structures, however it is equally important to avoid hypoglycaemic events. A sudden drop in blood sugar, hypoglycaemia, can result in dizziness, unconsciousness and finally death if not treated promptly.

2.1.2 The diabetic foot

The diabetic foot is a complex problem caused by both PVD and consequent DPN, often leading to ulcer formation [14, 15]. The reduction in blood supply reduces the body's ability to transport oxygen to the tissues of the body and manage metabolites. As a consequence the tissues become susceptible to trauma and infection, exacerbated by a reduction in cross sectional area and elasticity of the vasculature.

The reduction in blood supply may also cause damage to the local sensory nervous system limiting or eliminating the sensation of pain, pressure and temperature sensitivity, and with it the ability to detect tissue damage prior to becoming critical. Other neural functions such as the ANS, which mediates haemostatic control, including blood flow and sweating, are also impaired by PVD and hyperglycaemia [16]. As a consequence the diabetic foot represents a significant increase in health risks associated with vascular or neuropathic related ulceration

It should also be noted that although a significant fraction of diabetic ulcers are caused by external insults to the plantar (sole of the foot) tissue the majority are of internal origin and are difficult to detect visually, particularly within the critical early stages. In the United States of America (USA), it has been estimated that 15% of the diabetic population as a whole and 25% of those over the age of 60 suffer

with foot ulcers with 30% of those aged over 40 experiencing some level of lower extremity disease.

2.1.3 Existing management and devices

Acute foot, where trauma or ulceration is present in the diabetic foot, is a medical emergency requiring prompt remedial action. This can range from cleaning and applying sterile dressings to pressure relieving orthotics, surgical debridement, revascularisation, minor (distal) amputation to complete lower extremity amputation (LEA). The diabetic foot accounts for 90% [17] of non-traumatic and nearly 50% [4] of all lower limb amputations in developed countries. Early detection of the condition greatly improves the prognosis, reduces recovery time and lowers costs. Unfortunately this is currently difficult to achieve.

Current best practice is for clinical examination by a specialist, or specialist team, annually for low risk patients, every 3-6 months for those at moderate risk, every 1 to 2 months for those at high risk but no immediate concern and every 1-2 weeks if there is immediate concern all with daily monitoring by the patient. For those at moderate or high risk who are unable to monitor their own feet NICE recommend increasing the frequency of examination further [18]. For some populations where this is accomplished dramatic reductions (44-85%) in hospitalisation have been observed [3]. Foot examination is heavily dependant on specialist training, clinical acumen and experience with many measurements being subjective (qualitative) rather than quantitative in nature. NICE maintains best practice recommendations for the management of the diabetic foot [18] outlined in Table 2.1. However, many patients fail to receive this level of clinical monitoring from their care providers for a variety of reasons.

Self-examination Regular self examination by those living with diabetes is recommended where practicable [6].

- Visual examination of the foot for lesions and signs of infection.
- Thermal measurement and comparison of the plantar aspects of the feet to detect infection. IR thermography is recommended over 6 to 10 critical points on each foot [19, 20, 21].

Self examination is complicated by patients being susceptible to retinopathy causing poor eyesight, being overweight with limited mobility, having limited or no sense of pain, lacking energy or motivation and other confounding pathologies. Consequently ulceration rates remain high despite international agreements to reduce the impact of diabetes on society [1, 6, 22].

Table 2.1: Diabetic foot assesment

Pathology	Routine examination	Advantage	Disadvantage
Neuropathy	10g monofilament	Low cost	Low accuracy qualitative device
	Calibrated tuning fork	Fixed excitation frequency	No amplitude control qualitative device
	Biothesiometer	Quantitative result	High cost
Assessment of vascular disease/ limb ischemia	Measurement of the ankle brachial pressure index	Quantitative result	
	Palpation of pulses	Low cost	qualitative
	Measurement of capillary refill	Low cost	qualitative
Charcot arthropathy/ foot deformity	Physical examination	Low cost	qualitative
	Examination of shoes	Low cost	qualitative
Gangrene	Odour	Low cost	qualitative
	Discolouration of the skin	Low cost	qualitative
Ulceration	Odour	Low cost	qualitative
	Temperature	Low cost	qualitative
	Waxy skin	Low cost	qualitative
	Skin colour	Low cost	qualitative
Callus	Physical examination	Low cost	qualitative

One of the diabetes-related objectives of Healthy People 2010 [23] was to increase to 60%, from the 1998 baseline level of 40%, the proportion of individuals with diabetes who receive formal diabetes education [22, 24]. Education plays an important role in the treatment of diabetes as it is necessary for the patient or carer to be diligent in their management of the condition. When blood glucose is used to measure the effectiveness of diabetes related education as an intervention, a short-term improvement in glycaemic control is found, however without further education average blood glucose returns to the higher pre-intervention base line level over 3 months. This suggests that a rolling cycle of education is required [22].

2.1.4 What are the costs of the diabetic foot?

The diabetic foot is a chronic, debilitating and degenerative condition affecting millions of people the world over [25], which has grave economic and social costs to both the individual and society. Current statistics show that annually 2-3% of those with diabetes will suffer with foot ulceration with 15% suffering ulceration during their lifetime [26]. A USA study calculated the annual post operative care cost, adjusted to 1998, to be USA$16 437 for non- ischaemic lesions to USA$64 265 for major amputation [2]. DF ulceration and amputations were estimated to cost USA healthcare providers USA$10.9 billion in 2001. The NHS in the UK currently spends between £0.6 and £1 billion pa on lower limb amputations due to DF [27].

In the UK 100 lower leg amputations are performed every week due to diabetes of which 85 could be avoided [28]. NICE reports about 5% of people with diabetes will develop a foot ulcer in any year and amputation rates are approximately 0.5% pa [6]. 20% of those that undergo amputation do so within 12 months of being diagnosed as diabetic [29].

Although this is a huge financial burden, the true cost to society is much higher. With the individuals loss of mobility and increasing morbidity comes loss of autonomy, independence, identity, self-worth and consequently family and social networks suffer. Couple this to loss of income and medical insurance (in the USA) and it becomes apparent that this is a very serious condition. It is important to note that LEA overcomes the immediate risk due to infection but has a high mortality rate in its own right. In “Diabetes in America” [4], Ronald Aubert reports mortality rates following amputation of 6% in 30 days post operation, 20-50% at 3years and 39-68% at 5 years (1989-92) using several populations. These rates are largely unchanged from those reported for 1976 78 [30]. In developed, countries diabetic foot care accounts for up to 12-15% of total diabetic healthcare resources, though it is difficult to be precise as some healthcare costs can remain hidden due to local costing strategies [28] and co morbidities.

2.1.5 Peripheral vascular disease

It is well understood that PVD in both the macrovasculature and microvasculature in the legs is a major contributor to the development of DF [31]. Sustained hyperglycaemia leads to a stiffening of the macrovasculature causing a number of mechanisms to deteriorate. The reduction in compliance mechanically restricts generation of myogenic tone in the small vessels, reducing effective control of the blood supply to the skin. This effect is exacerbated by further rarefaction of the microvasculature (arterioles) reducing the effective exchange of oxygen and metabolites to and from the tissue. There is a corresponding increase in the density of arteriovenous shunts and blood flow through the shunts [32]. These mechanisms culminate in poorly supported tissues that are prone to ulceration, infection and necrosis.

With viable methods of measuring perfusion of the microvasculature, capillary refill time, heart rate, oxygenation and assessment of ANS activity via wearable sensors [33, 34], together with measurements of mechanical stress affecting plantar blood flow in the living environment, will aid the differentiation of risk of tissue damage. Monitoring these factors in the free living environment would help provide an enhanced understanding of the pathogenesis of ulceration and tissue degradation and investigate commonality in subjects.

2.1.6 Diabetic peripheral neuropathy

DPN, affecting sensory, motor and autonomic nerves [35], is experienced by up to half of all people with diabetes. Reduction or loss of sensory nerve function significantly increases the risk of damage to the foot from thermal, fatigue or direct mechanical damage in both internal and external tissues. The lack of a protective pain response not only allows the original injury to pass unnoticed but also allows the development of ulceration and finally necrosis without detection [35]. Although this progression can be rapid, prompt care generally reduces the severity of any problems.

Fine motor control is often affected which, together with the loss of pain response, results in changes in gait that can exacerbate stress on the soft tissues [36, 37]. In the early stages of neuropathy there is a significant increase in pressure applied to both fore-foot and rear-foot during perambulation. In the later stages there are significant changes in the fore foot - rear foot loading ratio (FR) [38]. It is currently not clear from the literature why this would occur though it is certainly a significant factor in the increase of plantar stress.

The ANS controls homoeostasis by regulating local blood flow and controlling sweating. Screening and monitoring for ANS degradation by GSR is already established EZSCAN [39, 40] and others [41]. Another method of observing sweat exists for the palmo/plantar skin [16] utilising a colour changing chemical to indicate the presence of sweat. Monitoring ANS activity in free-living individuals offers the

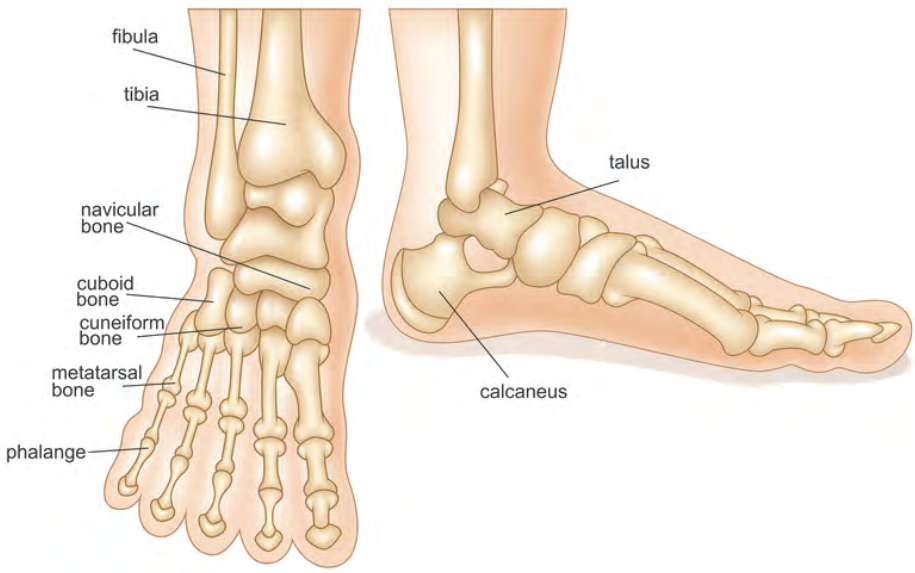

Figure 2.1: Skeletal structure of the feet defining the major bones. Figure courtesy of https://www.dreamstime.com

opportunity to monitor neuropathic pathology.

2.1.7 Structure of the foot

The skeleton is a near rigid tissue structure in the body used to transmit loads to the environment. The foot is the lower extremity of land dwelling animals and, in the case of humans, allows us to exercise bipedal perambulation. The joints and their supporting structures allow constant adjustment of gait in response to the environment. The skeletal structure of a healthy foot is shown in Figure 2.1. Note that the metatarsal bones and respective phalanges are in-line in the dorsal (left view). The arch of the foot is shown in the lateral (right view) between the calcaneus bone and the metatarsal phalangeal joint being well defined contact points with the ground.

The articulation of the joints and reaction of loads involved in locomotion is performed by the skeletal musculature. These muscles operate in response to the motor control neural system, with blood flow and low level, homoeostatic, control being mediated by the sympathetic nervous system. The plantar fascia, sometimes called the plantar aponeurosis, is the tendon that joins the heal bone (calcaneus) to the toes (phalanges) hence supporting the arch of the foot. The plantar fascia also transmits load from the Achilles tendon to the forefoot allowing us to apply pressure preferentially to the forefoot to aid running. These ligaments enable the forefoot to absorb shock, adapt to uneven ground and transmit the resultant load to the lower leg muscles. There is an abundance of muscles in the plantar region, see Figure 2.2, of the foot that are of limited use in the modern world enabling the flexing of toes, presumably as an aid to climbing, but these do provide an ability to

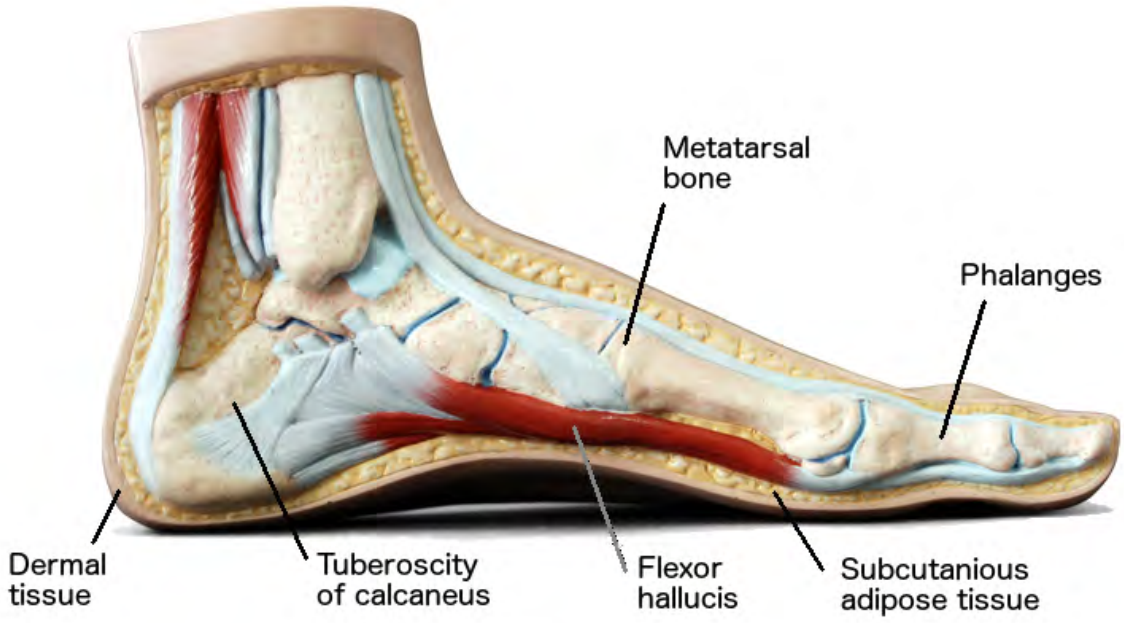

Figure 2.2: Lateral exposure of the foot structures. Reproduced from https://www.dreamstime.com

distribute stress from the skeleton to the softer tissues.

The subcutaneous fat, shown in Figures 2.2 and 2.3 separates the musculature and plantar fascia from the dermis. This provides cushioning, a thermal barrier, a level of energy storage and a support mechanism for the vasculature serving the dermis. The dermis is a living bed of tissue supporting the vasculature and containing the eccrine sweat glands, sensory nervous system including Meissners corpuscles responsible for high sensitivity touch. The lower dermis is covered by the papillary dermis that contains the microvasculature allowing effective oxygen and metabolite transport to the tissues. The final layer is the epidermis that is a layer of harder, densely packed, dry, dead skin cells that defend the soft fragile tissues beneath from mechanical damage or infection. This structure is a tough, compliant, elastic material.

2.1.8 Mechanical properties of the foot tissues.

The tissues of the foot are affected both as a direct consequence of hyperglycaemia and as a result of ulceration. The properties of elasticity, flexibility, stiffness, tensile strength, compressive strength, shear modulus, together with changes in thickness, homogeneity and isotropy need to be considered. Each of these parameters affects either the local stress concentration or the stress that can be tolerated by the tissue.

Reduction in tissue elasticity due to diabetes and consequent stiffening have been attributed to both post ulcerative scarring and increased cross-linking of the

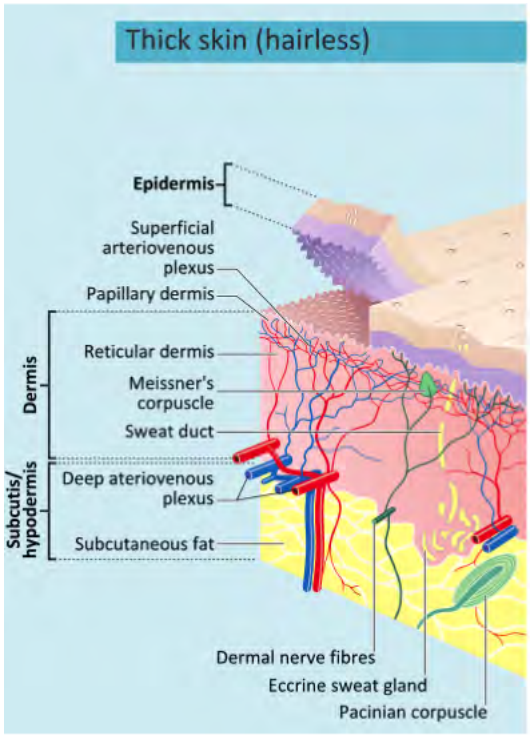

Figure 2.3: Section through Thick Skin figure courtesy of https://commons.wikimedia.org

collagen. This causes elevated stress at the site of previous lesions [42] in an area of reduced vascularisation (due both to scaring and diabetic pathology). Diabetic tissue has been found to be approximately twice as stiff as non-diabetic tissue [43] and elasticity is negatively correlated with stiffness [44]. It is also worth noting biomechanical properties in healthy patients are non-homogeneous over the plantar surface in that tissue properties under the sub calcaneal tissue and sub metatarsal tissue exhibit different responses to loading in a time variant manner [45]. The stress limit, as either a function of ultimate tensile load, fatigue limit or principle stress, can also be negatively affected by diabetic pathology.

The atrophy of the plantar muscles [46] logically leads to reduced ultimate tensile strength and consequently fatigue tolerance of the muscles in question. These muscles also provide a level of cushioning and isolation between the dermal tissues and the skeletal system reducing the stiffness gradient of the tissue without pathological disturbance. Any muscle atrophy reduces this cushioning and increases the local stiffness gradient. Diabetic anisotropic tissue with increased local hardening has been estimated to increase local stress due to pressure and shear in the order of 50-55%. This is also associated with large stress gradients [47].

2.1.9 Charcot neuro-arthropathy

Charcot neuro arthropathy (CNA) has uncertain aetiology but is thought to happen due to trauma in the skeletal structure of the neuropathic foot [48]. This pathol-

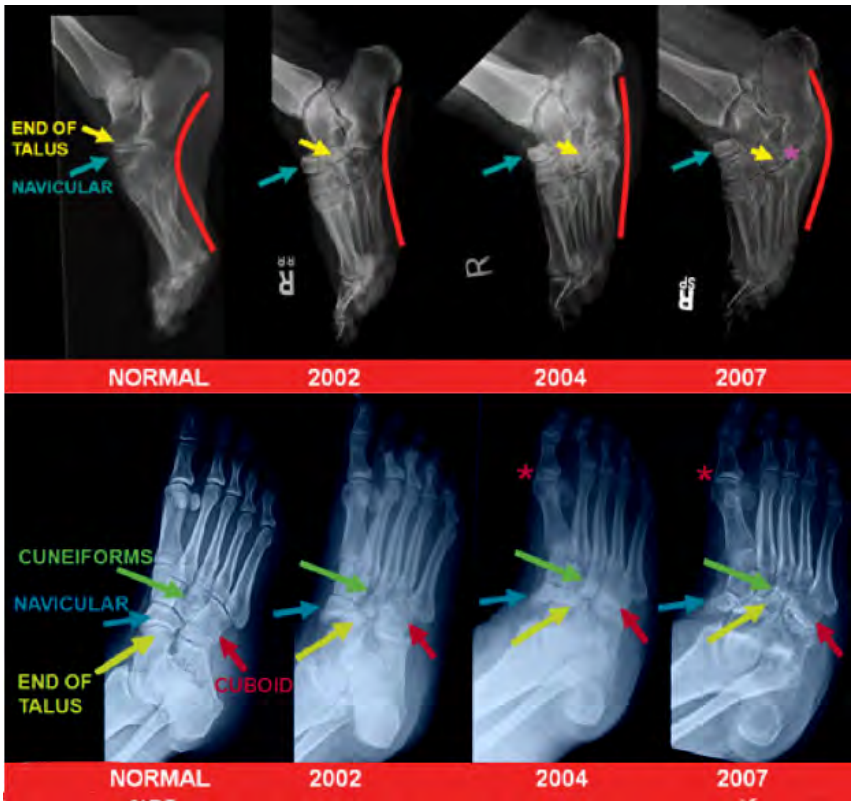

Figure 2.4: Charcot neuro-arthropathy is a chronic condition common in the DF that progresses over a period of years. Figure courtesy of Endocrine Today Nov. 2009

ogy occurs in either the atrophic or hypertrophic form and once established causes deformity in the supporting structures of the foot. Changes in structure lead to undesirable load cases in the surrounding soft tissues which in turn lead to increased stress and hence ulceration in the plantar tissues [15]. Ulcers resulting from Charcot neuro-arthropathy are known to have a unique temperature signature as discussed in section 2.2.7

Changes to foot morphology are progressive over time as can be seen from the lateral x-rays in the upper section of Figure 2.4 and require specialist management over an extended period. In the instance shown, the arch of the foot collapses over a period of years as shown in the dorsal x-rays (Figure 2.4) in the lower section the talus, cuneiforms navicular and cuboid bones are all displaced. Regardless of the individual pathology, CNA fundamentally changes the pattern and magnitude of load expressed by the skeletal structure on the soft tissues of the foot. This presents challenges to instrumentation and monitoring as it is not possible to predict where tissue stress will increase in the short to mid term and hence where to place sensors.

2.1.10 Diabetic ulcers

Diabetic ulcers usually occur in the plantar tissues due to a combination of PVD, neuropathy, mechanical stress or other environmental hazards, though any part of

the foot is at risk. Ulcers are generally classified as either neuropathic or ischaemic depending on the primary causation.

As a healthy person walks or runs, a complex and poorly understood feedback system controls balance, gait and sweating. The purpose of this system is to ensure efficient locomotion in any set of physical circumstances. These could include flat or uneven ground, hot or cold, humid or dry climates etc. The body must maintain a homoeostatic internal environment while constantly adjusting balance to account for external hazards and internal wear or damage for effective locomotion. With the onset of DPN a number of factors are affected that degrade the efficacy of the feedback control that informs proprioception [49].

The most obvious neuropathic effect that a person may experience is painful neuropathy with chronic pain either as a response to normal activity or without provocation. A less obvious form of sensory neuropathy is the gradual partial or complete loss of the senses of touch and temperature. The effect of neuropathy on the motor control system and autonomic nerves is often insidious requiring explicit investigation to be observable in the early stages [50].

Sensory neuropathy can limit or remove the protective pain sensation and hence the ability to sense the destruction of tissue by mechanical, thermal or chemical action [50]. In this pathology it is common for a patient to be unaware of ulcers in the sub-dermal or dermal tissues until chronic infection occurs. Sensory neuropathy also denies the patient of the ability to offload tissues by changing gait or footwear. An associated loss of fine motor control increases the risk of damage to the structures of the foot.

Changes to the ANS affect the fine control of blood flow in the tissues by influencing the myogenic response controlling the pre-capillary sphincter. ANS also mediates the sweat response and hence local temperature control, skin hydration and consequently affects skin stiffness/elasticity [51, 52, 53].

Ischaemic ulcers are caused by poor perfusion of the tissues causing oxygen and nutrient deficiencies at the cellular level. This is caused by increases in the stiffness of the microvasculature resulting in restrictions in blood flow within the tissues. These wounds are often intensely painful and are very difficult to resolve. The at risk patient will present with poor capillary refill, lack of palpable pulse, the skin may also appear shiny and be lacking hair.

2.1.11 Pathologic response to trauma

Trauma causes changes to the bodies tissues that are observable. These may include swelling, changes in blood flow and temperature to name a few. Understanding these processes offers an insight into possible techniques for monitoring tissue status. With the onset of the inflammatory response changes in the balance of intra and extra cellular fluid are experienced. To the Engineer this equates to change in

the balance of resistive and capacitive pathways in the tissue.

The body's initial response to trauma, however it is instigated, is to incite an inflammatory response. This response starts when the tissues are exposed to excitation beyond some critical level, may change as part of the ageing process, change in exercise regime, diabetes or other pathologies.

Increased vaso-perfusion and increased permeability of the vessel walls allow extravasation into the interstitial space between the cells. This fluid carries fibrinogen and other proteins into the damaged area which wall off the area of damage to prevent the spread of infection and limit the scope of the inflammation. Extravasation is the migration of white blood cells including polymorphonuclear leukocytes needed to manage infection and necrotic tissue. Once any infection is dealt with these cells die and become pus, which is removed over time by the lymphatic system. As this system must operate faster than any spread of infection to be effective, changes in the efficacy of the vasculature can have a dramatic effect on this repair mechanism.

Scar tissue is formed as part of the healing process where a lesion has occurred in tissues of the body. Scar tissue is characterised by an increase in the cross-linking of collagen fibres that forms the parent tissue, an increase in tissue stiffness, reduced vasculature, impaired mechanical properties and an absence of sweat glands (if the skin is involved). Scars can be hyper-tonic, atrophic or keloid in nature. It has been found that soft tissue affected by hyperglycaemia with a history of ulceration and scarring exhibits increased stiffness, which significantly increases the risk of re-ulceration [42].

2.1.12 Effect of exercise on the tissue

Exercise can be very beneficial to those living with diabetes by reducing blood pressure, improving insulin sensitivity, reducing weight and improving general fitness. However this also imparts a level of risk that is a significant disincentive to partaking of exercise as trauma can lead to ulceration if not carefully monitored. Providing a sensor suit to provide tissue monitoring may go some way to alleviating the concerns.

Finite Element Analysis (FEA) studies indicate that contact stresses may rise by 38-50% whilst internal stresses may increase by 82-307%. This suggests that it is more likely that lesions occur internally than externally [54, 55] which concurs with observations of the lesion locations seen in clinic. However, reducing exercise does not mitigate risk and long-term is believed to be detrimental to the patient. Previous studies indicate that patients with diabetes generally have scope to increase their exercise [56]. Weight bearing exercise does not increase the pressure exerted on the plantar tissue, as such both weight bearing and non-weight bearing exercise pose little extra risk to insensate plantar tissue when properly monitored and

with gradual increase in workload [57]. Maluf and Mueller suggest that the atrophy of plantar muscles increases the risk of tissue damage at low stress levels [58], though the weight bearing tissues must be carefully monitored to prevent ulcers developing.

Holt et al observing the effect of shear in healthy patients noted that the whole skin exhibited strain hardening while the dermis-only demonstrated stress softening under step-stress [59]. It has not been possible to find equivalent data for skin affected by diabetes. Even if this mechanism remains unchanged rather than being degraded by some mechanism it is reasonable to assume that these changes will negatively affect the stress response of the skin.

2.2 Injury and monitoring requirements of the diabetic foot

There is extensive evidence in the literature demonstrating correlation between mechanical loading of diabetic plantar tissue and the occurrence of plantar ulcers [60, 61, 62]. Although this is not surprising in itself, it is unfortunate that it has not been possible to define any viable metric and measurable threshold for predicting ulceration. The current understanding and consensus of sensing modalities will be discussed including the effects of, pressure, shear, compound stresses, and fatigue alongside other sensing modalities. It is important to note that even for tissue unaffected by age, injury or pathologic process the limit of shear, compressive and tensile stresses can be radically different from one-another and anisotropic in nature so the three variables must be considered separately and in concert. Allowable stress limits are affected by exercise, age and pathology on both a macro and micro timescale causing extra complexity in application.

2.2.1 Stress and stress raisers

Stress can be thought of as an expression of the internal forces exerted by adjacent particles on one another in a material under load. Any load on a material will result in some level of stress be this compression, tension, flexure, torsion or shear. In stressed components it is important to avoid features that concentrate this stress such as a sudden change in cross section or material properties as these are the areas where early failure is most likely. In non-living materials these failures usually occur as small cracks that propagate rapidly through the material. Within living tissues the cell structure that forms the tissue becomes disrupted until a lesion forms. This can occur at the local interface of two different materials such as bone resting on a muscle or the interface of scar tissue to undamaged tissue for example. As each material and material condition has a stress limit and this stress raiser preferentially loads a small volume of material causing early failure (fatigue is discussed

later 2.2.6).

Tissues affected by diabetic pathology are prone to changes in structure leading to local deleterious changes in their mechanical properties. This reduces the tissue's acceptable stress limits pre-disposing the tissue to further damage. Cheng et al utilised finite element analysis (FEA) of the diabetic foot to estimate that tissue stress is increased by a factor of 3 where stiff bony structures meet soft tissue [54]. This goes some way to explaining why ulceration often occurs in the deeper tissues remaining hidden until infection is well established.

This form of analysis is not viable for monitoring at risk tissue due to the requirement for detailed models of the foot topology and tissue properties together with accurate high resolution data for all input stresses applied to the tissue to predict tissue failure. As tissue properties are unstable and prone to sudden change in the diabetic foot, constant re-validation of the mechanical properties would be necessary.

2.2.2 Pressure

Current studies investigating peak pressure (PP), peak plantar pressure (PPP), peak pressure gradient (PPG), and pressure time integral (PTI) have attempted to estimate threshold levels of stress that predict ulceration, however there is no consensus on a viable threshold. Lavery *et al*.concluded that foot pressure is a poor tool by itself to predict foot ulcers [63]. This may indicate the involvement of another mechanism or mechanisms acting alongside pressure.

Other investigators have reported changes in FR pressure ratio in the diabetic foot but noted that significant increases only occur in severely neuropathic patients [38]. Significantly both, fore foot and rear foot pressures were increased in the mild to severe neuropathic condition. No threshold values were suggested from this study. As FR pressure changes during the course of the pathology but ulcers may occur at any point, becoming more prevalent with disease progression, FR is also unlikely to yield a single threshold value to predict ulceration.

Analysis of FR and PPG have also been investigated. PPG is defined as the spatial change in pressure around the point of PPP, hence including some information on pressure distribution across the whole foot. This is indicative of changes in local stiffness of the tissue. As elasticity and pressure distribution will be affected this could have a profound effect on the stress in the tissue.

Lott *et al* suggests that PTI may be useful in predicting ulceration in plantar tissue but does not offer any definitive level where tissue damage can be usefully predicted as significant overlap in the results occurred [64]. Yavuz *et al* found increased PTI values in the diabetic foot compared to normal controls but no increase in PPP [62].

Pressure is almost invariably measured using force cells with the assumption

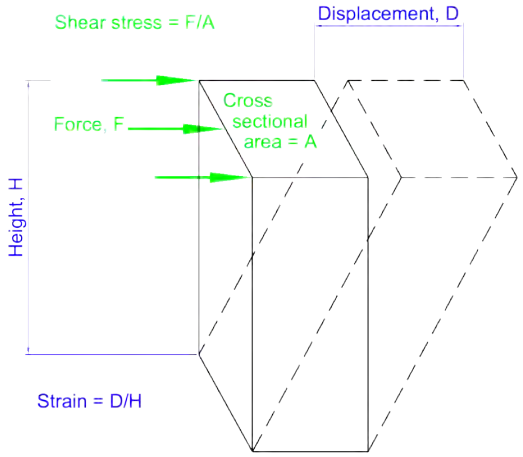

Figure 2.5: Shear Diagram.

that the actuating load is evenly distributed over the entire sensor surface. With small sensor areas, typically 5 x 5 mm, this is a valid assumption but interfacing to a high density sensor array is complex and expensive.

2.2.3 Force

To mitigate the overheads associated with interfacing a high density pressure sensor array the use of larger format force sensors is proposed. Utilising a single sensor under each point of interest to measure peak load will enable the gathering of salient information in an economic manner. In this configuration where the larger sensor area may or may not be in full contact with the sole of the foot surface only force can be measured with certainty not pressure. Force sensing resistors are typically $\approx 0.2 - 0.5\mathrm{mm}$ thick, flexible and commonly available in a range of sizes from $\oslash 3.8 - \oslash 25.0\mathrm{mm}$ from companies such as Tekscan [65] .

2.2.4 Shear

Shear stress occurs where one plane of a tissue sample is displaced laterally to a parallel plane. In a three dimensional representation Figure 2.5 where shear is exerted on a square section of material the sample tends towards a parallelogram.

Shear sensors work by measuring the lateral displacement of two parallel surfaces. There are a number of technologies available including piezo, capacitive and strain gauge but commercially available gauges are all designed for measuring surface shear [66]. The flexible thin film sensor system being developed by Piotr

Laszczak et.al. at the University of Southampton provides both pressure and shear measurement for stump socket for amputees in a discrete conformable package [67, 67]. This greatly improves the existing technology that is both bulky and rigid.

Many researchers have investigated the effect of surface shear on the plantar tissue as current sensors are only capable of measuring this phenomena. Surface sheer stress is largely caused by locomotion, however sensors of this type do not measure the shear caused in the sub-dermal tissues due to static or dynamic loads and as such are deficient. Mathematical studies have shown sub-dermal stress to be of greater concern than surface shear, see Figure 2.6. Perry *et al* correctly stated that shear is technically challenging [68]. This statement is important as there are no direct measurement techniques that enable a sensor to measure shear in the sub dermal tissues. FE models show this is not the site of maximum shear stress. Maximum shear occurs adjacent to the bony masses in the foot and does so primarily as a response to static load as the elastic tissue tries to flow around the bone. As such it is not possible to infer meaningful internal shear forces by resolving pressure and shear at the surface. This would explain why mathematical modelling predicts that shear is significant but empirical data investigating surface shear fails to provide a useful metric.

The literature is contradictory with Yavuz *et al* observing higher shear stress for subjects with diabetes compared to controls. In addition, the relative increase in shear was greater than that observed for pressure [62]. In contrast, Lord and Hosein [69] did not observe a difference in peak shear between subjects with diabetes and controls. They did however observe significant differences under the metatarsal heads; subjects with diabetes had lower magnitude of stress under the third and fourth metatarsal, but higher stress under the first two metatarsals [69]. This may indicate a reduction in the roll motion in the foot but maintaining the yaw.

2.2.5 Principle stress, combining the stress factors

An engineering perspective leads one to ask the question of how tissue is affected by multiple stress sources acting simultaneously. The combination of all stresses acting on a material is referred to as the principle stress which can be calculated from either empirical or analytical data. By applying each stress to an appropriate vector in a three dimensional vector model the resultant principle stress can be derived. In a Finite Element Model see Figure 2.6 [54] this is estimated using the Von Mises Criterion [70, 71]. This method gives a greater understanding of the stress concentration in the tissues but does not generally differentiate between different tissue types and does assume that the material is isotropic, though as discussed earlier in Section 2.1.8 this is not the case for 'healthy' tissue. However this method does improve the understanding of the stress exerted on the foot and plantar tissue. FEA can also give us a greater understanding of the effects of mechanical changes

in pathological tissue but only for specific cases and is not suitable for real time analysis. Currently there is no evidence that principle stress has been investigated using empirical data for the diabetic foot.

Despite the fact that the plantar tissue experiences three dimensional loading during gait, only the vertical component has been studied thoroughly. This may be attributable to the fact that measurement of the horizontal or shear components, anteroposterior (AP) and mediolateral (ML) is technically challenging and that the subsurface stress is difficult to derive from the surface measurements.

Yarnitzy concluded"... that internal deformations and stresses in the plantar pad during gait cannot be predicted from merely measuring the foot-shoe force reactions. Internal loading of the plantar pad is constituted by a complex interaction between the anatomical structure and mechanical behaviour of the foot skeleton and soft tissues, the body characteristics, the gait pattern and footwear" [72]. Investigating simple stresses as has been done is valid if they act alone or the other stresses are insignificant in comparison. Yavuz *et al* investigated the spatial relationship between peak pressure and shear, hypothesising that peak stresses in the same area of the foot could lead to skin breakdown. They found that peak sites were on average 2.4cm apart, and observed no significant difference between distance for subjects with diabetes and controls. It was, however, highlighted that two out of the 10 subjects with diabetes had peak shear and pressure in the same area, compared to none in the control group of 38 volunteers without diabetes [73].

The stresses depicted in Figure 2.6 are the FEA outputs for the stresses incurred during a typical gait cycle. This model assumes that the soft tissues are isotropic and as such does not investigate the limiting stress of each tissue. To estimate failure, each soft tissue would have to be modelled and analysed against a known safe limiting stress. However, this model is useful to elucidate the absolute stress across the plantar aspect and connecting tissues. It should be noted that the maximum stress (0.31 MPa) occurs under the 1^{st} metatarsal (B & E), however significant stress (.15 MPa) occurs under the 5^{th} metatarsal (F). The stress shown between the 2nd and 3rd (D & C) metatarsal heads at 0.1 MPa is not supported by bone so is largely due to static shear. This internal static shear is not measurable by surface mounted shear sensors.

Chen *et al* noted that the peak stress occurred where the soft tissue interfaced with irregular bony tissue under the metatarsal heads [54]. Petra also noted the same phenomena and also that the fat pad helped to distribute the load [74]. This is broadly in line with Gefens findings which predicted significant stresses under glycation stiffened tissue under the 1st and 2nd metatarsal heads [55].

Gu *et al* assessed the role of heel skin stiffness in ulceration using an FE model. The model predicted that an increase in skin stiffness resulted in slightly increased skin stresses, while softer skin caused a change in pressure distribution [75]. Thomas *et al* used an FE model to compare controls and subjects with diabetes. They re-

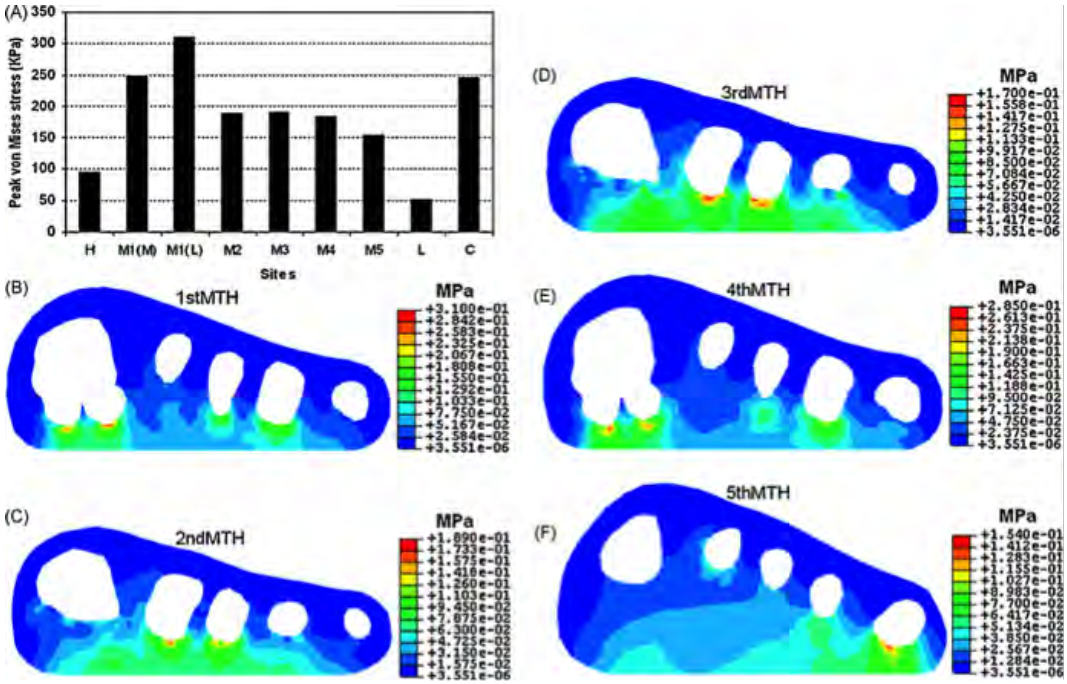

Figure 2.6: FEA model Von Mises stress at the metatarsal heads. This model presents stress and the stress concentrations experienced by the tissue. The soft tissue is assumed to be isotropic and therefore this model does not express the stress as a function of the local limiting stress [54].

ported that non-uniform hardening of the sole of the foot and decreased tissue thickness, as seen in subjects with diabetes, led to increased inter-facial stresses [47].

Yarnitzky *et al* attempted to overcome the complexity of whole-foot FE models by applying the method only to areas of the foot of most interest. The method coupled analytical modelling of the whole foot with FE analysis of the heel and metatarsal heads. This simplification allows for real-time analysis when used with force sensors. Use of this method is relatively limited as the paper reports use on only four subjects. The model suggests that internal deformations and stresses in the foot cannot be predicted from foot-shoe/ground interactions alone, nor from anatomical characteristics alone [72]. It should be noted that this method can only work where an accurate model of the patient's foot and plantar tissue is available.

All of the above studies suggest that the material properties and morphology of the tissue play an important part in predicting tissue stress accurately. However, an accurate foot model for each patient would be costly to produce and would require regular review where active pathology is present.

Existing sensors that measure surface loading are incapable of measuring the at-risk tissue directly. The use of these sensors is a pragmatic attempt to monitor the subsurface stresses, even though there is general agreement that this is not a practical means of determining deep tissue stress.

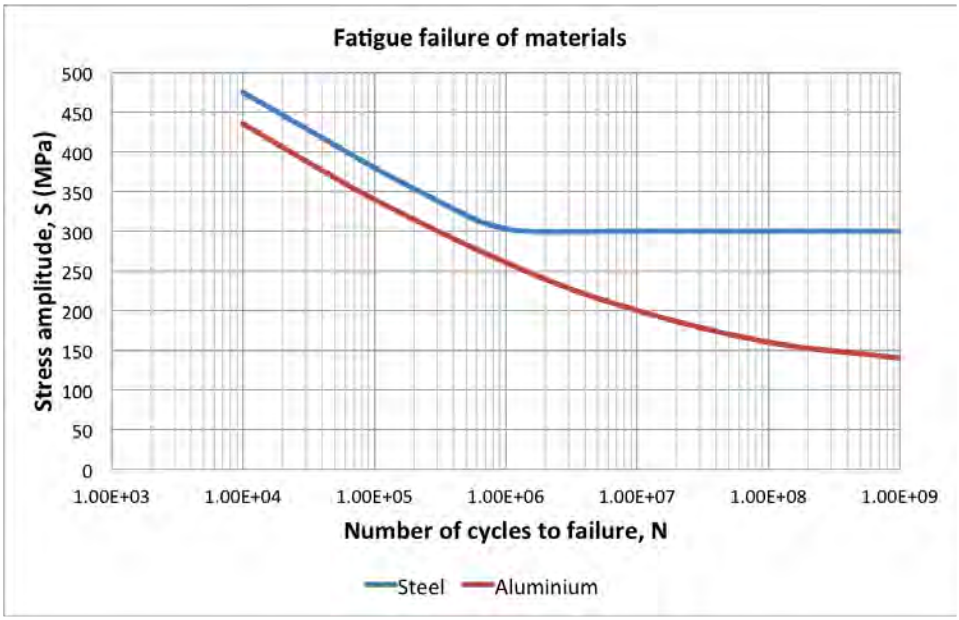

Figure 2.7: S-N curves for Steel & Aluminium. Fatigue affects differ by material type and condition. In the cases shown the steel effectively has an infinite life if exposed to a cyclic stress of less than 300MPa, whereas the aluminium has no verified fatigue limit.

2.2.6 Fatigue - the measure of accumulated damage

The ultimate stress that a material in a structure is capable of withstanding is rarely of interest as this represents the single cycle stress required to cause failure, fatigue is almost invariably the factor of concern. Fatigue is the measure of the accumulative damage incurred by a structure over a number of load cycles. The estimation of failure is usually accomplished with the use of Stress Number of cycle (S-N) curves. These estimate the number of cycles that a material can tolerate for a particular magnitude of the applied stress. Consider the S-N curves shown in Figure 2.7 the aluminium 2014-T6 could be expected to fail at around $1x10^6$ cycles for a repetitively applied load of 260 MPa.

In certain critical structures strain relief or annealing is performed to normalize the stresses prior to, or even after, commissioning. In living tissue this would be analogous to recovery time or resting. Thus, if fatigue was considered to be the source of a problem, it is possible that a relatively simple no-decompression model could be used to manage the tissue status and ensure tissue was maintained within manageable limits. Decompression modelling estimates the maximum level of work that could be under taken without damage being done; when a threshold is approached a warning to cease the activity with a required period of rest is issued. Though there may be merit in this approach, studying the potential benefits of these is beyond the scope of this research.

Looking at the load or stress applied to a material alone is not particularly enlightening and so far we have seen much research on PPP, PPG, PP etc. but fatigue

remains poorly investigated. A few researchers, including Yavuz [62], have stated there would be merit in investigating fatigue failure of the plantar tissue. Yavuz suggests this should relate to shear. Hall & Brand observed that moderate stresses can be responsible for tissue breakdown [61, 76]. Moderate applied stress is often observed where fatigue is the underlying mechanism of failure so this statement alludes to fatigue rather than stating it is the problem directly. In an observation made in 1979 Maluf and Mueller used the product of PTI and step count to determine cumulative plantar stress over seven successive days for similar groups. Though not strictly fatigue they did suggest that under use of the limb contributes to muscle atrophy and consequently increased soft tissue stress at lower cycle count and lower accumulative tissue stress, accumulative stress being fatigue [58]. For a study of this nature to be valid, measurements of actual loads applied to the tissue over time would be necessary, with a means of examining tissue state before and after testing.

2.2.7 Temperature, homoeostasis and infection

Environmental temperature and the body's response to it is important for the maintenance of homoeostasis. Skin is the main thermoregulation organ of the body with the vasculature being functionally and anatomically central to effective thermal control. As temperature rises in the body, shunt flow increases near the skin surface promoting radiative and evaporative heat loss. Diabetic pathology can affect this mechanism, making it a useful metric for monitoring the foot.

Flynn, Edmonds, Tooke and Watkins demonstrated that shunt flow is increased in the feet of diabetic patients (14 participants) with neuropathy compared to the control group (14 participants) [77]. Edmonds states mean temperature in the neuropathic foot as $33.5°\mathrm{C}$ compared with $25.8°\mathrm{C}$ in control subjects [78]. It is expected that measuring bilateral skin temperature in a worn device would enable viable ulcer detection. Bharara *et al* noted that the neuropathic foot had a delayed thermal recovery after cold or warm water immersion, when compared to healthy feet [79, 80]. By comparing local temperature to environmental temperature and calculating heat flux a useful measure of energy usage can be obtained as done in the SenseWear armband [81]. Consequently measuring skin temperature at multiple sites and environmental temperature can be expected to provide useful information on long-term tissue status. Where a step response in ambient temperature occurs it may be possible to estimate the pathological status.

Skin temperature is also a useful analogue for infection or pathological change. If the same sites are compared bilaterally it has been found that a ΔT of $2.2°\mathrm{C}(4°F)$ is a reliable indicator of infection according to Lavery *et al* [21]. This is usually measured daily or twice daily by the patient or carer over 6 -10 sites on the sole of each foot with non contact IR thermography with manual comparison [19]. Arm-

strong also noted that ΔT was also an effective indicator of the pathology with Charcot neuro-arthropathy and neuropathic ulcers having distinct characteristic ΔT of $4.6°\mathrm{C}(8.3°F)$ and $3.1°\mathrm{C}(5.6°F)$ respectively [20]. Thus temperature is a simple quantitative measure for incorporation in the multi sensor device.

2.2.8 Activity/Acceleration

Activity in the diabetic patient is known to decrease over time exacerbating muscular atrophy and increasing the likelihood of stress related damage to the plantar tissue. Little is known about the actual activity levels that people with diabetes experience in their daily lives and most methods of ascertaining this are unreliable, e.g. self-reported questionnaire. Only Valletta *et.al.* have measured the energy expenditure and related glucose level in those living with type 1 diabetes [82]. This is a small study, 23 people for 12 days that offers some quantitative insight into the lifestyles of the study group utilising the SenseWear armband in a physically active cohort.

Activity levels and patterns can be approximated using accelerometry devices ranging from simple step counters to multiple-axis accelerometers. Measuring this parameter offers a means of evaluating fatigue due to stress cycles together with pressure/shear and an improved understanding of activity levels in those being treated for diabetes. To be effective this needs to be undertaken in-vivo in the free-living environment [83]. Lau and Tong have investigated this technology for event identification [84] vertical acceleration range of $1.0 - 3.2g$ was measured for a non pathological group (n =3).

Monitoring gait utilising single or multiple accelerometers could be employed to enable the analysis of impact load, fatigue and levels of activity in both daily life and the longer term. With the addition of suitable haptic feedback it is probable that the use of an electronic surrogate neural path could help to reduce applied stress by informing the wearer of impeding or actual damage to the tissue [85]. Placement of accelerometers and gyrometers is technically less challenging than pressure or force sensors in the sole of the shoe where electrical conductors are constantly being flexed. Effort should be made to approximated pressure or force from accelerometery data.

2.2.9 Blood pressure and pulse

Blood pressure and pulse are important diagnostic factors in the diabetic foot as both macro and micro-circulatory vessels are affected by the pathology. Measuring the pedal pulses allows the estimation of arterial sufficiency and adequacy of blood flow to the microcirculation. Large artery dysfunction is often observable prior to a diagnosis of diabetes and progresses over time [86]. Microvascular function is also

important in the diabetic foot as microvascular rarefaction and increased arteriovenous shunting restricts oxygen and nutrient transport at the cellular level [86]. This reduction in metabolite and oxygen transport is exacerbated in the plantar tissues due to pressure and shear dependent occlusion of the vasculature.

The effects of ischemia in the plantar tissues and its links with ulcer development have not been extensively researched. This is primarily due to the historical difficulty in measuring ischemia in vivo and particularly in the free-living environment. Cobb and Claremont compare three different techniques for assessing microvascular function; laser Doppler as discussed in section 2.2.10, measurement of transcutaneous oxygen tension, and near infra-red spectroscopy [34]. Yudovsky *et al* have demonstrated the use of hyper-spectral tissue oximetry to retrospectively assess risk of ulceration[87]. This technique, as presented, is only viable in the clinical environment due to size of the equipment required. It remains to be seen if this approach could be adapted for utilization in a worn device.

Photoplethysmography (PG) is a simple, cost effective, non invasive technique for monitoring blood volume changes, blood pressure, oxygen saturation, heart rate assessment of peripheral circulation and large artery compliance and assessment of autonomic function [88]. Although not fully developed, examination of blood flow in a tissue under test appears to have potential for elucidating the effect of environmental effects on plantar tissue. PG potentially allows the investigator to examine ischemia and recovery in the plantar tissues caused by standing and perambulation.

2.2.10 Blood perfusion

Blood perfusion is a measure of the amount of blood passing through a particular tissue sample. There are many mechanisms that affect blood perfusion in all tissues but the skin and sub-dermal plantar tissues are of special importance in the diabetic foot.

Blood is a complex fluid that has evolved to carry oxygen and metabolites, performs an important first response to injury and acts as a heat transfer fluid to cool the body amongst other functions. The control of blood flow to the tissues is an important and delicate task and consequently one prone to disturbance. Neuropathy may cause disturbances to the ANS and hence control of blood flow, while micro and macro vascular disease presents challenges to the maintenance of the blood supply to tissues. This may take the form of high perfusion levels indicating ANS dysfunction or occasionally proliferation of capillaries, causing elevated shunting from arteries to veins. These problems are exacerbated by loss of sensation preventing the patient noticing temperature change or numbness caused by pressure-induced ischemia.

Laser doppler flowmetry (LDF) is a technique that indicates relative perfusion

within the tissue being measured, as opposed to flow [89]. It is an effective measure of red cell velocity and concentration in a tissue sample over time but not absolute blood flow. Cobb and Claremont investigated the use of LDF in a worn environment [90]. In their testing it was possible to determine differences in capillary refill time for non diabetic, diabetic with DPN and diabetic with PVD. However this technique is prone to movement-induced error so care must be taken when analysing results from a worn device and may even preclude using LDF in a worn device if movement artefacts cannot be ameliorated. Cobb and Claremont state that it is only possible to measure without movement artefacts within the swing phase of gait.

2.2.11 Humidity

Humidity and moisture is known to have deleterious effects on the feet even causing trench foot in healthy individuals in extremis. Moisture causes a reduction in tissue strength, changes the elastic properties and enables softening of the tissue. This increases the probability of mechanical damage or microbial infection. With the accessibility of small, cheap, reliable humidity sensors this parameter can be readily measured.

At the other extreme dry skin such as seen in diabetic foot disorder [50] is prone to cracking allowing the ingress of infectious agents. With in-shoe humidity being related to the evaporation of sweat it is possible that humidity monitoring could be a useful non-contact surrogate for GSR to estimate skin moisture or *vice versa*.

2.2.12 Bioimpedance

Bio-impedance measures a biological tissues ability to impede or conduct AC. Living tissue conducts electricity through ionic conduction utilising free ions in the intra and extra cellular fluids as charge carriers. Where there is a continuous electrical pathway, the extra cellular fluid DC and AC. can flow being measured as a resistance. However, the intra cellular fluid is electrically isolated from the extracellular fluid (ECF) by the plasma membrane making it capacitively coupled to any current flow. When the frequency of the current increases this intracellular fluid (ICF) becomes capacitively charged and discharged allowing a second current path to become available. This pathway can be explicitly examined as the resulting conduction has a phase lag due to the capacitive charge – discharge cycle. The concentration and type of ions, cross section, length and balance of pathways affect the impedance measurement.

This analysis technique has proven effective as a measure of body composition, the identification of various forms of malignancy [91, 92], monitoring fluid balance of dialysis patients [93], investigation of dental caries [94], diabetic skin condition [95] and a number of other conditions.

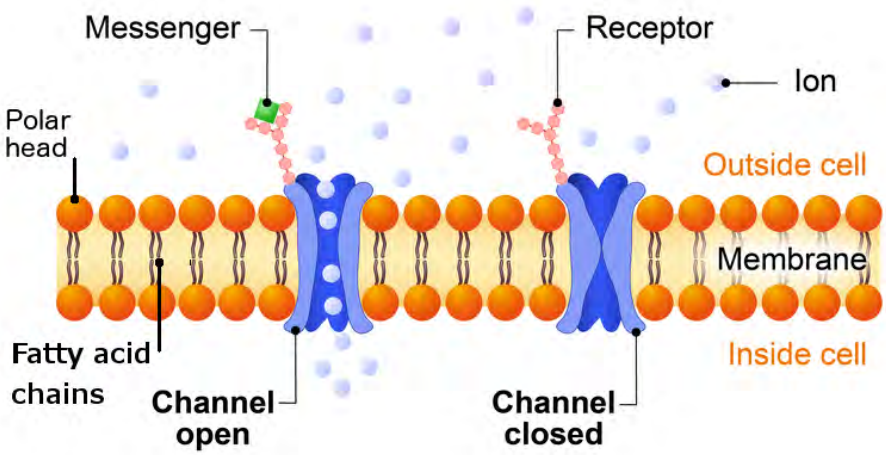

Figure 2.8: Cell Plasma Membrane structure. The hydrophobic fatty acid chains and hydrophilic polar heads create an electrically insulative membrane between the extra and intra cellular fluids. Reproduced from https://www.dreamstime.com

The cells of soft tissue are bounded by a plasma membrane, Figure 2.8, where the fatty acid chains forming the mid structure are hydrophobic in nature and consequently ensure the ICF and ECF are electrically separated. The ECF is present throughout most of the body, though only having nominal presence within the bone and epidermal tissue, constituting a continuous conductive pathway through the body. The transmission of electricity within biological samples is ionic, meaning that the electric charge is carried by anions (-) and cations (+) within a given solution, hence resistance/impedance is proportional to the concentration of the solution. The resistance of each tissue is proportional to the cross-sectional area, ionic concentration and the length of the electrical path.

The electrically isolated fluid bodies can be modelled as a capacitance and investigated via electrical frequency, or bio-impedance analysis. By comparing the frequency response of a tissue or tissues over a known range, usually $0Hz - 1\mathrm{M}Hz$, various pathologies can be identified due to characteristic changes in the ICF/ ECF as functions of volume and ionic concentration (see figure 2.9 & Figure 2.10 for the schematics of the single cell & single tissue conductive pathways). Figure 2.9 depicts the equivalent electrical pathways of electricity passing around and through a cell. Pathway R_e represents the purely resistive pathway of the extra cellular fluid, R_m represents a leakage path through the cell membrane largely due to the transmembrane ion channels. C_m represents the capacitance of the cell being measured.

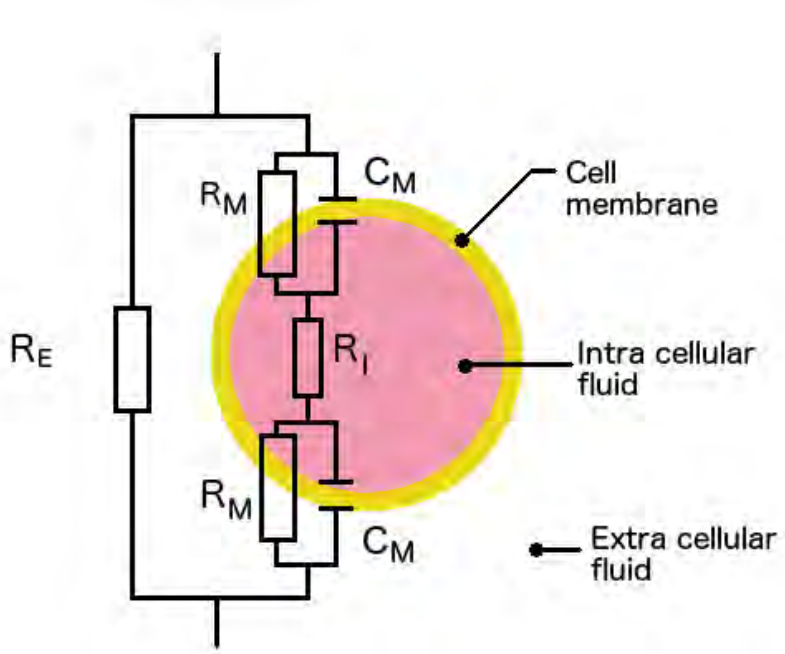

Figure 2.9: Single Cell bio-impedance diagram with superimposed electrical equivalence diagram.

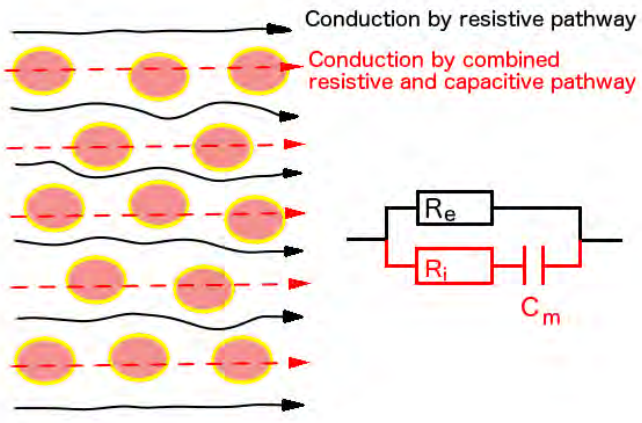

Figure 2.10: Single tissue bioimpedance diagram defining resistive and capacitive pathways with equivalent electronic circuit.

Figure 2.10 depicts the effective electrical circuit through a single tissue. Resistance R_E is the resistive path through the extracellular fluid. R_l is the resistive path that charges capacitance C_m. C_m is a simplified model ignoring the leakage path shown in Figure 2.9.

As discussed in section 2.1.11 the body's primary response to trauma is the inflammatory response. Extravasation changes the balance of intra/extra-cellular fluid in the tissues and hence the resistor capacitor (RC) network balance. By analysing the tissue over a known frequency range changes in the ratio of capacitive and resistive power conduction can be measured, which indicate changes in the tissues being measured. Changing the pitch of the electrodes to control the depth of penetration achieved by the injected current, allows the investigator to target particular tissue volumes of interest.

As demonstrated by the application of a capillary refill test, soft tissues become ischemic under the application of stress above a threshold level and re-perfused with blood on relaxation of the stress [96]. This process can be altered by diabetic pathology where peripheral arterial occlusive disease (PAOD) reduces the systemic response to physiological stress [97]. As has already been discussed, the reduction in exercise that most people with diabetes experience has a deleterious effect on the plantar muscles causing an increase in stress for other tissues. It is likely that bioimpedance will give insight into the tissue condition, enabling the optimisation of remedial action. Analysis of the data from instrumented insoles will identify the critical parameters and measurement techniques required to utilise this measurement technique.

Electrolytic conduction

Conductance (S) is the accepted measure for liquid electrolytes and is the reciprocal of resistance

$$\mathrm{S} = \frac{1}{R} = \frac{I}{\mathrm{V}} \tag{2.1}$$

As the measured conductivity is dependent on the geometry of the fluid volume being measured it is necessary to normalise this against a cell constant (K). The cell typically consists of two plates each with an area $(A)1\mathrm{m}^2$ placed $(d)1\mathrm{m}$ apart. This assumes a totally enclosed cubic volume of $1\mathrm{m}^3$ with no field effects outside that volume.

$$K = \frac{d}{A} \tag{2.2}$$

$$\sigma = \mathrm{S} * K = \frac{\mathrm{S}}{\mathrm{m}} \tag{2.3}$$

$$conductivity = \sigma, \;\; cell\ conductance = S, \;\; cell\ constant = K$$

Typical values		
Tissue	$\mathrm{S/m}$	Ω/m
Blood	0.7	1.43
Muscle	0.05 – 0.4	20 – 2.5
Bone	0.005 – 0.06	200 – 16.7
Skin – wet	10^{-5}	10,000
Skin – dry	10^{-7}	100,000

Table 2.2: Typical values of conductivity

For a GSR test, DC is applied between two exposed areas of epidermis and the resistance measured between the two points. The current flows through all tissues between the two contact areas with the resistance measured being the sum of all resistances in the current path. As can be seen from equation 2.2 and equation 2.3 the typical values of resistance using the muscle as the conductive path we can see that even $1\mathrm{m}$ of sub-dermal muscle tissue of $100\mathrm{cm}^2$ section a resistance of 0.25 – 2.0 $\mathrm{k}\Omega$ would be expected. For two layers dry skin of $100\mathrm{cm}^2$ each $0.5\mathrm{mm}$ thick $1000\mathrm{k}\Omega$ or $10\mathrm{k}\Omega$ for wet skin would be expected and $10x$ these values for dry skin. The skin is the major contributor to resistance of DC and other resistances can be largely ignored as a result.

Electrical safety

Applying a current source to any living body needs to be undertaken with extreme care. Where a current is passed across the chest, e.g. from left to right arm, a current of $18 - 22\mathrm{mA}$ can cause contraction of muscles and cessation of breathing. Increasing this to $22 - 75\mathrm{mA}$ disruption of the heart and between $75 - 400\mathrm{mA}$ ventricular fibrillation may be induced. Paradoxically currents higher than this are considered less dangerous, following removal of the current source as less permanent damage is caused to the heart and normal operation can be regained [98].

The IEC 60601 directive [99] provides best practice electrical design guidance for medical devices. This provides a safe patient applied current limit for an externally applied current of DC $10\mu\mathrm{A}$and AC $100\mu\mathrm{A}$for both earthed and floating applications.

2.2.13 Electro Dermal Response (EDR)

Most bioimpedance measurements are interested in tissues deep in the body, the heart, lung, fat, neural systems etc. which have weak signal strength hidden behind the highly resistive stratum corneum. To successfully undertake these measurements it is normal practice to overcome this high resistance with the use of

wet electrode technology, the stripping of the layer of skin known as the stratum corneum Figure 2.3 or micro-needle electrodes that pierce this outer layer thus electrically bypassing the skin resistance. The electrodermal response however specifically investigates the response of the skin as a useful metric in its own right in the form of changes to resistance or changes to the μV emitted by the skin over time.

Féré (1888) was the first to suggest the existence of the electro dermal response (EDR), utilising an exosomatic method, which is linked to sweat gland activity in the skin and proven by Fowles (1986). As sweat is primarily a conductive solution of NaCl in water and the sweat glands pass through a highly resistive layer of tissue, the epidermis, it is possible to measure changes in both exosomatic, from external source, and endosomatic from internal source, current via the electrodermal response. The former is regularly utilised in the more familiar form of GSR.

Goadby and Downman utilised GSR and plethysmography to demonstrate that the vasomotor response reflexes where significantly impaired in diabetic patients with neuropathy [100]. Shahani *et.al.* [101] utilised EDR to investigate the sympathetic skin response in unmyelinated axon dysfunction in peripheral neuropathies and found that the response was completely absent in axonal neuropathies.

Galvanic Skin Response (GSR)

The Galvanic Skin Response utilises exosomatic DC to investigate changes in skin resistance (R) over time. This can be achieved by either inducing a fixed current (I) to flow through the skin and measuring the resultant voltage or by employing the subject to be measured as one half of the divider, then measuring the resultant voltage over the skin the resistance can be inferred according to equation 2.4. The resistance of a component can be calculated if the current flowing through it and the voltage drop measured across it are known. By measuring or calculating the voltage drop across a known resistor we can calculate the current flowing in the circuit. It can also be demonstrated from this equation that as the current is constant through the circuit, each resistance is directly proportional to the voltage drop measured across it, hence the ratio of voltages measured across each resistance is proportional to the ratio of resistances. From the drive voltage applied (5V Figure 2.11) and having a known reference resistance the whole body resistance can be calculated. GSR has been widely utilised as a measure of physiological and psychological arousal over many years, primarily due to the simplicity of the device[53, 102]. This methodology is further investigated in chapter 4 and in combination with other sensors in the SenseWear armband utilised by Valletta *et.al.* for the estimation of daily energy expenditure [103].

$$R = \frac{\mathrm{V}}{I} \tag{2.4}$$

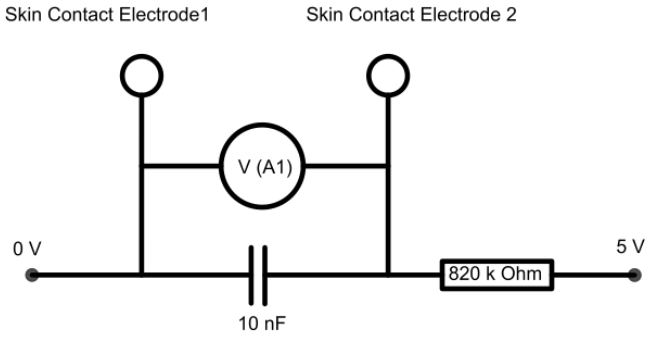

Figure 2.11: GSR circuit for the foot

Endosomatic investigation

The second EDR technique is the measurement of endosomatic voltages emitted through and by the skin. These exist in the range of -70 to $+10\mathrm{mV}$ (measured from the middle palmer aspect of hypothenar eminence, referenced to the anterior forearm)[104]. Though these measurements were first introduced by Tarchanoff (1889) and are known to have similar properties to exosomatic measurements their interpretation is not as well understood. This method of measurement however, does not suffer from polarisation complications common to GSR as there is no requirement for an externally applied current and the endosomatic current is insufficient to cause polarisation.

Human sweating has three main functions, thermoregulation, emotional response and the release of pheromones [105]. Thermoregulation is the most important function as it is necessary to maintain homoeostasis. Together with vasodilation, sweat released by the eccrine sweat glands evaporates releasing heat from the body and lowering the core temperature. These sweat glands produce sweat formed primarily of water and NaCl that is odourless and colourless. The second function, Emotional Sweating is a stress response and is most evident on the palms and soles, which serves to increase friction, reducing the likelihood of slipping when running or climbing in a stressful situation. Eccrine sweat glands are distributed over the body at an average density of $200\mathrm{cm}^{-2}$ (though this varies from $65 - 700\mathrm{cm}^{-2}$) being at a maximum density on the palmo-plantar aspects.

The action of the eccrine sweat glands is mediated by the sympathetic nervous system, a subset of the ANS, and to a limited extent by adrenergic control. This infers that endosomatic investigation would be of use as a means of monitoring ANS however, though the voltages stated above can be measured in the laboratory, doing so in a dynamic environment would be extremely challenging due to movement artefacts and electrical noise pollution.

2.2.14 Acoustic impedance

Acoustic impedance is a useful measure of a material's resonant frequency, elasticity and damping characteristics. These change as a function of hydration, scar tissue formation and tissue density. These changes are fundamentally the embodiment of the mechanical degradation of the tissue and are directly observable in the tissue [44]. Quintavalle *et al* concluded from a study of 119 patients that high resolution ultrasound was a viable means of monitoring the soft tissue changes due to ulceration. They also noted that although subdermal oedema was detectable via ultrasound before any visible changes in the external tissues could be seen, dermal oedema was only present with subdermal oedema [106]. From this they concluded that the inflammatory response, originates within the deep tissues rather than from the surface. This insight directs the investigator to consider the measurement of the deeper tissues of primary importance where traditionally surface conditions have been considered. It is also likely that complex stresses are involved in the initial tissue insult which would be difficult to monitor/deconvolve from surface inputs.

Acoustic impedance, in the form of ultrasound, is often utilised in the diagnosis or monitoring of conditions relating to changes and lesions in soft tissue from pregnancy, gallstones, kidney disease and monitoring diabetic skin [106, 107, 108]. However, there are some concerns with the long-term use of ultrasound arising from the heat generated in the tissue being studied and the generation of cavitation in the tissue [109]. This would suggest that this technology should be used sparingly, or at a frequency that drastically reduces these side-effects. Another possibility would be to measure the propagation of sound generated by the act of walking though this has not been done before.

One matter of practical concern for the continuous/long-term application of ultrasound is the necessity to use an impedance matching gel to ensure the effective transmission of sound to and from the tissue. This would be an unacceptable impediment to the use of this technology so any application of this technology would have to work with dry contact with the foot and in an acoustically noisy environment. These concerns may prevent the use of this technology in a worn device for use in the free living environment and in the application area considered in this thesis.

2.3 Modelling pathology as a system

In the field of control engineering there are traditionally two methods of modelling an observable process, the mechanistic and black box methodologies. In the mechanistic approach the process is modelled on the laws of nature controlling the system for example the temperature resistance curve for a thermistor allows one to calculate temperature from resistance directly. In a black-box model the behaviour

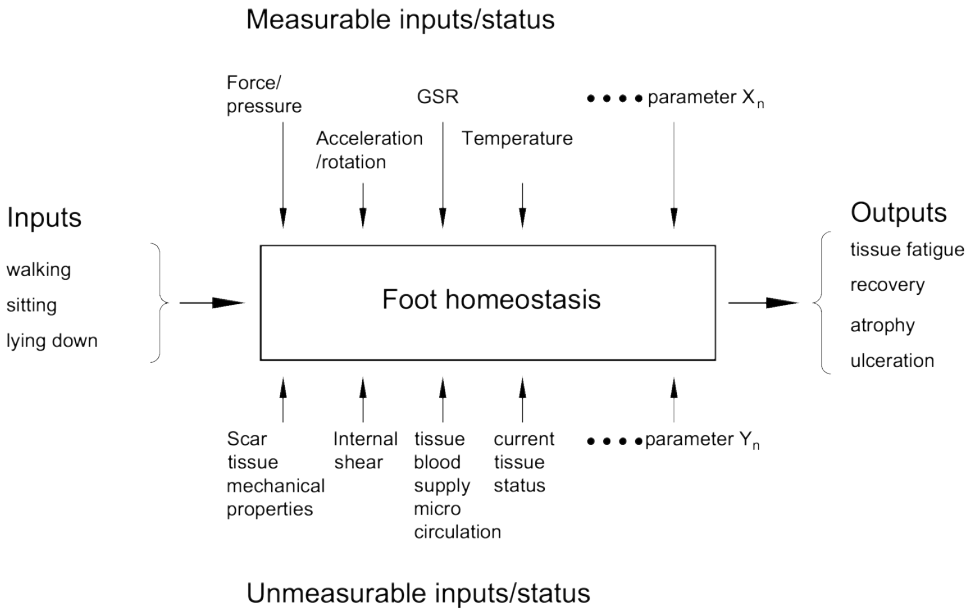

Figure 2.12: General model of foot homoeostasis showing the complex inputs to the foot status. Some are known and/or measurable while others are not. The unknown factors are confounding factors for accurate predictive models.

is characterised against known inputs and outputs without reference to the actual process, for example measuring an ulcer temperature at $33.1°C$ is an indicator of Charcot-neuro-arthropathy but the mechanism for this is immaterial to the sensing mechanism.

A black box approach is useful in observing biological systems, particularly where the mechanism is poorly understood such as the diabetic foot as valid inferences can be made from abstract measurements. Figure 2.12 presents a simplified model where inputs and outputs are subject to disturbing influences of process and material properties. While we may not yet understand the process certain measurements or more likely groups of measurements may predict the outcome of the process. Where all the influences are understood and characterised with a relatively simple mechanistic model can often be derived. Where this is not the case a black box model may be used to good effect. This approach may be necessary as our knowledge of the process is simply too immature to develop the mechanistic model or because the mechanistic model is too complex to be practical.

The aim of this research is to be able to predict tissue breakdown in the diabetic foot in the free-living environment in a timely manner. To be robust this must take into consideration factors that can not be defined or even predicted in advance. Consequently a solution relying on the sensing of inputs can never fulfil this role so it will be necessary to employ sensors for the estimation of skin condition against measured parameters both individually and in concert.

2.4 Haptic feedback

Morley *et al* proposed supplying feed-back from their data acquisition system in 2001 though there is little evidence of this being investigated at present [110]. Providing haptic feedback, meaning to touch, directly to the patient in a timely manner has the potential to ameliorate some of the effects of sensory neuropathy [111]. Implementation via mechanical resonance or direct electrical stimulation to a suitably enervated site has potential to provide a surrogate sensory pathway.

Some patients with advanced neuropathy are currently able to walk, however, they exhibit a characteristic pathological gait where increases in foot pressure to both fore and rear foot progresses to a change in forefoot/rear-foot pressure ratio. Providing a surrogate feedback system enables the investigator to explore techniques of reducing foot-fall stress in fully neuropathic patients. Timely haptic feedback offers the potential to investigate and possibly restore gait in a novel manner.

2.5 Summary

In 2011 Ewings reported, "There is a lack of prospective, longitudinal studies". Many studies are retrospective and consider differences between subjects with diabetes and controls, or those with a history of ulcers and controls. Such studies will not reliably inform about the causes of ulceration, and may fail to take into account the effect ulcers have on any observed differences [7]". This remains true today.

There is a paucity of studies employing continuous measurement, with most analysis based on a small number of steps. Furthermore, measurements are generally taken in a clinical environment and are not necessarily relevant to free-living conditions that subjects routinely experience. Devices for measuring pressure in free-living conditions, such as F-scan [112], are very cumbersome and far from ideal for use during normal activities.

A number of variables are associated with ulceration, although no single variable appears able to predict ulcers with accuracy. In particular, no thresholds exist that are able to predict ulceration with sufficient sensitivity and it is unclear if changes in properties of the foot, over time, could be used to predict future ulceration.

It appears that plantar surface pressure is unable to predict internal stresses, and hence its use as a surrogate for internal trauma is limited. Measuring shear has proved difficult and there is only limited information regarding the association of shear with ulcers. Measuring temperature, as a surrogate for inflammation, has proven effective in reducing ulcers in two studies. Measuring pulse strength, blood pressure, tissue perfusion and oxygen saturation are useful metrics for understanding tissue viability as are monitoring of the mechanical changes in the tissue.

Examining the tissue with multiple sensing modalities and investigating interdependencies in the data is a logical progression of the existing research. The work

reviewed above is important in three main areas. The first, investigating established analysis techniques and practices used in the area of study. Secondly, it is possible to elucidate where there is a paucity of research at this point, for example in the examination of tissue fatigue data or the availability of data from the free-living environment. Finally, the specification of the sensing device to be designed, relies heavily on the work of others, as without this it would not be possible to define the sensing modalities required, the useful ranges, acceptable tolerances or the temporal requirements of each sensing modality.

In the next chapter a new multisensory device will be discussed that is capable of obtaining longitudinal data in the free-living environment with multiple sensors. This device will be utilised to investigate the foot and in shoe environment. Test data gathered will be utilised to investigate interdependencies in the measured phenomena and elucidate the mechanisms of tissue failure in a manner that will aid prediction of failure and/or detect early stage failure.

Chapter 3

Sensing at the foot, sensor selection and specification

3.1 Introduction

Currently there are no composite devices available that can address the sensing requirements of this study, necessitating the design of a bespoke multi-sensor platform. This chapter will establish the necessary sensor ranges, resolutions, and accuracy required for the complete sensor set. Sensors will be chosen and sample data gathered for later incorporation into a multi-modal in shoe sensing ensemble.

Existing lab based gait analysis tools, such as Tekscan and AMTI force plates [112, 113, 114] have stood researchers in good stead over the past decade, however, they are cumbersome and not suitable for use in the free-living environment. These devices concentrate on measurement in an artificial (laboratory or clinical) environment. Expanding the number of measurement metrics will change this paradigm.

With recent developments in miniaturising microprocessors, sensors, battery technology and data storage coupled with low power wireless technology, such as Bluetooth, BtLE, ANT and ZigBee unobtrusive wearable sensing platforms have become feasible. The open source technology community has made embedded processing accessible to a wider audience than was possible even ten years ago. With the advent of low cost single board computers, such as the Arduino [115], Raspberry-Pi [116] and Beaglebone [117] it is possible to develop low cost/low power sensing solutions in a timely manner.

Some valuable work has been done by Cobb and Claremont [34, 80, 90, 118] amongst others, covering temperature measurement, plantar blood flow, microvascular function and pressure sensing for monitoring the diabetic foot in wearable devices. This is showing a clear move towards multi-sensor devices that can be used easily in the free-living environment. Others such as Segeve-Bar [119] have concentrated on the problems of designing and implementing wearable systems. Nahapetian et al. [120] have done much to develop the field of wearable sensors

in recent years and techniques such as printable flexible circuits, sensors mounted in clothes, low power electronics including an orthotic shoe combining measurements from a thin film force sensor and an accelerometer have been utilised [121]. Chan et al [122] have shown that the supporting technology for smart wearable sensors is maturing and this offers opportunities to health monitoring in the living environment.

This chapter will present the rational for selection and validation of sensors for use in the skin health sensing platform, together with the development of the sensor interfacing system. Sensor interfacing, output, robustness, resolution and accuracy will be validated here to ensure suitability for integration into the composite device.

3.2 Data aquasition

3.2.1 The Arduino Micro-controller

Having defined the parameters of interest it is necessary to select a micro-controller with which to gather the data and transmit it to a host device. There are many embedded processors available that could be used to implement the control and interface for these sensors but the Arduino is a pragmatic choice of cost, functionality and available code base with on-chip I^2C, analogue to digital converter (ADC) and serial output capability in a small form factor. With a large user group with extensive software libraries, though intended as a teaching aid it has also become a useful embedded prototyping tool. The Arduino family of devices provide a pre-built host environment for a specific embedded processor, complete with power supply, timing crystal, universal serial buss (USB) programming interface in a plug and play package which significantly reduces development time. Thanks to the Arduino project started by students at the Interaction Design Institute Ivrea 2005 the Arduino Nano, shown in Figure 3.1, embedded processor board is available. This is an $8bit$ microprocessor running at 16MHz with 8 x $10bit$ analogue to digital ports, 14 digital pins, 1 UART (Serial port), I^2C interface and USB programming in a package 0.73 x 1.70. This was used as the embedded processor which interfaces with all the sensors listed in Table 3.2.

3.3 Sensor selection

The sensing requirements for each sensing modality are discussed in sections 3.4 to 3.13 with the measurement range, tolerance, resolution and units listed in Table 3.1 below. The sensor selection, Table 3.2, lists the sensors selected for possible inclusion in the sensor set. Where available pre calibrated off the shelf systems such as accelerometer, gyrometer, environmental humidity and temperature sensors where

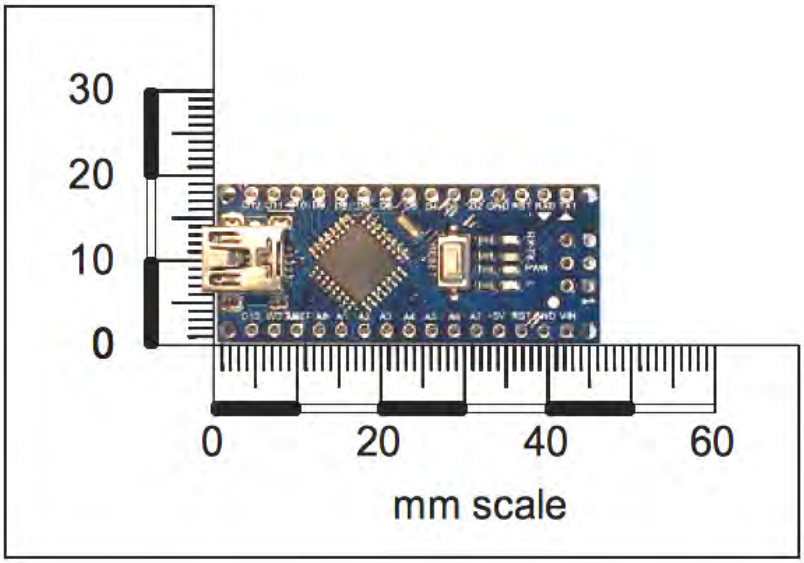

Figure 3.1: Arduino Nanao - single board computer used for inshoe and environmental monitoring. Scale 1:1

selected, utilising the inter intergrated circuit serial buss (I^2C). This allows plug and play connection with pre-calibrated devices that are individually addressable simplifying the programming requirements.The remaining sensors, pressure, force, flex, skin temperature, heart rate, oxygen saturation and bioimpedance have analogue output to the processors' ADC. These require signal conditioning and calibration or validation.

3.4 Environmental monitoring

The environment in which the foot exists is an important consideration where we are measuring sweat response and temperature, as such it will be useful to measure both the macro and micro environment. To this end laboratory environment will be monitored adjacent to the exercise surface, within $1.5\mathrm{m}$ horizontally and $0.2\mathrm{m}$ vertically. In shoe environment will be monitored proximal to mid arch position on the foot. The lowest humidity measured in the UK in the last year (2015) is 24% [123]. As the device will be used in a shoe and hence a moist environment 30% humidity is set as the lower limit with the upper limit of 100%.

3.4.1 Temperature

Environmental temperature will range from $15.0 - 35.0°C \pm 1.0°$ with a resolution of $\pm 0.1°C$. This is a practical limitation due to the sensor systems available in a package suitable for embedding in the shoe. The same technology will be utilised

Table 3.1: Sensor requirements summary table

Parameter	Range		Tol±	Resolution	Units
	min	max			
Acceleration	-4	4	0.01	0.001	g
Rotation	-400	400	5.0	0.5	$^{\circ}\,\mathrm{s}^{-1}$
Force	0	150	5.0	0.5	N
Humidity in shoe	30	100	2%	0.2%	%
Humidity of environment	30	100	2%	0.2%	%
Temperature in shoe	15	35	1.0	0.1	°C
Temperature of environment	15	35	1.0	0.1	°C
Temperature of skin	20	40	1.0	0.1	°C
GSR	10	1000	10%	1.0 %	kΩ
Bioimpedance gain	-30	+30	1.0%	0.1 %	dB
Bioimpedance phase	-90	+90	0.1	0.01	°

for both external and internal environmental measurement.

3.4.2 Humidity

Measurement range will be $30-100\%$, resolution 0.2%, accuracy $\pm 2.0\%$ for humidity. The choice of range is pragmatic in that they are the best available in a small package and no reference data is yet available for this metric in shoe. This tolerance is equivalent to the best electronic sensors only being exceeded by chilled mirror dewpoint hygrometer ($+/-0.5\%$).

3.5 Acceleration

Acceleration will be measured below the lower end of the fibula. This provides a convenient, prominent datum while reducing the risk of accidental sensor damage. The measurement range will be a minimum of -4 to $4\mathrm{g}$, the anterior posterior acceleration for a healthy subject under normal walking conditions will peak at $4\mathrm{g}$. Resolution will be $0.001\mathrm{g}$, accuracy will be $0.01\mathrm{g}$, [84].

The MPU 6050, measuring acceleration and rotation rates is mounted just below the lateral malleolus on the outside of the shoe to prevent impact with the opposite foot while walking. This maintains consistency with other work in the field [124]. The accelerometer was set in the default state of $\pm 2.0\mathrm{g}$ with the on board digital filter disabled to enable a short prototyping cycle and rapid validation. Implementing then validating range and filters was only necessary after concept validation. Data shown in Figure 3.2 demonstrates output from the accelerometer sensor verifying that the data acquisition system capability. For the purpose of validating the accelerometer operation ranges were left in the default state of $\pm 2.0\mathrm{g}$ with the on

Parameter	Sensor Manufacturer	Device	Range		Resolution	Units	Interface	Supply V
			min	max				
Acceleration	Invensense	MPU-6050	-2	2	16 bit	g	I^2C	5
			-4	4				
			-8	8				
			-16	16				
Rotation			-250	250	16 bit	$^\circ/s$		
			-500	500				
			-1000	1000				
			-2000	2000				
Force	Tekscan	A401	0	25	0.5	N	0-5 V	As exciter circuit
Humidity in Shoe	IST Innovative SensorTech.	HYT 271	0	100	0.10%	%	I^2C	5
Temperature in shoe			20	40	0.2	°C		
Humidity environ.	IST Innovative SensorTech.	HYT 271	0	100	0.10%	%	I^2C	5
Temperature environ.			20	40	0.2	°C		
Temperature skin	ATC Semitec	JT104	20	40	0.2	°C	0-5 V	As exciter circuit
GSR	Self buit		10	1000	1%	kΩ	0-5 V	As exciter circuit
Bioimpedance Gain	Analogue devices	AD8302ARUZ	0.01	100	0.1	unitless	0-1.8 V	2.7-5.5 V
Bioimpedance Phase			-45	45	0.1	°		

Table 3.2: Sensor selection

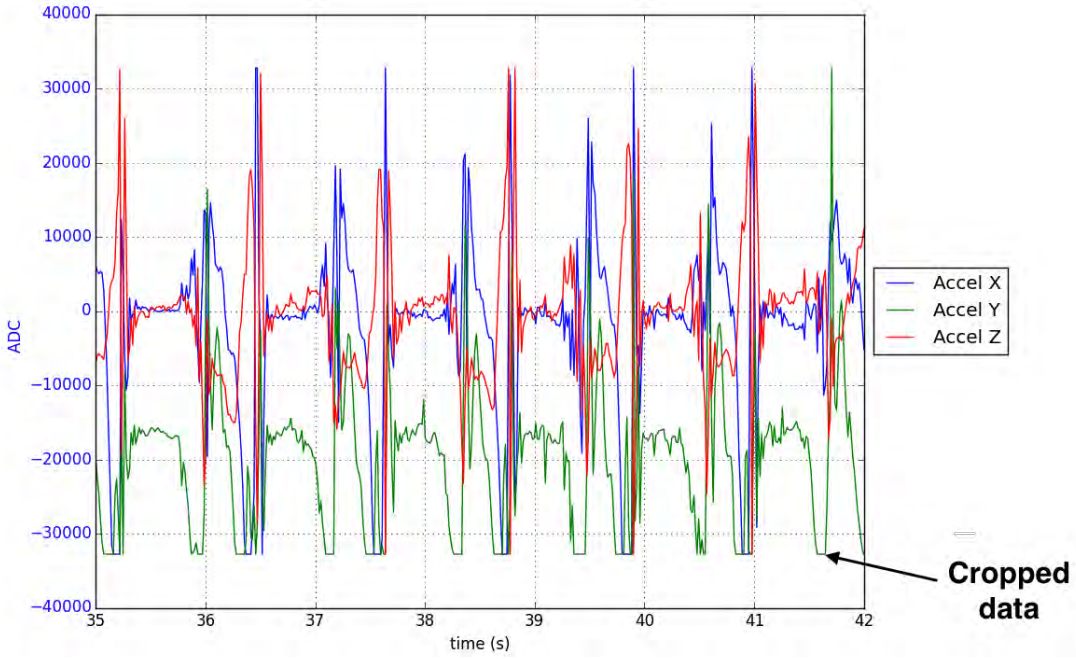

Figure 3.2: Sample in shoe accelerometer data demonstrating data capture of three orthogonal channels over wireless connection during perambulation. Note that the Y acceleration (vertical acceleration in this instance) is cropped due to inadequate range in the default condition.

board digital filter disabled allowing rapid. Acceleration along the Y axis (vertical in this implementation) is cropped at $-2.0\mathrm{g}$ requiring the range to be increased to a minimum of $\pm 4.0\mathrm{g}$. This sensor test data was taken walking on a flat level surface at a volunteer selected speed for the purpose of sensor data collection validation. The accelerometer was set with the Z - Y plane parallel to the floor with +Y pointing in the direction of travel on the right foot and against the direction of travel for the left foot.

Validation of the correct accelerometer output was established by exposing the accelerometer to $+1.0\mathrm{g}, 0\mathrm{g}$ and $-1.0\mathrm{g}$. This was achieved by fixing the accelerometer to a cubic block and placing it on each face in turn. A plot of the output data can be seen in Figure 3.3, note acceleration Z is deliberately offset by $+2.0\mathrm{g}$. This is discussed in greater detail in section 5.3.1.

3.6 Rotation Rate

Rotation rate will be measured at the same point between ankle and the ball of the foot as acceleration that will provide a reliable datum for the foot and protect the device from accidental impact. The measurement range will be a minimum of $\pm 400^\circ\,\mathrm{s}^{-1}$, Lau and Tong measured this as the maxim rate of rotation, resolution will be $0.5^\circ\,\mathrm{s}^{-1}$, accuracy will be $+/-5^\circ\,\mathrm{s}^{-1}$ [84]. Morio [125] records plantar/-

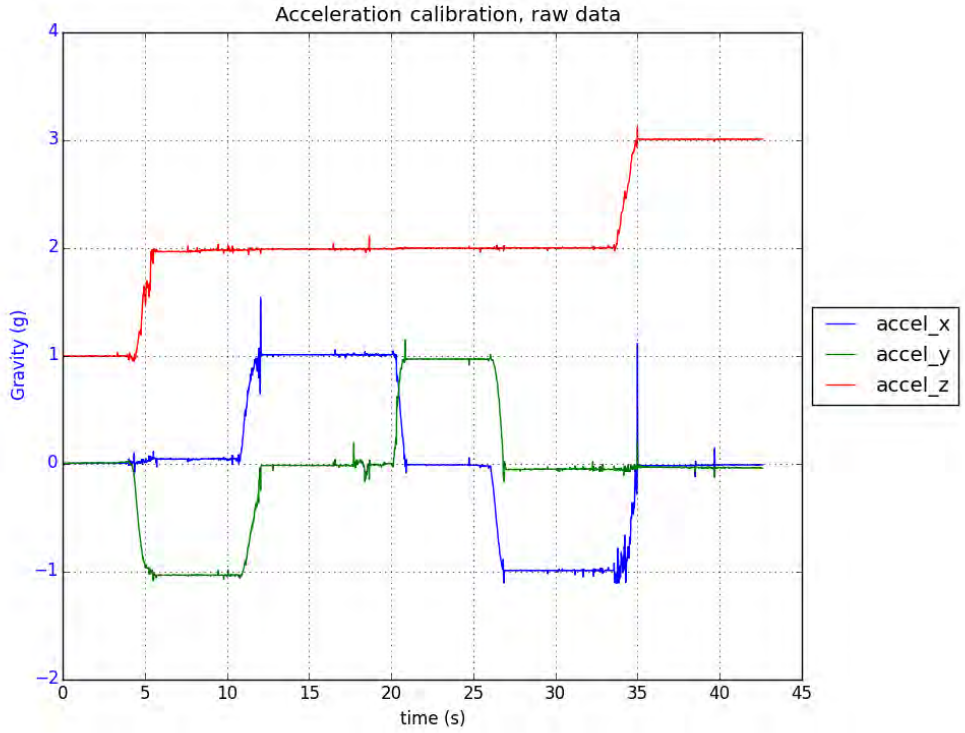

Figure 3.3: Accelerometer validation. Accelerometer fixed to a cube and rotated over all faces. ± 1.0g on each face verifies correct accelerometer operation. The plot of acceleration in the Z axis is offset by +2g for clarity.

dorsiflexion of $\pm 10\,\mathrm{deg}$. This is in line with the motions recorded during system testing. All three rotational degrees of freedom will be measured.

Data shown in Figure 3.4 demonstrates output from the MPU6050 gyroscopic sensors, demonstrating stable angular acceleration output. Rotation rates were left in the default state of $\pm 250^{\circ}\,\mathrm{s}^{-1}$ respectively with the digital filters disabled for simplicity of sensor validation. In Figure 3.5 rotational rate data in Yaw is clipped requiring the range of $\pm 250^{\circ}\,\mathrm{s}^{-1}$ to be increased to a minimum of $\pm 500^{\circ}\,\mathrm{s}^{-1}$ for use in the composite device. Filters will be set at half the data sampling rate to ensure the Nyquist sampling theorem is satisfied.

Validation of the correct gyrometer output was established by rotating the gyrometer through $90\,\mathrm{deg}$ around each axis in turn. This was achieved by fixing the accelerometer to a cubic block and placing it on each face in turn and integrating the result with respect to time. A plot of the output data can be seen in Figure 3.4. This is discussed in greater detail in section 5.3.2.

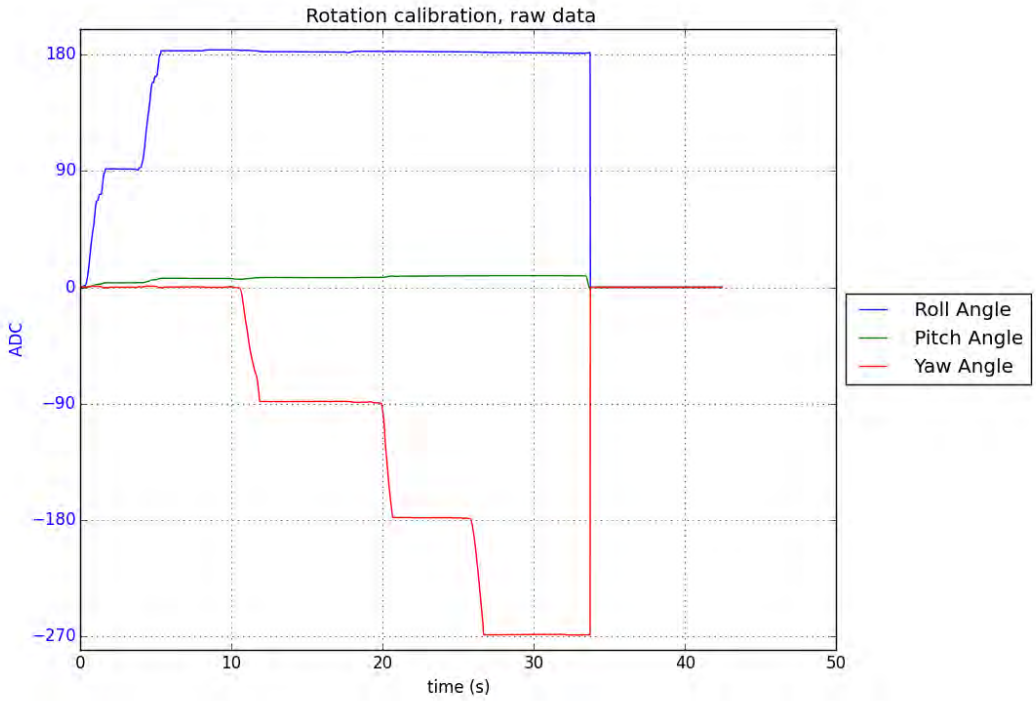

Figure 3.4: Gyrometer validation. Gyrometer fixed to a cube and rotated over all faces. Integration of output with respect to time yields the angle rotated. Note pitch angle failure.

3.7 Pressure

Pressure will be measured under the 1st and 5th metatarsal heads, the great toe and the calcaneus protrusion, a total of four sensors. These sites have been selected as being the primary load bearing sites and known high risk locations for ulceration [14, 126]. The measurement range will be 0 – 0.3 MPa. Resolution will be $\pm 0.5\%$, accuracy will be $\pm 5\%$ which covers all peak pressures measured by Caselli in a cohort of 20 healthy people [38].

Pressure is measured as a force on a sensor which is assumed to have uniform loading over the sensing area. To measure pressure gradient over an area a number of separate sensors are required with spacial resolution being a function of sensor density which in turn is a function of sensor size. To do this under the sole of the foot multiple small sensors are utilised, assuming minimal pressure gradient across an individual sensor. Commercial sensor systems utilised in this field to measure PP, PPP, PPG and PTI utilise a sensor pitch of $5.1\mathrm{mm}$ in both X and Y directions, equating to 954 sensels per foot on the standard insole [112]. Though accurate, the high sensor density requires greater signal conditioning and processing requirements when compared to a smaller number of force sensors measuring peak force.

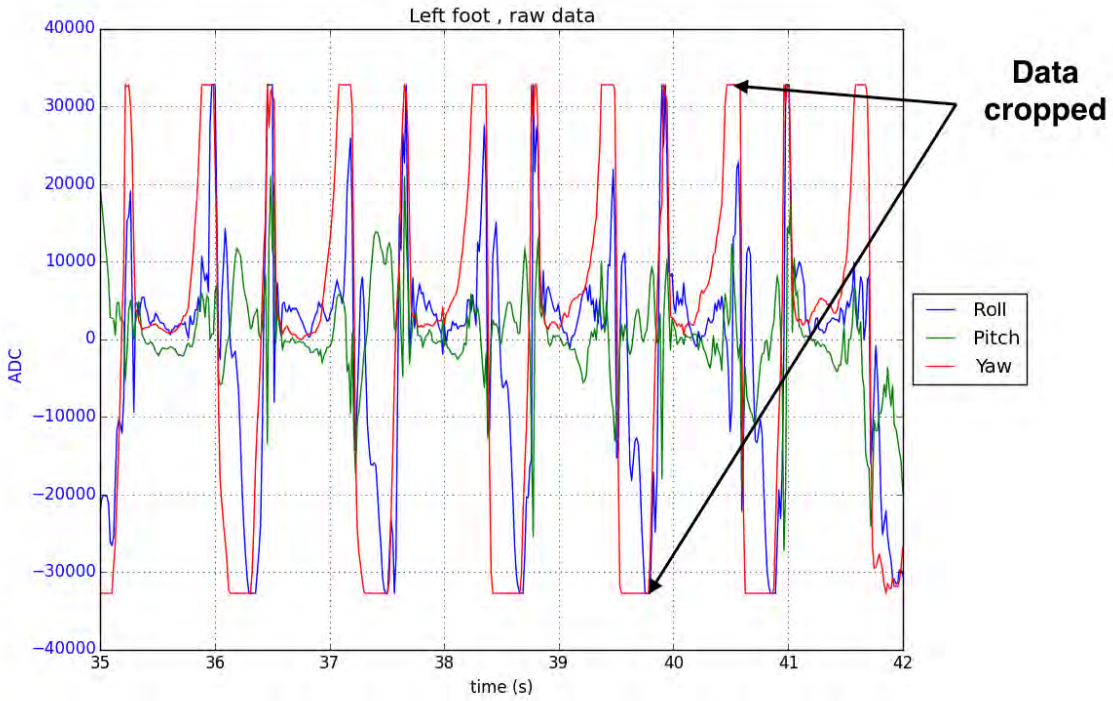

Figure 3.5: Sample gyrometer data to demonstrate system data acquisition capability using the author as a test subject. This data is only used as part of the sensor prototyping. It is also noted that the data is cropped as the default sensor range is inadequate for the desired measuring task.

3.8 Force measurement

Few investigators have utilised force as a measurement, so selection of the measurement range is derived from the pressure measurement above. The force is calculated from the pressure and desired sensor size. Utilising a $\oslash 25.0\mathrm{mm}$ sensor at $300\mathrm{kPa}$ would require a 0 -145 N calibration range ($F = P \cdot A$). Resolution will be $\pm 0.25\mathrm{N}$ and accuracy of $\pm 2.5\mathrm{N}$.

Initial validation of the force, temperature and forefoot flex was undertaken with a proto-board circuit, see Figure 3.6, to validate the multiplexed sensor selection. Sensors where driven at $-0.257\mathrm{V}$ with output multiplexed into an inverting operational amplifier with $R_f = 120\mathrm{k}\Omega$ in line with the manufacturers recommended drive circuit, see Figure 3.7. No filtering was used at this stage with all data being output in $10bit$ (0-1023) format. Sensor calibration is discussed in section 5.3.4.

Force sensors, Tekscan A401 [127], were placed under the calcaneus tuberosity, metatarsal heads and the pad of the great toe, see Figure 3.6 as discussed in section 2.2.3, which are sites known to be susceptible to increased loading due to diabetic pathology. This acted as a surrogate for pressure that minimises complexity, power and data requirements. Peak force may also better inform the investigator of the

loads passed to the skeletal system.

Figure 3.6: Analogue circuit prototype board, for the investigation of force, temperature and forefoot flexure

Force sensing resistors are designed to measure force rather than pressure. Only force should be quoted if the area exposed to the force is unknown. Figure 3.8 demonstrates why this is important. In this experiment a force sensor, an A301 from TekScan, was exposed to a range of loads, using both a $\oslash 5.0\mathrm{mm}$ and a $\oslash 8.0\mathrm{mm}$ load puck. Measuring sensor output with consistent force but varying surface areas/pressure as shown in Figure 3.8 demonstrates the sensor to be a force sensor.

Sensor output can be seen in Figure 3.9 where sensors mounted as described above measure in shoe forces generated by perambulation. All force sensors provide clear signals, though resolution could be usefully increased. Force sensing was chosen as the appropriate in shoe metric in lieu of pressure due to the simplicity of interfacing and certainty of measurement as discussed in section 2.2.3.

3.9 Forefoot flex

Flex will be measured over the ball of the foot in the sagital plane. Measurement range will be from $0 - 90°$ Resolution will be $\pm 0.25°$ accuracy will be $\pm 2.5°$. Currently there is no evidence of this being measured utilising in shoe sensors. Where foot flex is observed it is done by eye or occasionally video.

The Spectra Symbol flex sensor was investigated as a means of monitoring the forefoot flex. This sensor is $0.5\mathrm{mm}$ thick with a nominal resistance of $\approx 10\mathrm{k}\Omega \pm 30\%$

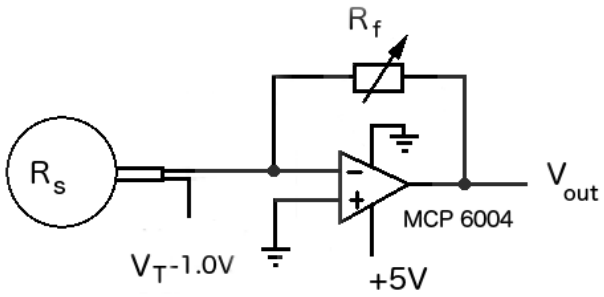

Figure 3.7: Force sensor recommended drive circuit. Maximum recommended current = 2.5mA

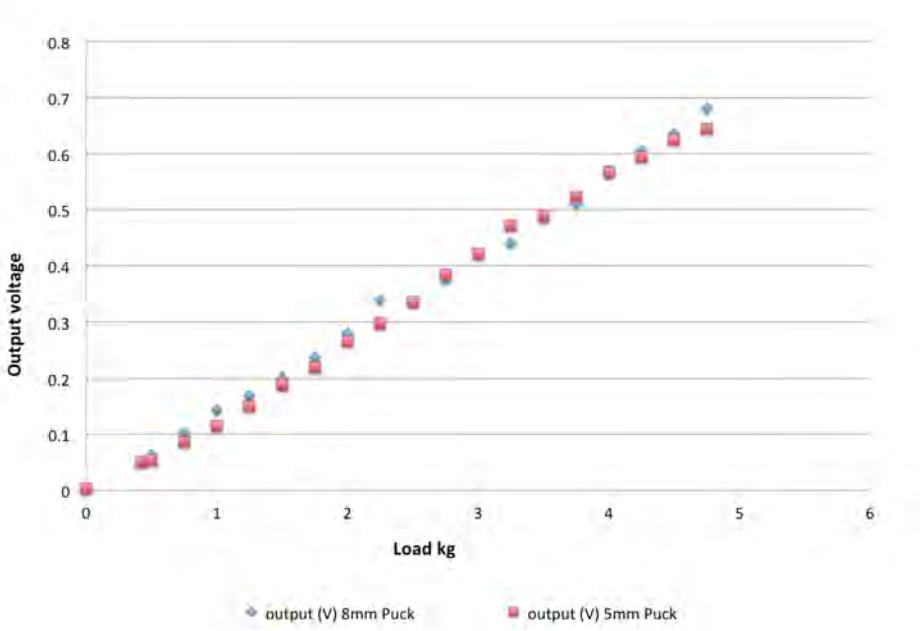

Figure 3.8: Load area comparison, demonstrating that the load cell (Flexforce A301) works as a true force cell not pressure. Measured using recommended circuit.

when flat and $>$ 2 x flat resistance at a $180°$ pinch bend. Resistances were measured over bend angles of $0, 30, 60, 90°$ with formers of radius $R = 29.0, 25.35, 21.75, 16.06\text{mm}$. An adjustable gauge was manufactured see Figure 3.10 and setting repeatability verified with a vernier protractor at better than $\pm 1.0°$.

Initial testing revealed that the sensors were sensitive to changes in both bend radius and the position of the bend along the sensor. The effects of these were investigated individually and in concert. The sensor manual stated that the tolerance for the inter-sensor variability was $\pm 30\%$.

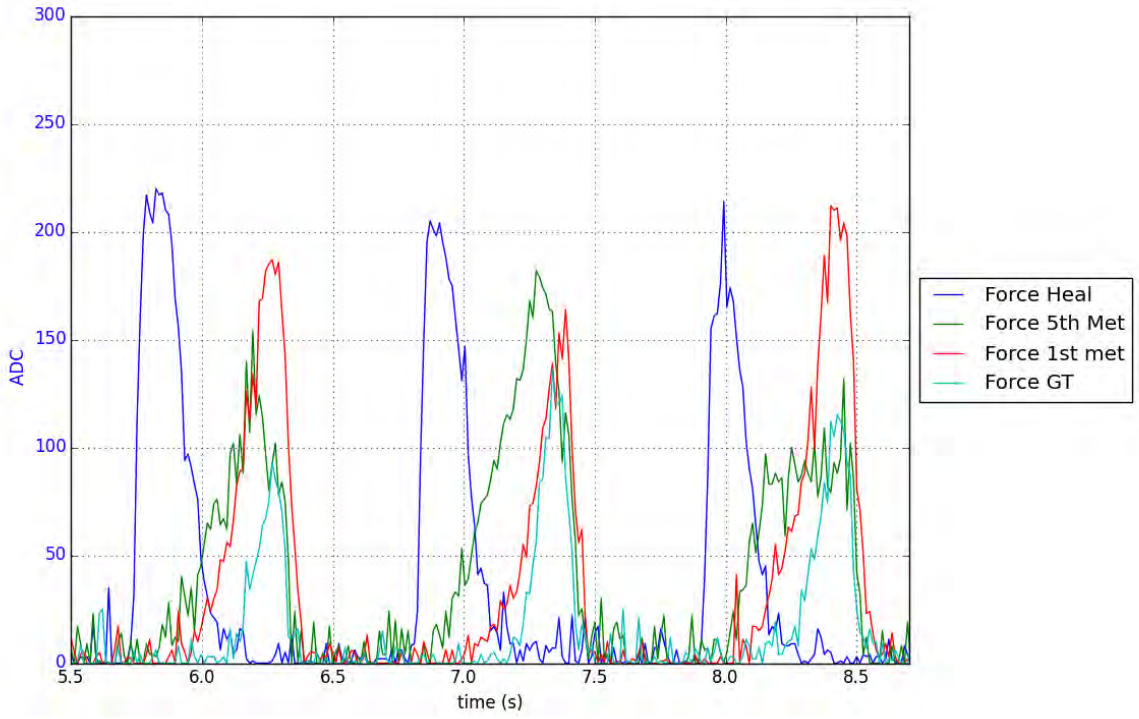

Figure 3.9: Prototype force sensor output for heal, great toe, first and fifth metatarsals of the left foot while walking at $5.0\,\mathrm{km\,h^{-1}}$.

The single bend point (offset 54.0mm), single radius (R25.35mm) test shows good repeatability of $\pm 2.0\,\mathrm{deg}$ over seven cycles see Figure 3.11. This is within the $\pm 2.5\,\mathrm{deg}$ required of the sensor.

As the ball of the foot may well change stiffness over the course of the day, the effect of changing the bend radius was also investigated. Testing sensor response at a single point with varying radii gives an error of $\pm 5.0\,\mathrm{deg}$ as shown in Figure 3.12. The flex centre of forefoot may change due to pathology compounded by in shoe movement so it was also necessary to quantify the error due to movement of the area of flex. Schepers *et al*. estimate heal centre of pressure varies by $\pm 6.0mm$ (n = 10) between individuals. As can be seen in Figure 3.13 the sensor output is not consistent along its length with $\pm 10°$ variation within $19\mathrm{mm}$. Due to these reasons this sensor was note utilised in the final device.

This type of sensor has proven to be too inaccurate for further consideration as part of this sensor set. However this remains an important source of data for foot geometry and should be included if a relliabel sensor could be sourced. Alternatively this angle could be inferred from other data where the hind foot angle could be measured from accelerometery with first metatarsal/ great toe force being used to confirm forefoot compliance with the ground.

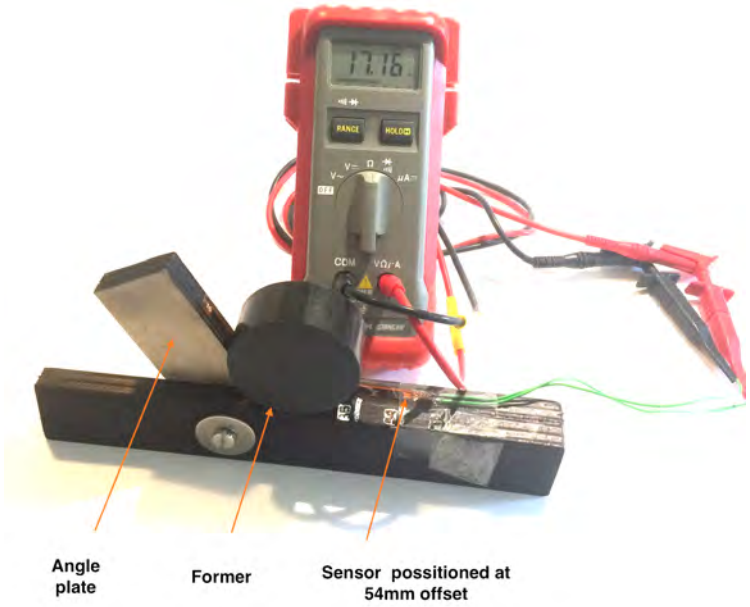

Figure 3.10: Flex sensor guage, with the theoretical corner set at 54mm from the base of the sensor with a radius 25.35mm former.

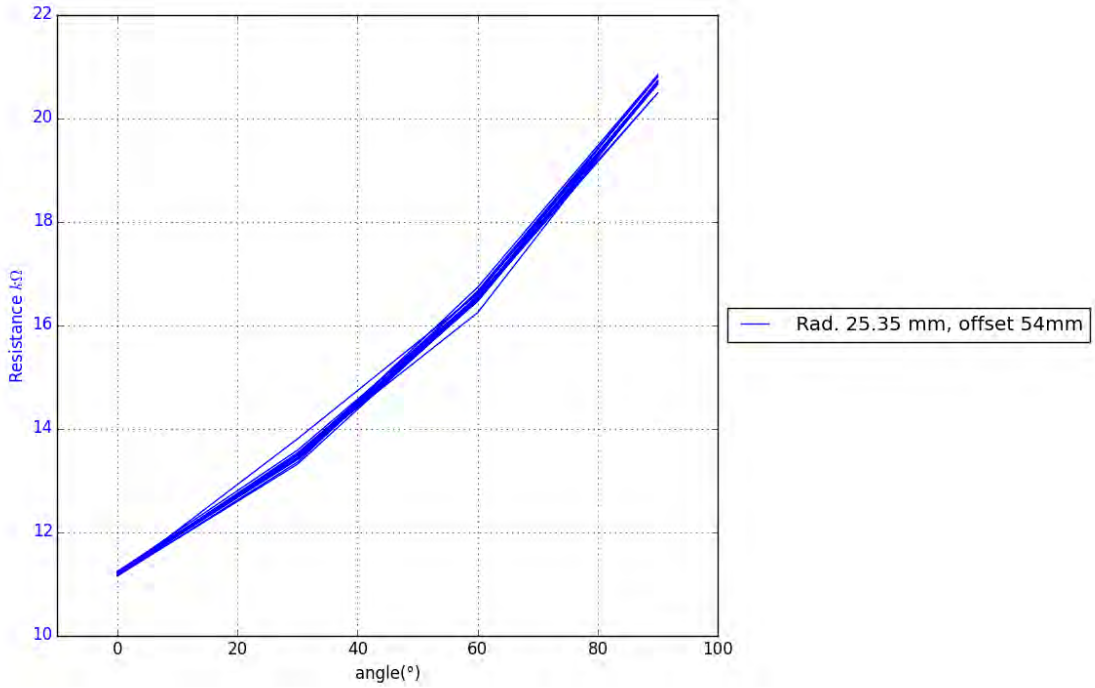

Figure 3.11: Flex sensor repeatability. Sensor cycled over a single radius at the same point flex point over $0, 30, 60, 90, 60, 30, 0°$. Error $\pm 2.0°$

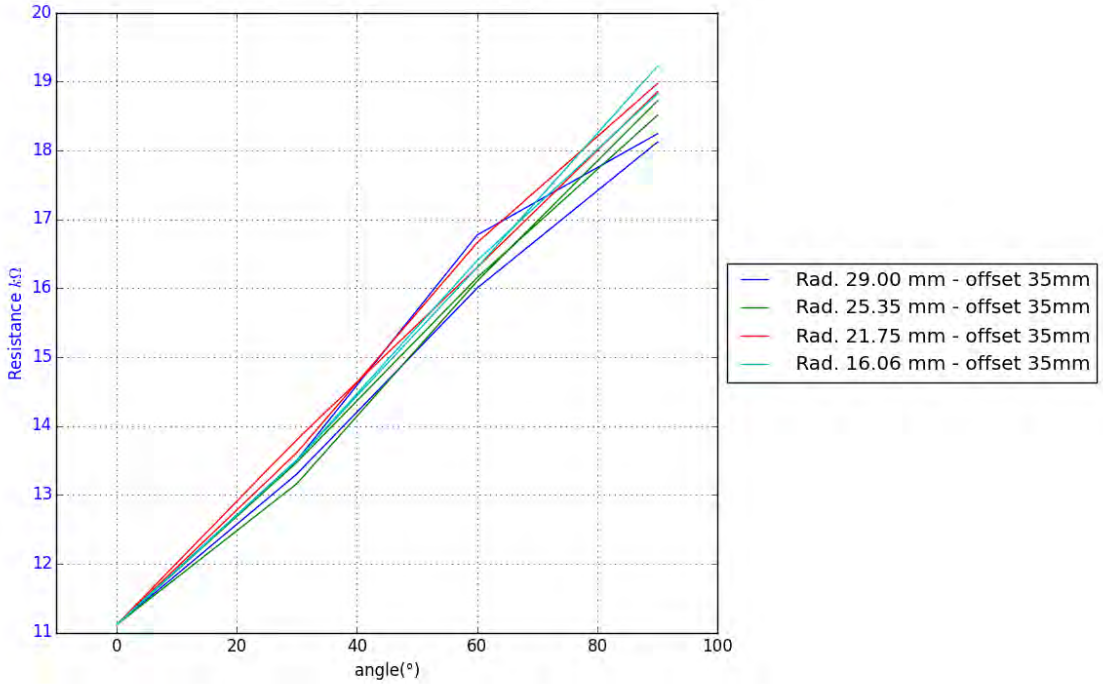

Figure 3.12: Flex sensor variation due to bend radius. Error $\pm 5.0\,\mathrm{deg}$. test n = 1.

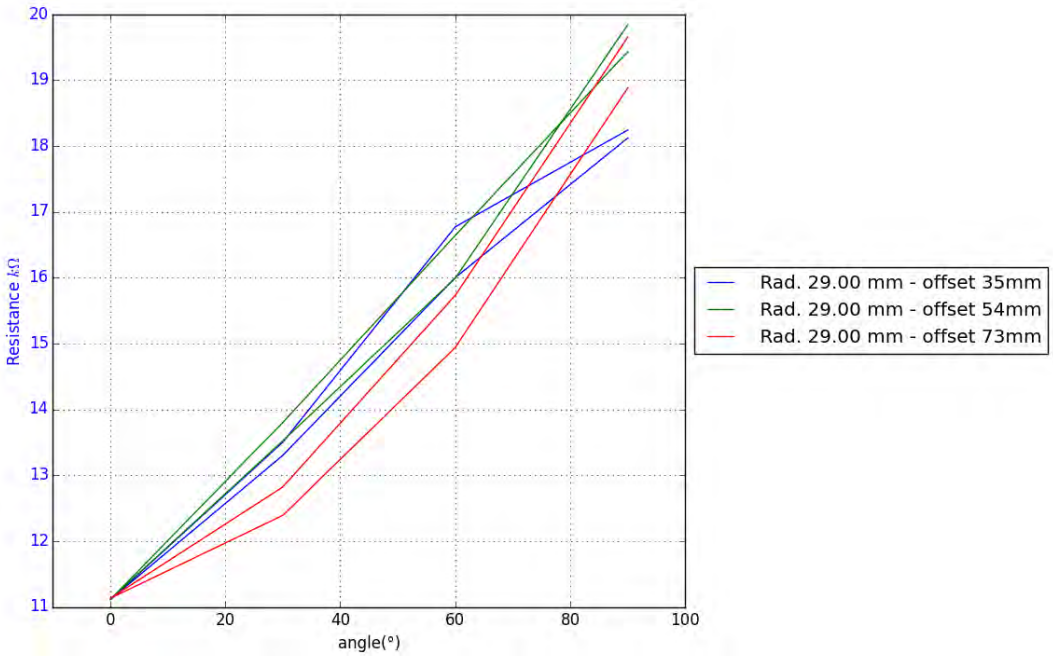

Figure 3.13: Flex sensor variation due to variable flexure point. Moving the point of flexure for a given bend radius generates a large error in the order of $\pm 10\,\mathrm{deg}$. This is unsuitable for monitoring foot flexure.

3.10 Skin temperature

Skin temperature will be measured under the great toe, the metatarsal heads [126] and calcaneus tuberosity. As the primary sites of infection in the diabetic foot these are useful target sites to gather validation data. The measurement range will be from $20 - 40°\mathrm{C}$, resolution $0.1°\mathrm{C}$, accuracy $\pm 1.0°\mathrm{C}$ to ensure discrimination of $\Delta 2.2°\mathrm{C}$. Measurements will be repeated at a period of no greater than 10 seconds. Temperature is expected to change slowly and as such presents no particular constraint on the choice of sensor. In shoe $15 - 45°\mathrm{C}$ Covill *et al* [128] shows that the in shoe temperature is expected to be $4 - 5°\mathrm{C}$ above ambient at $15°\mathrm{C}$ ambient and $0.3 - 1.2°\mathrm{C}$ above ambient at $35°\mathrm{C}$ for a healthy foot. As stated above Armstrong [20] also noted that ΔT was also an effective indicator of the pathology with Charcot neuro-arthropathy having a distinct characteristic ΔT of $8.3°\,\mathrm{F}$. The sensor upper limit will be set at $40°\mathrm{C}$ to accommodate this.

Skin temperature monitoring utilised a thermistor type 104 JT 025 from Semitec. This was driven by the same circuit as the force sensors in 2.2.3 to validate sensor operation. Figure 3.14 demonstrates a stable output though resolution could be usefully increased. Thermistor temperature measurement was demonstrated to be a suitable technique for monitoring podiatric skin temperature. Afoot discrimination of a $\Delta T = 2.2°\mathrm{C}$. Armstrong *et.al.* [19] utilised the same device on both feet so output must be repeatable within these bounds though absolute temperature is not as important for a relative measurement. The protocol for sensor calibration is discussed in section 5.3.5.

3.11 Heart rate

Heart rate will be mountable on the third or fourth toe or the ball of the foot to measure ischemia. The measurement range will be $50 - 150$bpm, resolution will be ± 1bpm, accuracy will be ± 1bpm. Discussions with other investigators have alluded to difficulty in getting reliable measurements of heart rate and SPO2 for the sole of the foot in a dynamic environment.

The 'Amped pulse sensor' chosen for testing utilised a light reflection principle where green light is directed at the tissue under test, while reflected light is measured with a high sensitivity photo diode. This technology is utilised where tissue is to be monitored from a single direction or the bulk of a transmission sensor is not acceptable. The photo diode output is low pass filtered to at $338\,\mathrm{Hz}$ and sampled at $500\,\mathrm{Hz}$ while DC drift was removed with an auto scaling feature utilising the max/min values of the previous 10 heart beats with signal dynamically re-scaled to aid pulse detection. Output was via digital to analogue converter (DAC) $0 - 5V$ centred around the mean output of $2.5\,\mathrm{V}(\mathrm{ADC}512)$. Output from the device is a time variant DC voltage, this is measured and processed by an external micro con-

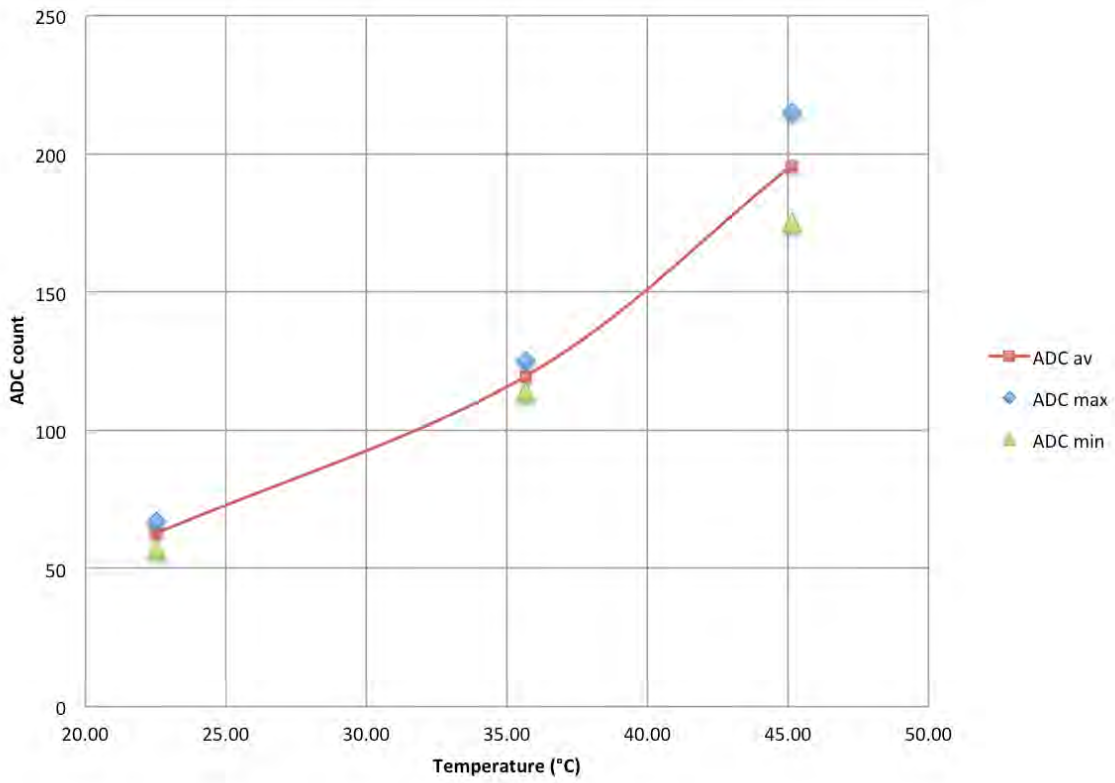

Figure 3.14: Protoype skin temperature sensor validation

troller, Arduino Nano in this instance. Output from the device is passed directly to the Arduino.

Tests undertaken comparing this device to a propriety Contec pulse-oxy-meter model:CMS50DL on opposing index fingers over a one minute test cycle agreed in all cases within $\pm$1bpm $n = 10$ tests, single volunteer.

Fitting the sensor to a shoe and testing in static and ambulatory modes revealed a susceptibility to movement artefacts as shown in Figure 3.16. The device accurately recorded heart rate in a static mode. However, the large increase in the magnitude of the signal and the similarity in signal frequency prohibited effective separation of the signals. As the signals could not be relied upon this sensor was eliminated from the sensor selection.

3.12 Oxygen saturation (SpO2)

Ideally SPO2 would be measured on the third or fourth toe or the ball of the foot to investigate ischemia in an area known to be a high ulceration risk. The measurement range would be $80 - 100\%$, resolution would be $\pm 0.5\%$, accuracy would be $\pm 1.0\%$ [129]. The reflectance technology used is the same as for heart rate and as

Figure 3.15: In shoe pulse measurement

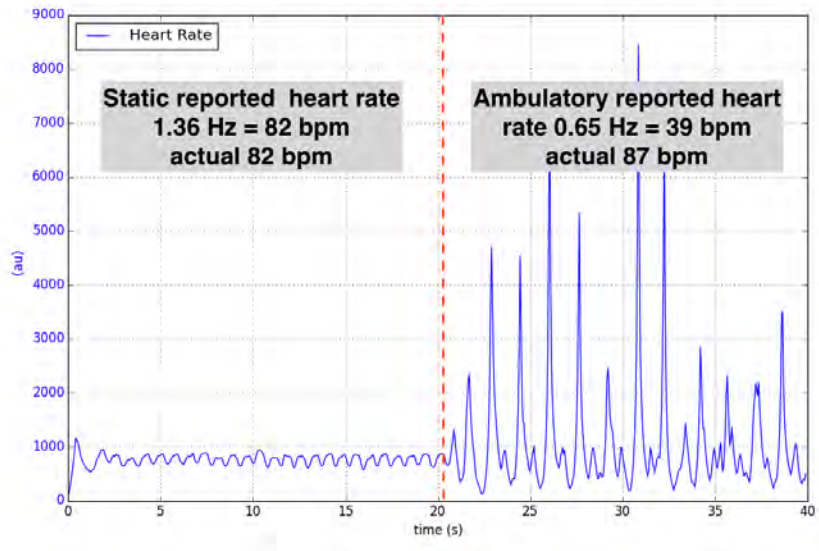

Figure 3.16: Static and ambulatory heart rate utilising light reflection technique. Heart rate is not reliably discernible from ambulatory data.

such suffers from the same movement artefacts and was consequently eliminated from the sensor suite.

3.13 Bioimpedance

Bioimpedance will be measured over the ball of the foot to measure changes in the tissue status at a single site where ulceration is likely to occur in the diabetic foot. The measurement frequencies will be 100kHz 1MHz in 100kHz steps. Accuracy will be $\pm 1\text{kHz}$. Phase measurement range will be $0 - 10°$, resolution will be $0.01°$, accuracy will be $0.1°$, gain will range from 1:100 to 100:1 resolution will be 0.1%, accuracy will be 1%. Capacitive coupling will eliminate the need for coupling gels and the possibility of tissue polarisation, improving comfort and safety.

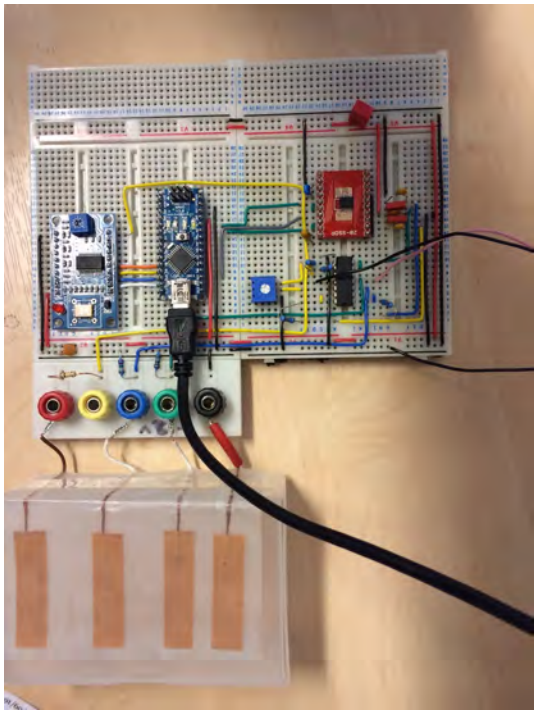

Figure 3.17: Bioimpedance sensor prototype on solder-less breadboard

A prototype capacitive (non contact) impedance sensor was built and tested for this application. The device was constructed by hand utilising copper film strips 10.0 x 40.0mm spaced $26, 24$ and 17mm apart, laminated between two $75\mu\text{m}$ polypropylene films as shown in Figure 3.17

Capacitance

$$C = K \times E_o \times \frac{A}{D}$$

$$K = 2.26$$

$$E_o = 8.85419 \times 10^{-12} \frac{\mathrm{F}}{\mathrm{m}}$$

$$A = 400\mathrm{mm}^2$$

$$D = 0.075\mathrm{mm}$$

$$C = 107\mathrm{pF}$$

E_o = permittivity of free space
K = relative dielectric permittivity

The prototype was driven from a signal generator connected to the outer electrodes of the electrode array with the ground electrode being $26\mathrm{mm}$ from the adjacent electrode. The signal was monitored between the ground electrode and each of the inner electrodes in the array, while drive signal was similarly monitored between the ground and driven electrode.

A sensitivity test was undertaken to investigate the devices' ability to determine changes in healthy tissue. Comparison of impedances measured laterally and longitudinally over the palm of the hand as presented in Figure 3.18 clearly demonstrate a response to the anisotropic nature of the hand. The palm of the hand was used in prototyping the bioimpedance sensor for convenience and as a courtesy to other lab users. Attenuation is of the same order. However, there is a clear $15.18°$ phase shift. This result does not prove the devices' ability to detect abnormalities in the tissue as there is a paucity of data regarding the necessary bioimpedance parameters necessary to investigate such a problem.

The principle of measurement was further developed so that it could be utilised in an embedded device. To enable the frequency generation and comparison of bioimpedance signal up to $1.0\mathrm{M}Hz$ utilising an $8bit$ $16\mathrm{M}Hz$ Arduino processor a bespoke circuit was devised. An Analogue Devices AD9850 was utilised to generate a $14bit 0 - 2.0V$ signal voltage, amplified to $0 - 4.0V$ to supply the sensor. This and the return signal voltage was analysed by an Analogue devices AD8302 phase gain detector. This device transmits the phase and gain as two independent $0 - 1.8V$ outputs, alongside a precision $1.8V$ reference voltage.

Safety of applied current - bioimpedance

The current passing through the circuit is important for user safety. Therefore the safe (AC) exogenic current limit of $100\mu\mathrm{A}$ should not be exceeded. The analysis

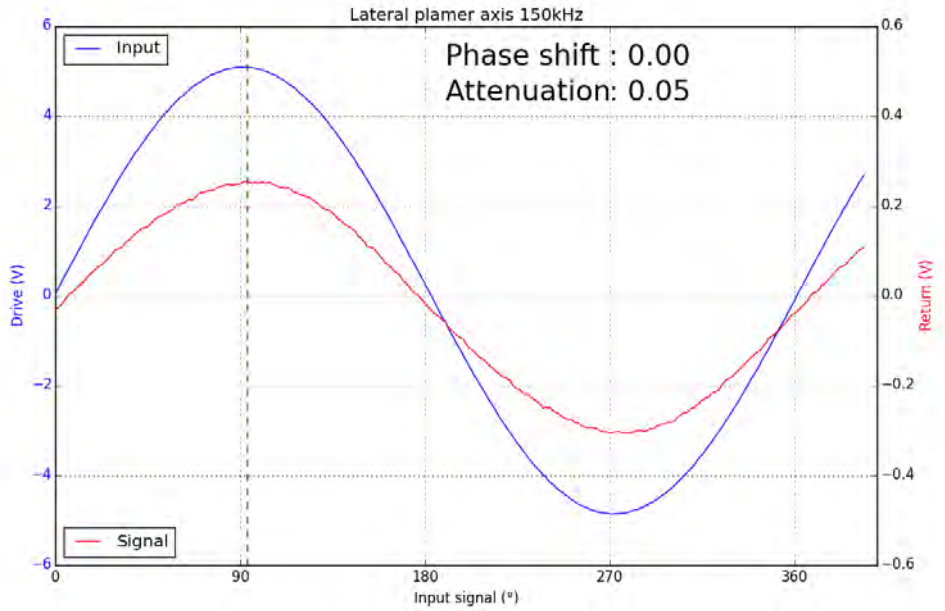

(a) Bioimpedance at $150\text{k}Hz$ - lateral palmer axis

(b) Bioimpedance at $150\text{k}Hz$ - distal proximal axis

Figure 3.18: Changes in palmer bioimpedance due to orientation

will ignore the body's contribution to impedance, assuming that the body has no impedance allows the calculation of the maximal current that the device can emit, thus erring on the side of safety. The circuit comprises two $107\,\mathrm{pF}$ capacitors in series driven at $\pm 5.0V$ at frequencies given below. Grimness and Martinsen show the range $100 - 1000\mathrm{k}Hz$ to have good dynamic range for conductance and susceptance when investigating dermal tissue[130].

$$X_c = \frac{1}{2\pi f C}$$

$$f = frequency Hz$$

$$f_{min} = 100\mathrm{k}Hz$$

$$f_{max} = 1\mathrm{M}Hz$$

$$X_{c(100\mathrm{k}Hz)} = 14.9\mathrm{k}\Omega$$

$$X_{c(1\mathrm{M}Hz)} = 1.49\mathrm{k}\Omega$$

Allowing for two capacitors in series

$$I_{100\mathrm{k}Hz} = \frac{V}{R} = \frac{5.0V}{2 \times 14.9\mathrm{k}\Omega} = 168\mu\mathrm{A}$$

$$I_{1\mathrm{M}Hz} = \frac{V}{R} = \frac{5.0V}{2 \times 1.49\mathrm{k}\Omega} = 1.68\mathrm{mA}$$

3.14 GSR

GSR would be measured proximal from the 5**th** metatarsal in an area of high sweat gland density, utilising the circuit defined in Figure 2.11. Though GSR can be used on any part of the body this thesis is interested in measuring the ANS/sudomotor activity in the foot. The measurement range will be $100\mathrm{k}\Omega$ - $10\mathrm{M}\Omega$ with a resolution of $\pm 2\%$, an accuracy of $\pm 5\%$ of measured value. Sensor validation is discussed in section 5.3.6.

Figure 3.19 demonstrates the GSR response to physiological excitation. In this experiment GSR was monitored while a sharp inhalation of breath was taken and held for $45\mathrm{s}$ and released. Both events induce an increase in sweating and a reduction in resistance. The underlying trend is a gradual release of sweat over time with typically smooth curves.

Figure 3.20 shows the GSR response to psychological excitation. GSR was monitored while the volunteer watched an extreme sport video. The response is more dynamic than that shown Figure 3.19 which is to be expected with a fear based response. Both figures demonstrate that a clear response is measurable with the devices as built.

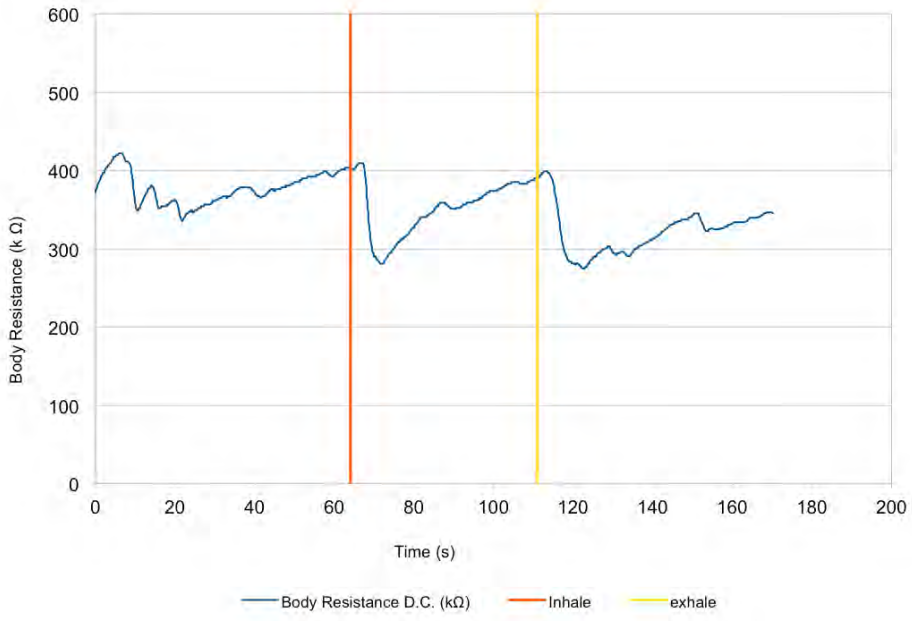

Figure 3.19: GSR measuring ANS response to rapid inhale and exhale. It is postulated that the rapid inhale causes sweating on the palms of the hand and soles of the feet as part of the fight or flight response to enable higher friction for running or climbing. Reduced sweat response is a known side effect of ANS neuropathy resulting from diabetes.

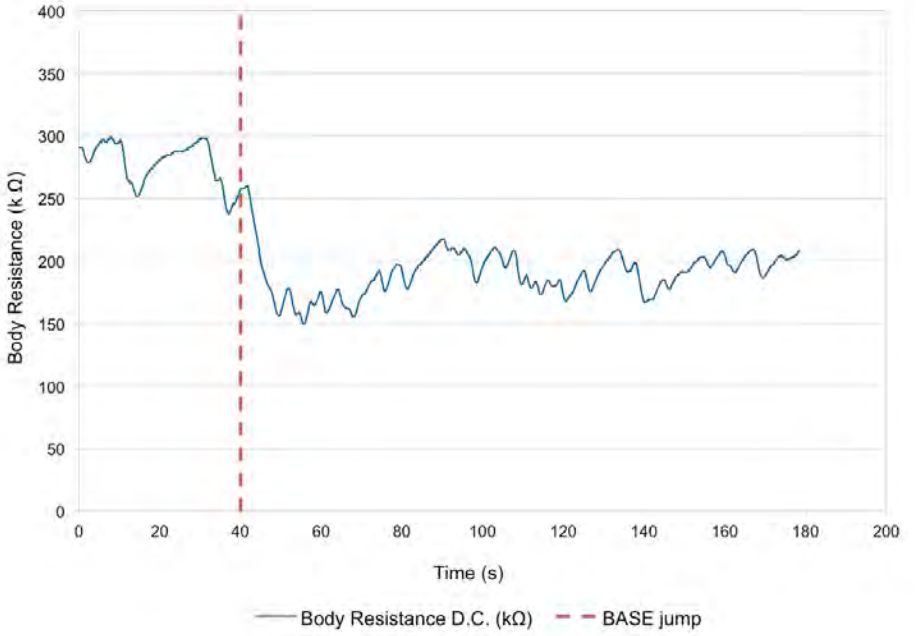

Figure 3.20: GSR measuring autonomic nervous system response to induced fear, utilising an extreme sports video

Safety of applied current - GSR

The current passing through the circuit is important for user safety. Therefore the safe exogenic (DC) current limit of $10\mu A$ should not be exceeded. Assuming that the body contributes no resistance to the circuit allows the calculation of the maximum current that can be applied.

$$I = \frac{V}{R} = \frac{5.0V}{820k\Omega} = 6.1\mu A$$

3.14.1 Design of data acquisition circuit

To integrate the sensors into a coherent data set, the design and manufacture of a signal conditioning circuit was necessary. This circuit provides six discrete functions.

1. Provide power to each section of the device at the correct voltage and current capability.
2. Connect digital sensors to the processor (I^2C).
3. Provide correct excitation to the analogue sensors.
4. Condition the return analogue signal and present it to the processor so that it can be read.
5. Apply calibration algorithm to the measured data.
6. Transmit the data to a host computer for collection.

A printed circuit board (PCB) was designed, see Figure 3.21, that would support a modular build with sensors being added over time see **Appendix B Figure B.1** for circuit diagram. Power was supplied via proprietary rechargeable $5V 1.6A\,h$ batteries normally used to charge mobile phones. These were used to power the Arduino on board voltage regulator and off-board amplifiers as required. Dual rail voltages for the op amps were generated utilising off board DC - DC converters to minimise the number of batteries and weight. This also enables charging from any desktop computer or USB charger for operational convenience. These will be mounted externally to the device and connected via a standard USB-A connector and also provides an easily interchangeable power source with good voltage control and easily managed recharging.

When choosing a sensor it is important to bear in mind the connection protocol as there are myriad protocols available to system designers. These range from analogue in either current, typically $4 - 20mA$ or voltage with $10 - 100mV$, $0 - 1.8V$, $0 - 5V$ or $0 - 10V$, being a few of the outputs available. Similarly there are myriad

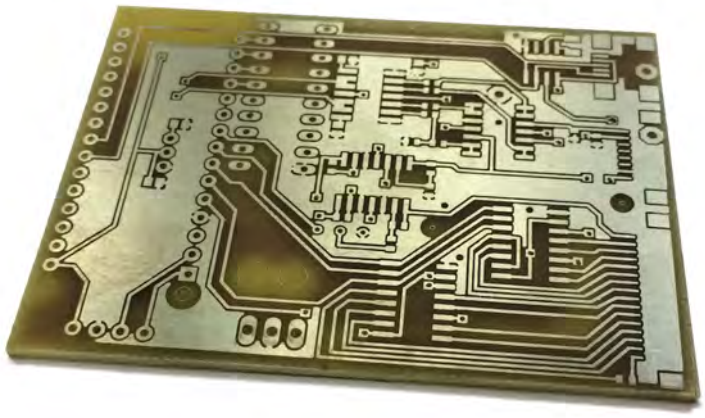

Figure 3.21: The second version of the data-aquasition PCB

digital interface protocols available with serial, parallel,I^2C, canbus, serial peripheral interface (SPI), pulse width modulation (PWM) to name a few. By designing the device using common interfaces for multiple sensors project risk and development time can be reduced while reliability is increased. Analogue sensors are usually cheaper to purchase than a digital equivalent but require more complex interfacing and often requiring calibration as the excitation and measurement circuits are external to the sensor, whereas digital sensors have this built in prior to the conversion to digital output and are often calibrated at source (though this must be validated periodically). Where a bus system is employed, multiple sensors can be added in a single chain without change to the host electronics much like a USB on a desk or laptop computer.

The sensors chosen for acceleration, rotation, humidity and in-shoe/ environmental measurements have been specified with anI^2C interface for speed, simplicity and cost. This will also allow for future expansion on the same interface if required. These sensors are factory calibrated within tight tolerances and are available at reasonable cost.

The bioimpedance measurement is based on Analogue Devices chip AD8302 ARUZ is a $0-1.8\mathrm{V}$ output for both gain and phase angle with on-board $1.8\mathrm{V}$ reference voltage. The Arduino has the ability to use this reference voltage as the upper limit on the ADC thus enables the Arduino to utilise the full $10bit$ ADC over this voltage range. However, as the voltage to be measured by the ADC must never exceed the reference voltage. This means that all other analogue sensors need to be restricted to this range as well, or the ADC must be re-set to internal $5.0\mathrm{V}$ reference immediately after a bioimpedance measurement is completed.

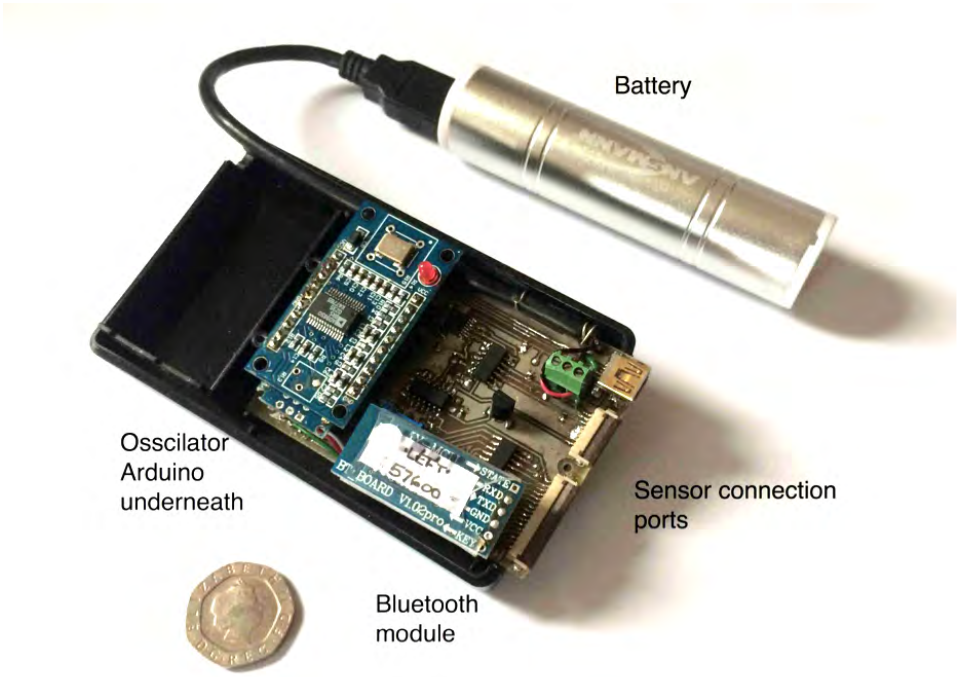

Figure 3.22: Embedded data acquisition device

The remaining sensors that measure force, skin temperature and GSR are resistive in nature and will be used as the input current control of an active circuit for maximum range and control. This provides simple voltage measurement at the processor interface.

The bioimpedance analyser requires a sinusoidal input for excitation which is provided by the Analogue Devices AD9850 direct digital synthesis chip [131].This is programmed via a serial link and provides a frequency range of 1Hz to 40MHz in a single device. These are readily available as fully configured development boards, simply requiring a power source and a host processor to provide the command signal.

Data is to be transmitted to the host computer via Bluetooth as it simply requires connecting to the serial port of the host processor. It is cheap, reliable and is available in most desktop/laptop computer systems. This allows the elimination of the wire tether to the host computer which would present a trip hazard and the discrete mounting of the data acquisition circuit under a trouser leg.

3.15 Combining sensor modalities, GSR, acceleration, environmental temperature and humidity

In the development board shown in Figure 3.22 there were five sensing modalities installed. These are:

1. Acceleration in (X,Y,Z) via I^2C interface.

2. Rotation rate (Roll,Pitch and Yaw) via I^2C interface.
3. In shoe environmental humidity via I^2C interface.
4. In shoe environmental temperature via I^2C interface.
5. GSR. via the analogue interface

Figure 3.23: Right foot sensor array

The GSR data presented was measured at the 1^{st} and 5^{th} metatarsal heads to measure changes in the ball of the foot. The prototype circuit utilised $5V$ over a voltage divider circuit for the duration of the test, it is proposed to change this to $\approx 250\mathrm{mV}$ to minimise the polarisation at the electrodes and the generation of local milieu while reducing load on the battery. An alternative to this would be to reduce the time that the tissue is exposed to the current/voltage source and to reverse polarity for each measurement cycle. It may be necessary to use different parts of the foot to gain better resolution or access tissue that is more sensitive to ANS perturbations.

The sensors were mounted in a pair of Regatta Harris sandals. This platform provides easy access to the sensing platform which can be removed and replaced at will, while presenting adequate features with which to locate the insole for reliable and reproducible sensor positioning. The sensors have been mounted on a proprietary 3.5mm foam insole spacer. This affords a suitable level of positioning accuracy, and adequate material thickness to position sensors without causing local pressure points. This platform is not ideal as there is a significant airflow to the

sole of the foot which will be incompatible with an enclosed shoe. However, this gives greatly improved access to the sensors and a repeatable platform for testing this concept.

3.15.1 Prototype sensor system output

The data shown in Figure 3.24 demonstrates multi sensor output from the GSR, acceleration, gyroscope, humidity and temperature sensors at frequency of $83Hz$ verifying that the data acquisition system was capable of suitable temporal resolution. Data clipping can be seen as it was not possible to set the accelerometer and gyrometer ranges at the time of testing.

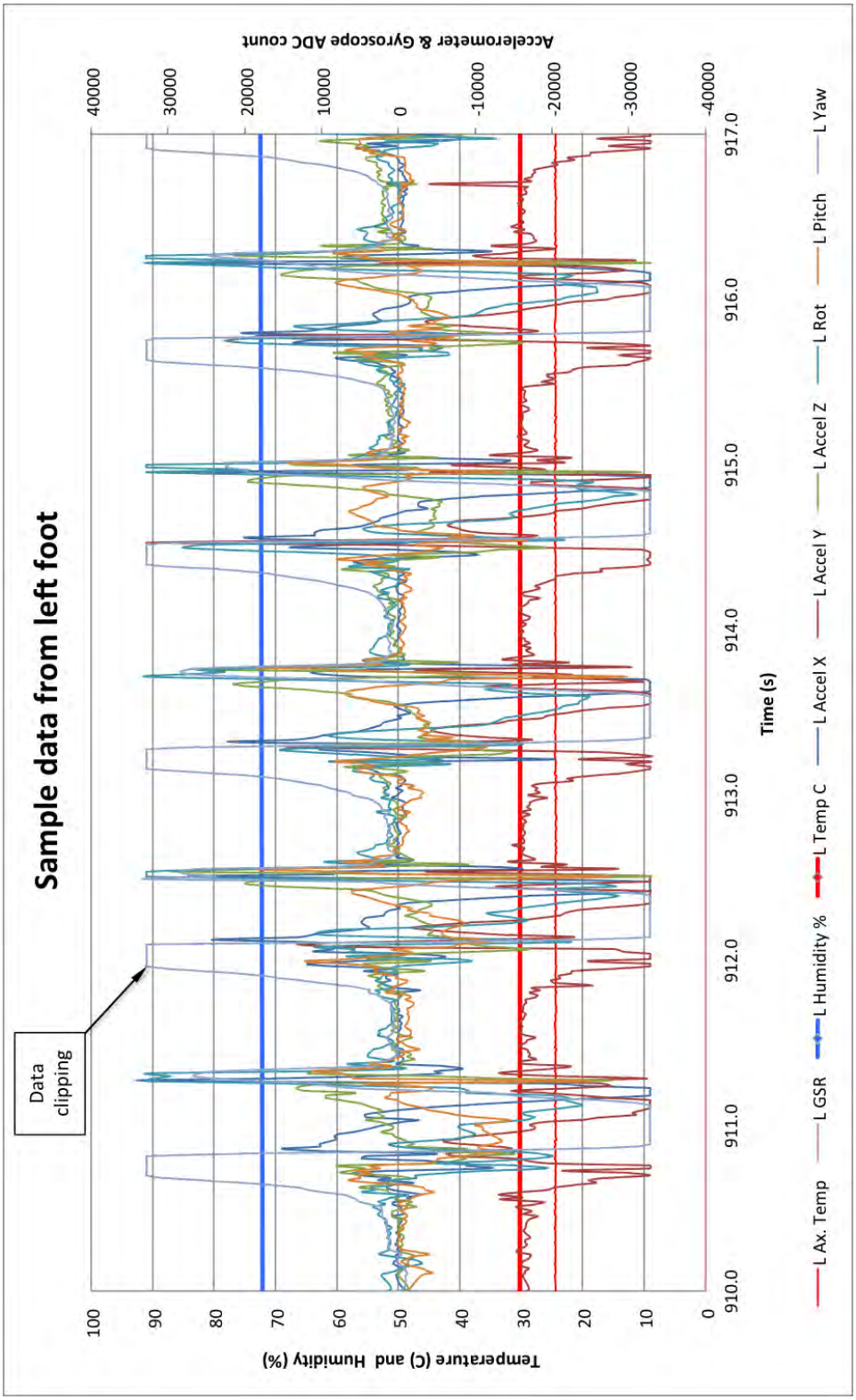

Figure 3.24: Sample acceleration gyroscope and humidity data

3.16 Summary

In this chapter a prototype circuit has been tested alongside a range of sensors. Table 3.1 details the sensing requirement to be implemented in the experimental sensor set. While Table 3.2 details the sensors selected against these criteria. A conceptual sensor layout is shown in Figure 3.25 to show how sensors may be integrated in later chapters.

Of the sensing modalities discussed above there are a number that are not practical to measure in the in-shoe environment using the methods we have investigated. These are heart rate, SPO2 and flex. It was decided to utilise force as a surrogate for pressure to reduce the interfacing load and to investigate it as an alternative to pressure.

The sensing modalities that have been successfully tested are:

- Environmental temperature.
- Environmental humidity.
- In shoe temperature.
- In shoe humidity.
- Acceleration.
- Rotation.
- Force.
- Skin temperature.
- GSR
- Bioimpedance.

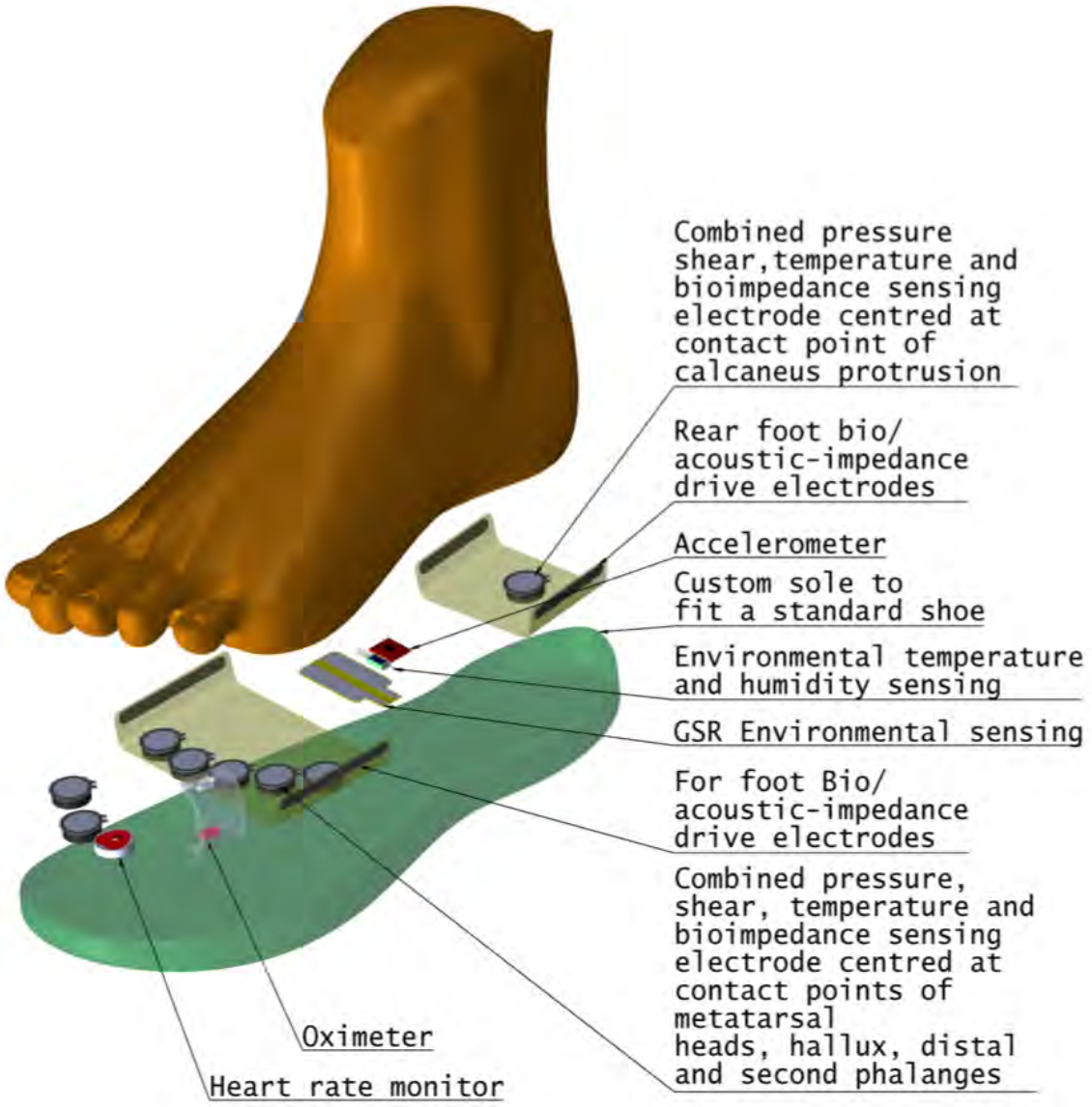

Figure 3.25: Multi-sensor preliminary sensor layout.

Chapter 4

GSR study

4.1 Introduction

This chapter demonstrates the development and implementation of a sensing modality. The same work flow and principles were used in other sensor design and implementation. GSR is a worthwhile subject for discussion as it measures the sweat response of the tissue under test. This response is controlled by the ANS which can be affected by DPN. Reduction and potentially cessation of perspiration in the diabetic foot is a known side effect of diabetes and is measured routinely with the Ezscan [39, 40] and Neuropad [16] tests. However these tests are currently only available in the laboratory or clinic environment so inclusion in the proposed sensor suit will ultimately enable the gathering of longitudinal data that will enhance knowledge

It has been suggested that the comparison of phenomena over different sites on the body is likely to provide insight into pathologic status. This is an accepted principle when measuring temperature and blood flow but [77, 78] has not been demonstrated with GSR, though Purna has demonstrated some level of hand to foot variability [132]. To this end a study was undertaken to investigate how GSR events are reproduced over the body. Five investigations were undertaken:

Comparing GSR between the fingers and foot in individuals believed to be healthy will give baseline data with which to elucidate expected 'normal' ranges prior to examining known diabetic patients. Comparisons of GSR in opposing feet to be used as an exemplar of coherence deviation measurements that would be observable by the proposed sensor suit acting as a 'normal' reference data set, showing the difference between local tissue state/function. Direct comparison of left foot/ right GSR data will be shown to examine differences in the timing of events and magnitude. GSR Data will be presented utilising caffeine as a disturbing agent for the autonomic nervous system. Other methods of analysis will be discussed.

The following topics will be discussed in greater detail in this chapter

1. GSR sensor data demonstrating the synchronous timing of ANS between

right foot to first and second finger of the right hand.

2. GSR sensor data demonstrating the synchronous timing of ANS events between opposing feet.

3. Data will be presented showing the effect of caffeine on the ANS while comparing GSR on the soles of opposing feet.

4. It will be demonstrated that GSR data can be gathered through a sock, without direct contact to the sole of the foot.

5. Finally intra-site GSR measurement of fingers, finger - foot, foot to foot and finger - pulse will be addressed alongside necessary changes in design and data acquisition rate.

4.2 Dual channel GSR, right foot to right hand

Figure 4.1: Foot to hand GSR measurement device

To investigate how timings of events may differ over the body GSR was synchronously measured at two different parts of the body utilising the foot to hand measurement device shown in Figure 4.1, namely the right foot and hand. The circuit used to measure GSR in the hand utilised a $180\text{k}\Omega$ biasing resistor while that circuit for the foot utilised a $820\text{k}\Omega$ resistor to optimise outputs for the expected

ranges. The ranges were established during earlier testing on this project. The volunteer was seated with contact being made to the right foot with the sandal shown in Figure 4.1. Electrodes were placed under the pads of the first and second fingers of the right hand with GSR recorded for 200 seconds with a manual termination of the test. A time series data set is presented in Figure 4.2 inset, which clearly shows that events that happen in both fingers and the sole of the foot are correlated temporally. Data was taken from a cohort of 14 healthy volunteers 7 male 7 female with an age range of 24-62. The wide cohort is used to generate a broad data set for non diabetic individuals. This will be used as baseline data for comparison with a diabetic population.

Sample data from a single volunteer is shown in Figures 4.2, 4.3, 4.4 and 4.5 that will be used to illustrate observable features in the data.

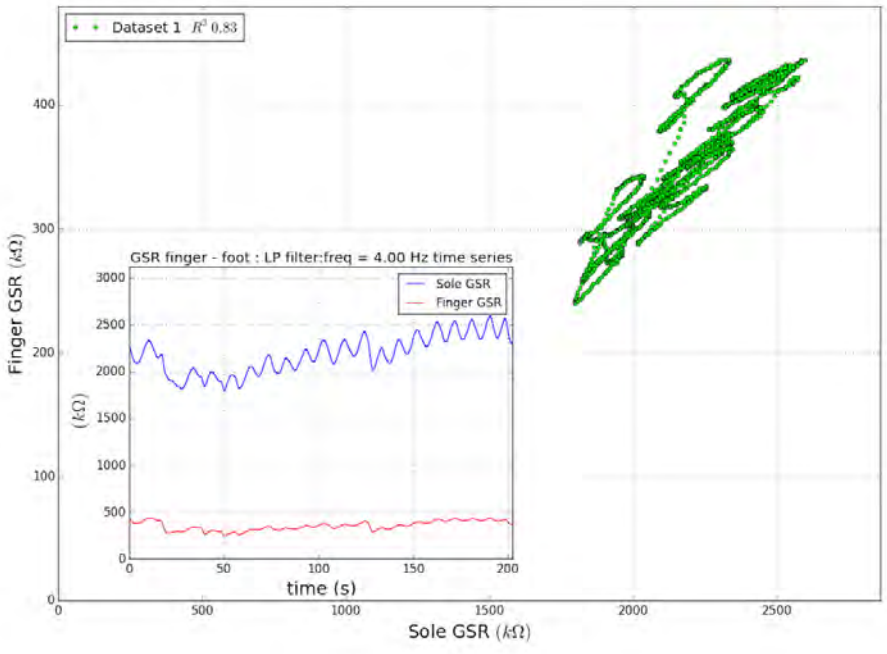

Figure 4.2: GSR coherence foot to finger signal. Male volunteer 45 years old BMI 27.4. The main figure shows finger to foot GSR coherence while the inset figure shows the same data as a time series plot for finger and sole GSR. With an $R^2 = 0.83$ this demonstrates high coherence between measurement sites.

- The red and blue plots are the finger and foot GSRs respectively with the green trace being the inter site coherence. From the time series data we estimate that the short term changes relative to the average respective baseline resistances are proportional to each other in terms of relative magnitude and timing $\Delta R_{foot}/R_{foot} = \Delta R_{finger}/R_{finger}$. The coherence measurement, of $R^2 = 0.82$ shows this to be a valid assumption for this data. If asymmetric ANS disease was present this would be expected to reduce the coherence, but due to the paucity of studies it is not currently possible to predict the level this effect.

- It should also be noted that there is a large swing in the resistance/amount of sweat at 18.5 and 127.8 seconds in this plot together with the mirroring of macro and micro trends suggesting that both sites are responding to the same control phenomena. These two larger changes in resistance are likely to be simply a function of homoeostasis rather than pathology as it is commonly seen in the majority of samples.

- It is possible to conclude that there is high coherence in the events observed. Coherence is a measure of how well one system is related to, or predicts the action of another, or conforms to a mathematical model that predicts its behaviour. A simple measure of this is the coefficient of determination (R^2 value) which calculates the deviation from a trend line trough the data with 0 being no correlation and 1.0 being perfect correlation. The signals measured in Figure 4.2 have high coherence with $R^2 = 0.83$. Isolating the physiologically significant frequencies of interest from Figure 4.2 with a band pass filter ($0.01 - 1.6Hz$) signals in Figure 4.3 also shows high coherence with $R^2 = 0.76$ for physiologically significant frequency bands of $0.01 - 2.0Hz$ [133][134].

Investigating event timings is possible for the data presented in Figure 4.4. Intra site latency of 0.15 to 0.4 (s) between hand and foot that have been observed but need to be verified by further investigation, Pruna expects a lag of 0.66-0.67 seconds for an induced response [132]. In the sample shown it should be noted that the finger lags the peak in GSR seen in the foot but leads the trough. This is in contradiction to Pruna where the hand lead the foot response [132]. The timing variations are small but greater than the resolution of the measured phenomena. However, it would be prudent to improve the temporal resolution before drawing any conclusions from such data. This also needs to be tested on the intra foot GSR device. It is expected that DPN would effect the signal strength and latency. Pruna noted a marked reduction in the magnitude of change for a single diabetic neuropathic patient compared to his control, but also noted exaggerated sympathetic activity even while resting [132]. The use of a high pass filter and peak/trough de-

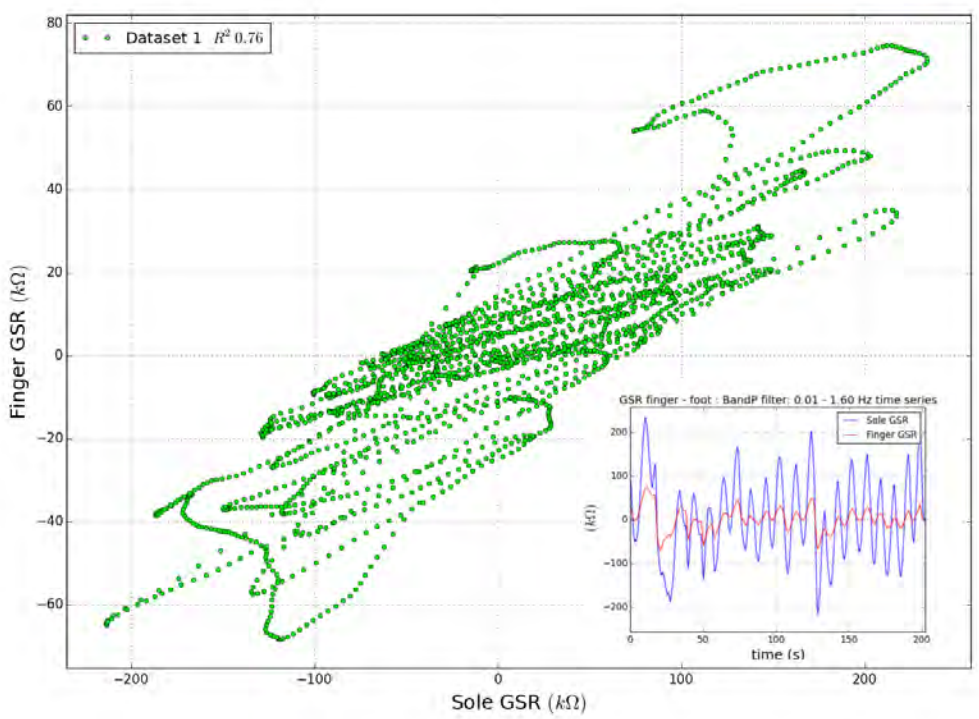

Figure 4.3: Finger to foot coherence with band pass filter set at $0.01\,\mathrm{Hz}$ to $1.6\,\mathrm{Hz}$. The $R^2 = of 0.76$ shows the signals are strongly coherent. The inset figure is time series data for the two measurement sites while the main figure is the coherence plot for the data sites.

tection algorithms will greatly aid the quantification of this phenomena as shown in Figure 4.4. Band pass filtering of the data as seen in Figure 4.5 presents coherent data as tending towards a diagonal with non coherent data, tending towards a horizontal or vertical.

Short term trends appear to be mirrored in both signals during stable ambient conditions Figures 4.3 and 4.4 though long-term trends may differ to some degree. This is possibly the result of haemostatic control of the body, but it is unclear why the body would elect to utilise occasional course control steps where regular fine control steps are also present. To investigate specific high frequency (HF)s of interest the use of a high pass filter between $0.02 - 0.01Hz$ cut off is utilised to remove DC/low frequency (LF) drift revealing the underlying signals in line with Stefanovska's frequency analysis defineing frequencies of interest [133]. The filtered signal reveals significant frequencies from both the finger and foot that are likely to be related to heart rate, breathing and metabolism. Qualitatively there appears to be good temporal coherence in the signals seen to date, which supports the findings of Pruna[132]. Those living with diabetes are at risk from dry skin and breakdown of the epidermis leading to infection. GSR is accepted as a measure of ANS activity which is often affected by the onset of diabetes, causing dry

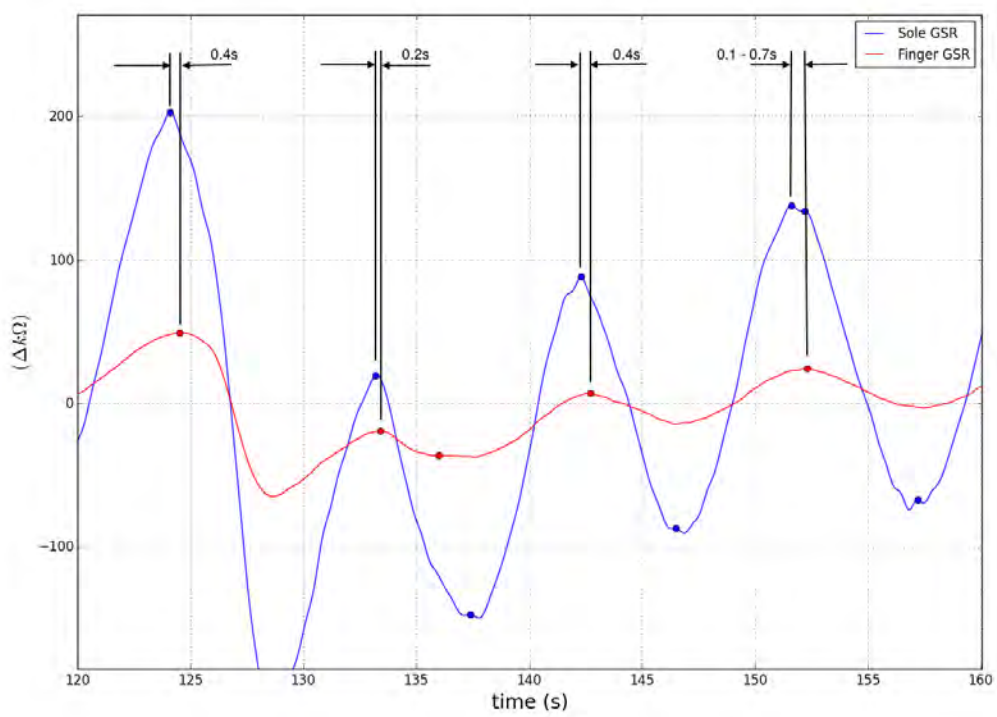

Figure 4.4: GSR latency finger to foot demonstrating the delay in signal from the foot being delayed when compared to the finger. This has been postulated to be caused by the difference in signalling path lengths from the signal origination point to the foot and hand [132].

and cracked skin. It is expected that those living with diabetes will have a higher skin resistance than others of a similar age and gender without diabetes, indeed a reduction of GSR signal has been observed in neuropathic patients by others. Surprisingly It has not been possible to find data comparing opposing feet to investigate whether a neuropathic foot can be monitored by this method or whether the DPN of the ANS is asymmetric or symmetric in opposing feet . Such a study would provide a contribution to the body of knowledge.

4.3 Dual channel GSR comparison of opposing feet

Comparing GSR at the finger to the sole of the foot, though interesting is not practical as a long term measurement as placing the necessary contacts on the fingers would present undue impediment to daily life. In the intended application of monitoring feet, utilising the next step is to measure the intra-foot GSR. For this a custom sensor was built that had identical measuring circuits, with constantly applied $5V$DC across $820\text{k}\Omega$ biasing resistors and calibrated against a +/- 1% decade resistor comparator to +/- 2%.

The intra sole GSR was tested utilising the intra pedal GSR measurement de-

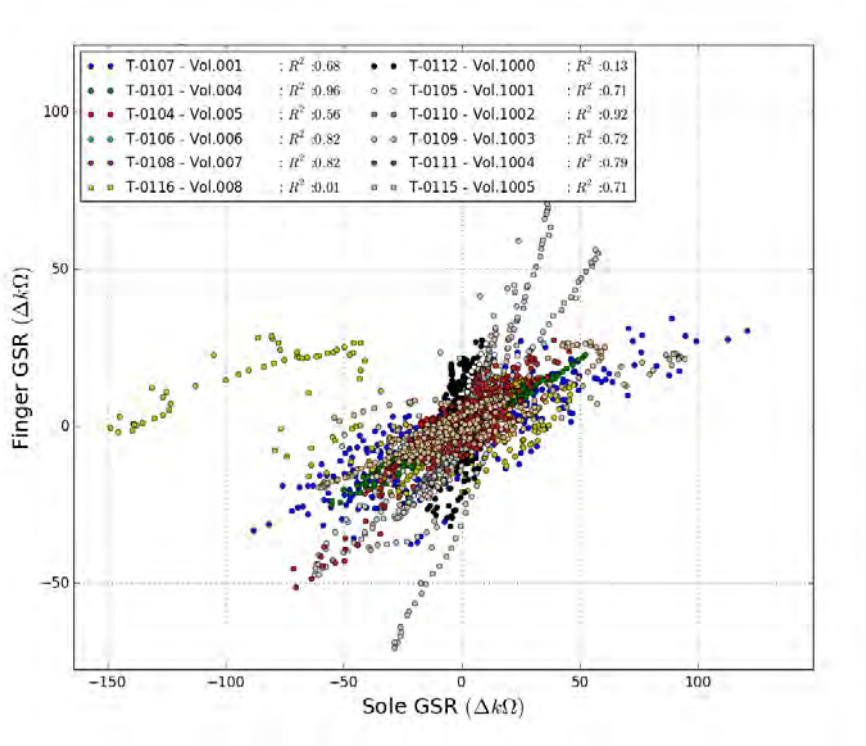

Figure 4.5: GSR finger to foot coherence for 12 volunteers band pass filtered at 0.01 - 1.6Hz. $R^2_{Average} = 0.65$

vice, Figure 4.6, with a data example shown in Figure 4.7 demonstrating a high level of coherence at $R^2 0.81 - 0.85$. Testing was undertaken on tissue without known pathology in which a high coherence is anticipated. Applying a band pass filter, removes LF drift and HF artefacts as seen in Figure 4.7. A $0.01Hz$ high pass filter was chosen to remove DC/LF drift with a $1.9Hz$ low pass filter to remove signal faster than the heart beat. Consequently it is also expected that lateral GSR comparisons will be able to measure ANS degradation. It will be necessary to test a larger cohort as currently this has only been tested on four individuals due to time pressures. It will be important to include a measure of skin and environmental temperature, alongside humidity to eliminate cooling of the limb as perturbation. Nonetheless, it is valuable to explore this here as there is no data available in the literature.

4.4 Multiple data sets

The data analysis methods for single tests have been examined in the first part of this chapter utilising a single volunteer. Here we will investigate multiple data sets utilising GSR.

A cohort of 12 volunteers utilising the time series data Figure 4.8 values ranged between $R^2 = 0.11 - 0.99$ and positive correlation was achieved with a single ex-

Figure 4.6: Intra pedal GSR measurement device

ception. It should be noted that the volunteer with the negative correlation also had the lowest coherence, has a family history of diabetes and the highest BMI in the study. The data for Figure 4.8 demonstrates that large ranges in the GSR response can be expected with finger GSR ranging from $70\text{k}\Omega$ - $831\text{k}\Omega$ and sole GSR 171 $\text{k}\Omega$ - $1.8\text{M}\Omega$ with the ratio of resistance between fingers and sole varying between 1:1.01 1:6.0. Band pass filtering the data as seen in Figure 4.5 at 0.01 - 1.6Hzisolates the biologically significant signals expected to be seen in the data according to Stefanovska [133]. An average of FFT's of the data sets shows that the only frequency of significance is centred around 1.37Hz. As this data was taken in a static condition this is likely to be the average heart rate of the cohort.

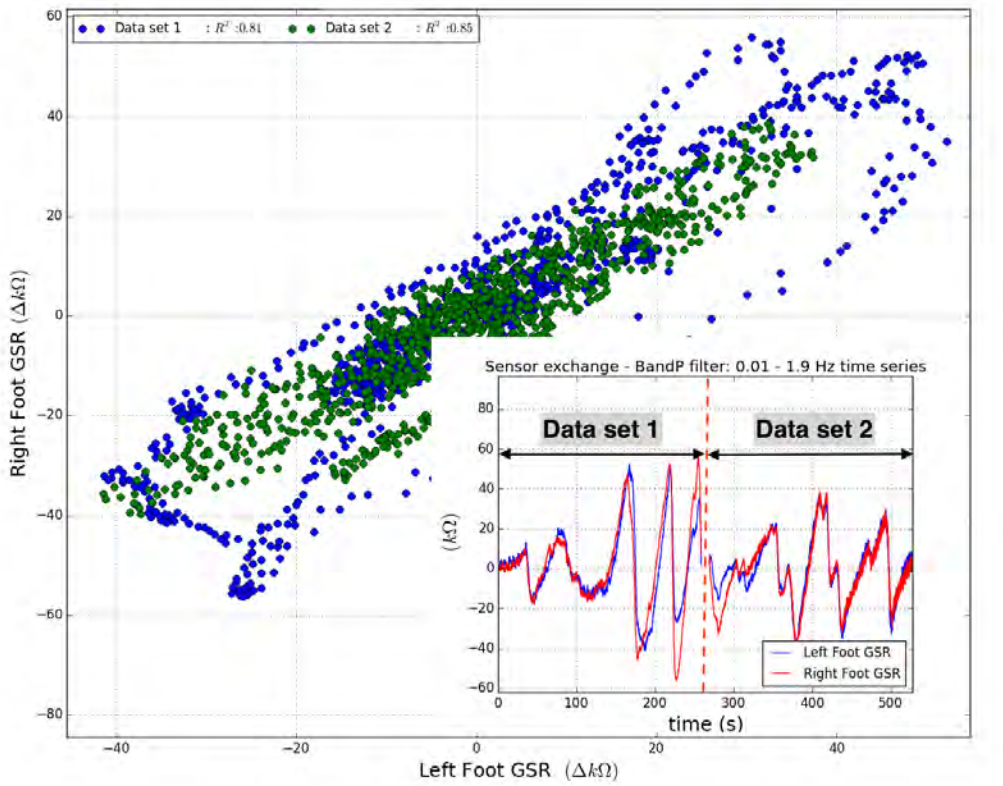

Figure 4.7: GSR Coherence between left and right feet, bandpass filter 0.01-1.9 Hz

4.4.1 GSR through socks

Hong et.al observed GSR being measured over clothes by using a 5 kHz AC source [135]. Measuring the GSR or any other phenomena through clothes is preferable to direct contact in in-shoe devices as socks can then be worn, improving foot hygiene. To this end a series of tests were undertaken to investigate the viability of using the as built GSR sensors through socks. The device used a DC source and consequently relies on a purely resistive pathway. A sock of man made fibre that is dry is an insulator. However, any sweat will reduce the resistance until an equilibrium is reached between sweat input and evaporation. It is likely that this method will also indicate when socks are changed or re-used on a daily basis as fouling of the material, from sweat and dead skin, will hold extra moisture and reduce the resistance from the sock. Poor foot hygiene is a particular problem for those with DF as it increases the risk of infection for any skin trauma and with the dry cracked skin prevalent with those suffering with DF. It may also be difficult for some suffering with diabetes to maintain good foot hygiene due to lack of mobility.

It is shown in Figure 4.9 that high intra-foot GSR correlation is observable where GSR is measured over socks. By consulting the data for Figures 4.10-4.13

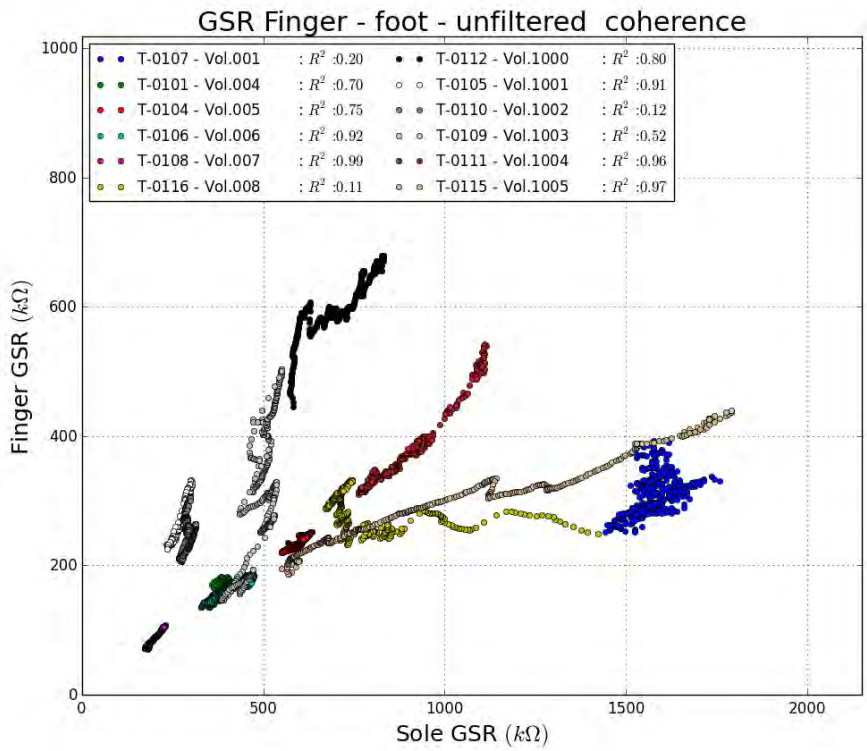

Figure 4.8: GSR finger to foot coherence 12 volunteers unfiltered data. $R^2_{Average} = 0.66$

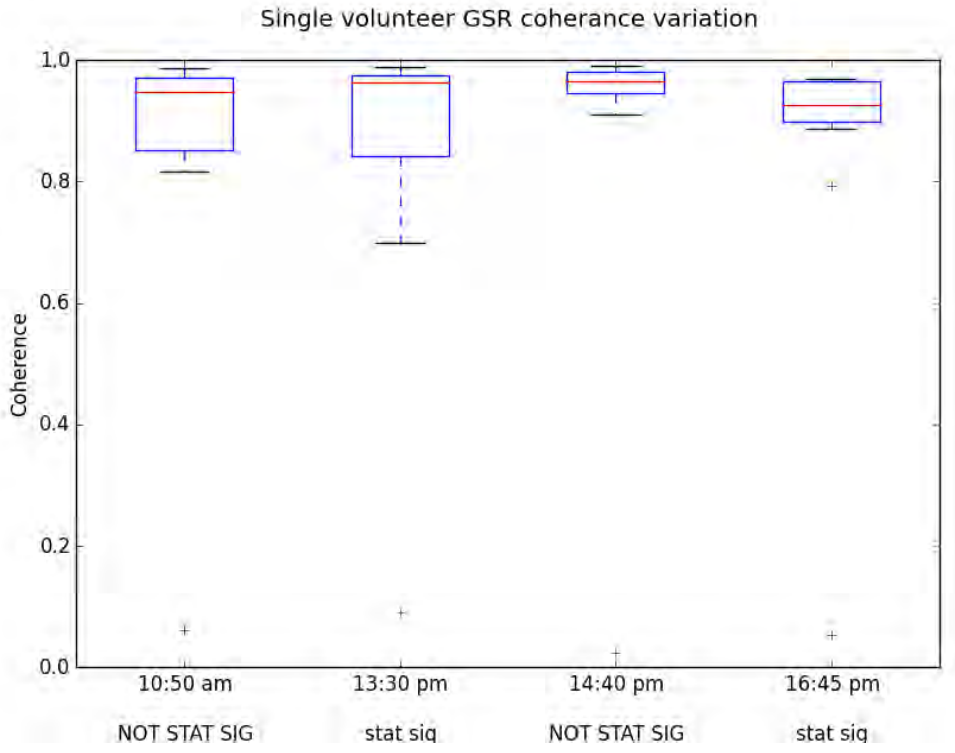

Figure 4.9: GSR daily coherence variation with socks

it can be seen that over the 6 hour period of testing that the GSR has reduced by a factor of 3, the reduction in resistance is expected as the humidity in the sandal increases above the ambient, due to restricted circulation. This causes an increase in moisture retained by the fabric of the sock and consequently increases dermal hydration. The concentration of salts will also increase as water vapour is released increasing the concentrations of sodium and chlorine ions. Figure 4.9 presents the intra foot coherence data for each of the previous figures as box and whisker plots. As is standard practice the median coherence value of each test set is represented by the red horizontal marker within the box, the upper and lower bounds of the box represent the upper and lower inter quartile range (IQR) . The whiskers represent bounds at ± 1.5IQR with data outside these bounds depicted as a $'+'$.

By contrast caffeine causes a reduction in coherence in the bilateral GSR data as demonstrated in Figure 4.14. Shapkin sites changes in the GSR response under the influence of caffeine [136] investigating increases in magnitude and delays in phase as evidence of the physiological effect.

Rossel et.al. reported impedances in the range of $10\mathrm{k} - 3.5\mathrm{M}\Omega\mathrm{cm}^2$ which correlates well with the resistances seen in this study [137]. Pruna [138] demonstrates foot to hand latencies of up to 2 seconds and Handler et al state latencies of 1– 3 seconds for excitation to electro dermal response [139]. Schapkin states that caffeine increases the time of response measured as both GSR and electromyography (EMG) [136]. However, no reference to the effect of caffeine on intra-foot/hand to foot GSR latencies is currently available.

There are however notable differences between the sensors in direct contact with the skin and those separated form the skin by a sock. The data presented in Figure 4.10 - 4.13 was taken from a single volunteer at 10:50 am, 13:30 pm, 14:41pm, 16:45pm on the same day. Data was taken at intervals during the day without removing the footwear. Examining the frequency spectrum shows considerable attenuation of frequency response but an increase in power over the observed frequency range where Low Pass filtering is utilised. It is also noted that there is a marked reduction in resistance over time. Neither effect is surprising as the textile acts as a reservoir holding moisture and increasing local humidity. This causes signal damping as sweat is retained rather than evaporating, causing an increase in local moisture and a corresponding sustained reduction of resistance as seen in the embedded coherence plots. Utilising a band pass filter of $0.002 - 1.9Hz$ over the whole data set as seen in Figures 4.15 and 4.16 significant power can be seen in three frequencies centred around $0.58, 1.0$ and $1.43Hz$ are clearly defined.

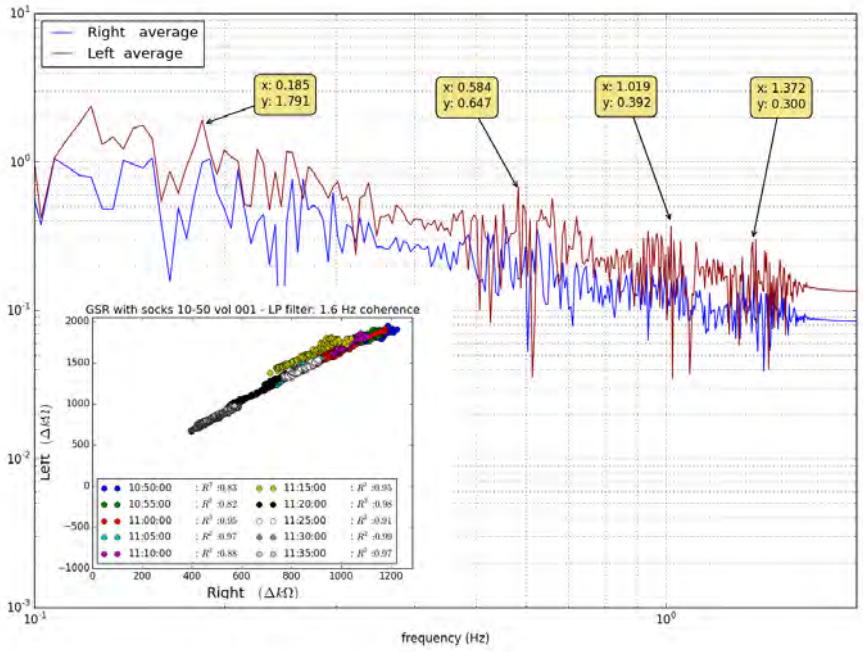

Figure 4.10: GSR conduction through socks. First test at 10:50 am. R^2 values are higher than previously seen due to the lack of evaporation creating a more consistent environment. The FFT presented is an average of all FFt's for all the data, though less pronounced than individual data sets, frequencies of interest can still be identified.

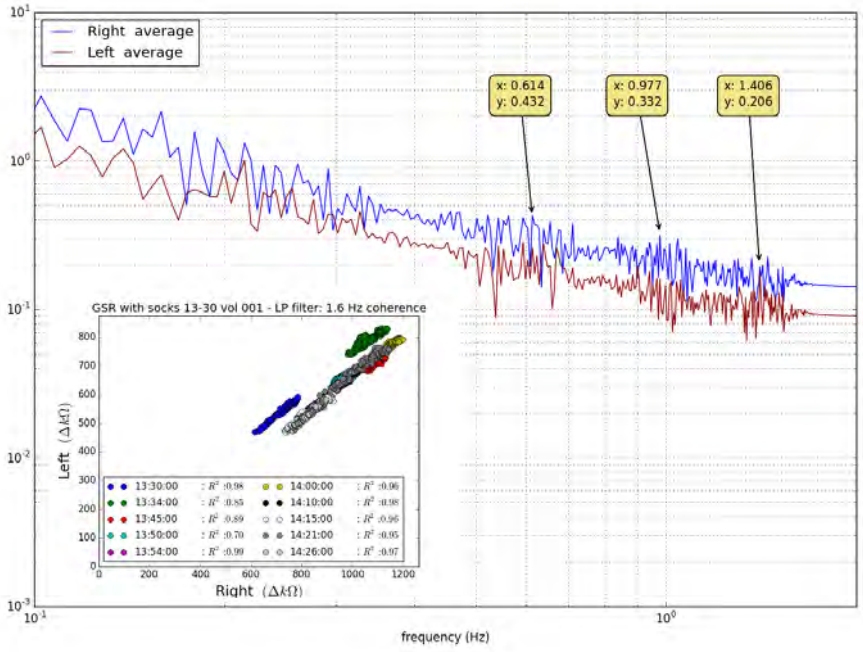

Figure 4.11: GSR through socks - 2

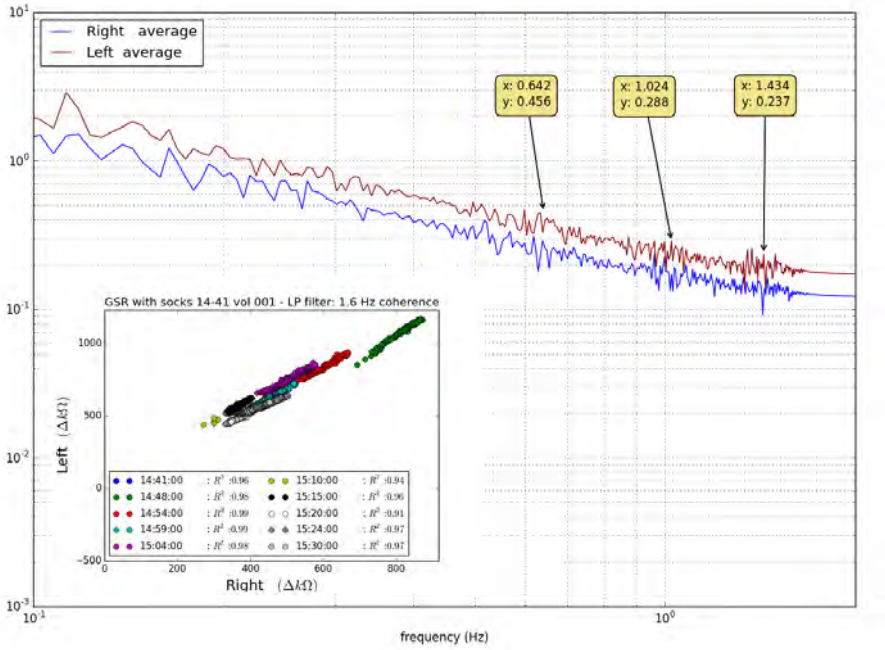

Figure 4.12: GSR through socks - 3

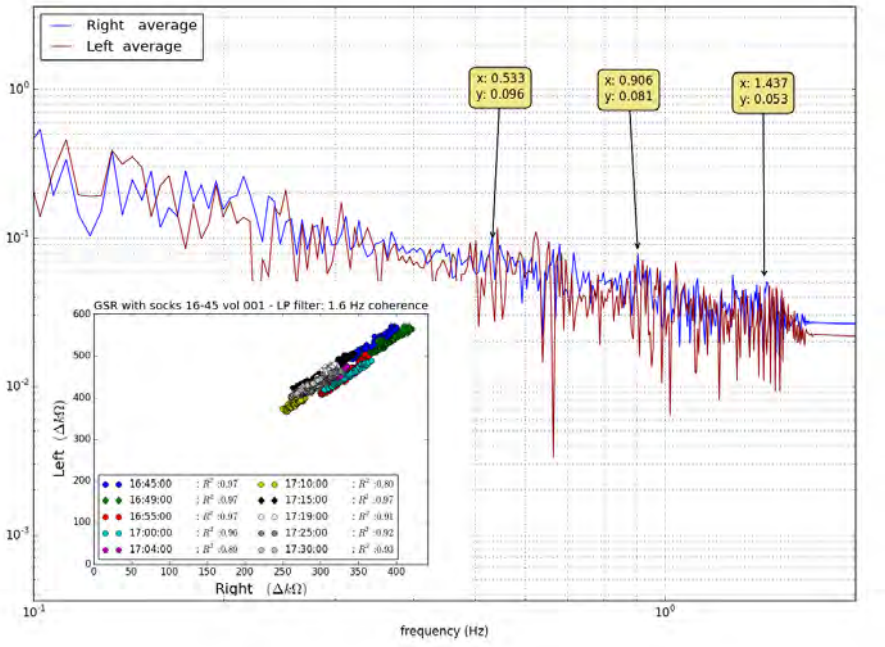

Figure 4.13: GSR through socks - 4

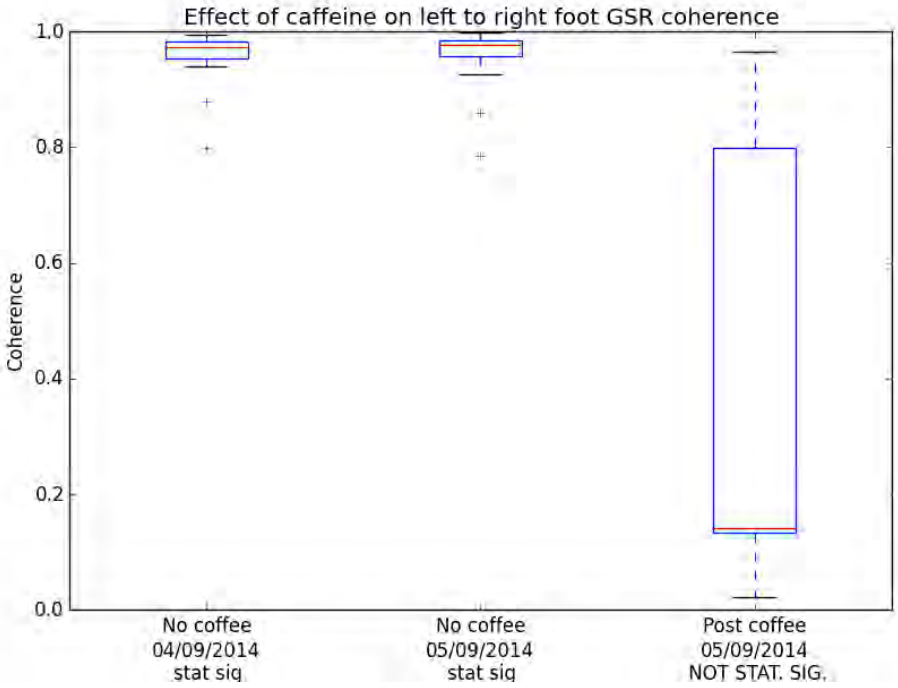

Figure 4.14: GSR effect of caffeine

4.5 Coherence deviation with and without caffeine as an ANS stimulant

Coherence measurement between feet has produced R^2 values of 0.9 to .99 with a few exceptions in the nominally healthy cohort of 14 individuals. Plotting the deviation from a norm is a useful method of characterising stochastic data and this was used to investigate the ranges of GSR coherence values in the data. Data already collected for GSR was compared to GSR with caffeine as an exciter. This data has 15 sets of GSR data of 200 seconds for each of two days, a large coffee was drunk and a further 4 GSR data sets taken. These data depicted in Figure 4.14 should be treated with caution as it did not reach statistical significance. However, the variation in GSR coherence seen after coffee is different enough to the data taken without caffeine to suggest that this analysis technique is worth further investigation. Caffeine is a known exciter of the ANS but little is known about how this effects GSR and particularly inter-site GSR the data presented here demonstrates that the effect is clearly measurable with very low coherence in the lower two quartiles.

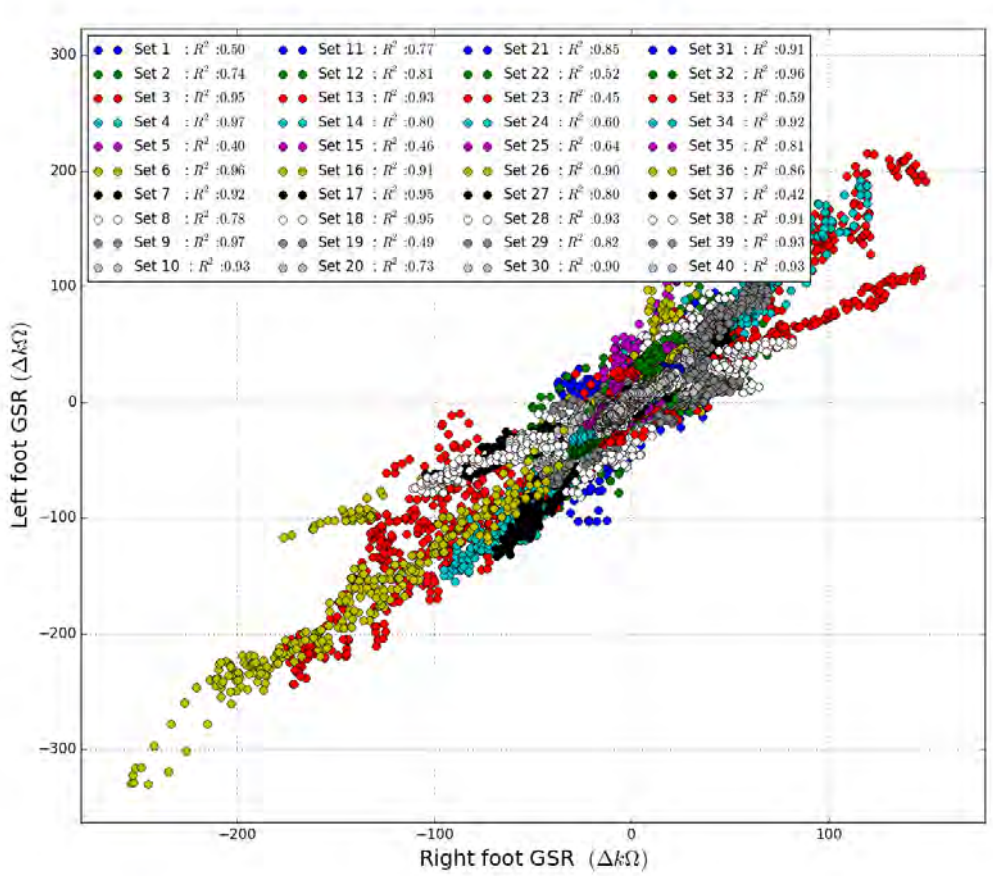

Figure 4.15: GSR through socks all data, BP filter 0.002 - 1.9 Hz. Four sets of 10 data sets taken at 10:50 am, 13:30 pm, 14:41pm, 16:45pm on the same day. $R^2_{Average} = 0.78$

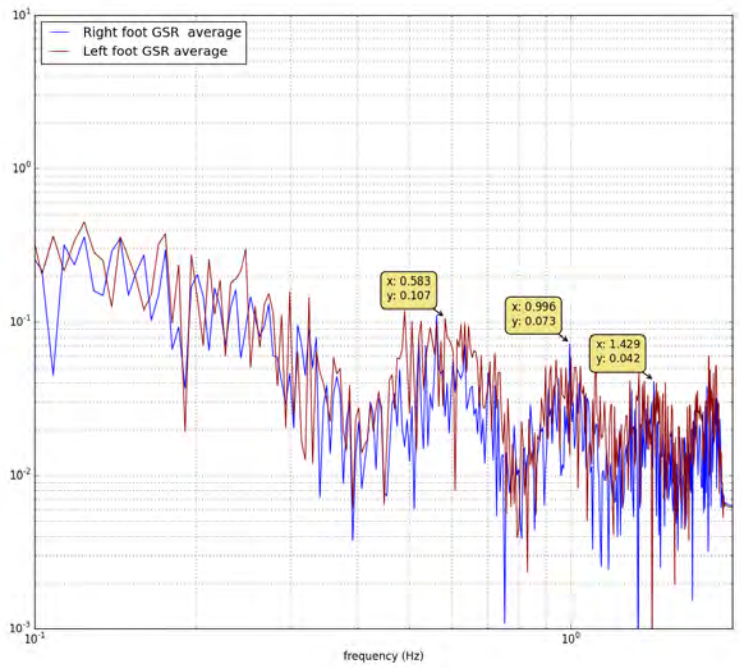

Figure 4.16: GSR through socks all data FFT, BP filter 0.002 - 1.9 Hz. FFT for Four sets of 10 data sets taken at 10:50 am, 13:30 pm, 14:41pm, 16:45pm on the same day.

4.6 Summary

In this section a typical process of sensor development has been demonstrated that was replicated for other sensor modalities. The development of test protocols, data conditioning and data analysis are shown together with the presentation of sensor data. Other sensor modalities were developed using similar processes during this project.

The following effects have been demonstrated:

- Coherence of GSR between the fingers and sole of the foot.
- Intra foot GSR coherence.
- The effect of caffeine on GSR coherence.
- GSR through socks.
- Heart rate measurement

The effect of caffeine on GSR coherence and the measurement of GSR through socks is novel.

Chapter 5

Platform build, experimental design and validation testing

5.1 Introduction

In this section we consider the configuration and validation of the experimental platform followed by the experimental design. Data and analysis from 3 volunteers is given to demonstrate the working system. The device incorporates metrics including temperature, humidity, applied force, acceleration, rotation rate, GSR and capacitively coupled bioimpedance as a means of measuring inflammation believed or likely to be useful in the detection or prediction of ulceration as a means of establishing a baseline multivariate data set [19, 21, 55, 140]. The sensors and instrumentation were mounted on each foot with data transmitted via Bluetooth to a Raspberry Pi single board computer (SBC) acting as data acquisition controller and user interface. The implementation of wireless technology enables the devices' use in many environments such as the laboratory, home, clinic, gymnasium or sports field without the incumbent trip hazard associated with wired sensors. The device is not limited to the observation of diabetic feet but holds promise for the monitoring of other conditions, non medical investigations such as sport optimisation or sensor testing.

The data acquisition system comprises five separate components with either wired or wireless interfaces dependent on function and physical location. Figure 5.1 shows the use of the Raspberry Pi operating as the master controller to capture both in-shoe, environmental and bioimpedance measurement devices while table 5.1 presents the chosen sensors. This design has been published in a special *Raspberry Pi* edition of *electronics*.

5.2 System modules

5.2.1 Master controller

Master control, see Figure 5.1 – module 1, Raspberry Pi 2 model B V1.1 SBC performs data acquisition, control, formatting and recording. The Raspberry Pi was chosen due to the low cost, availability, connectivity and the native python support. It is also notable that bluetooth integration on the Raspberry Pi was considerably more reliable than either an Apple or PC. Both the Apple or PC failed to reliably switch between bluetooth channels at the frequency required. Utilising the Raspberry Pi allowed the rapid development and deployment of the data acquisition system in a cost effective package.

Ambulatory data was gathered from the environmental monitor first, see figure 5.1– module 2, followed by the left foot, module 3, and then right foot, module 4, in shoe monitors with a single CSR 4.0 Bluetooth device being utilised to communicate with the in shoe sensors. With biological frequencies of interest being below $1.5Hz$ (heart rate while walking) [133] we utilised a sampling frequency of $20Hz$ to enable the gathering of larger data sets with the available hardware. With all biological frequencies of interest and step frequencies being less than $2.0\,\mathrm{hertz}$ sampling at $20\,\mathrm{hertz}$ allows limited over sampling of data without excessive data storage overhead. The frequency chosen is hence considered to be a pragmatic choice. Inputs were low pass filtered at $10Hz$ to obey the Nyquist sampling theorem, hence preventing aliasing while retaining valida data for the chosen sampling frequency. Utilising this sample frequency any signal of less than $10Hz$ can be accurately reproduced.

Bioimpedance data was gathered directly from the bioimpedance sensor, module 5, at 20 Hz.

5.2.2 Environmental monitor

The environmental monitor, see Figure 5.1 – module 2, controlled event timing for all data collected while providing environmental temperature and humidity monitoring for the test environment. Temperature and humidity were monitored by an HYT271 sensor locally controlled by a dedicated Arduino Nano with USB connection to the controller.

5.2.3 Humidity and temperature validation for in shoe and external environmental monitoring

The HYT271 combined humidity and temperature probe was chosen for in shoe and external environmental monitoring for the small package size and I^2C connection. This was provided with a $-40\ to + 125$°C and $0 - 100\%\ RH$ with a claimed calibration of $\pm 1.8\% RH$ and ± 0.2°C.

Temperature validation was undertaken in a proportional integral derivative

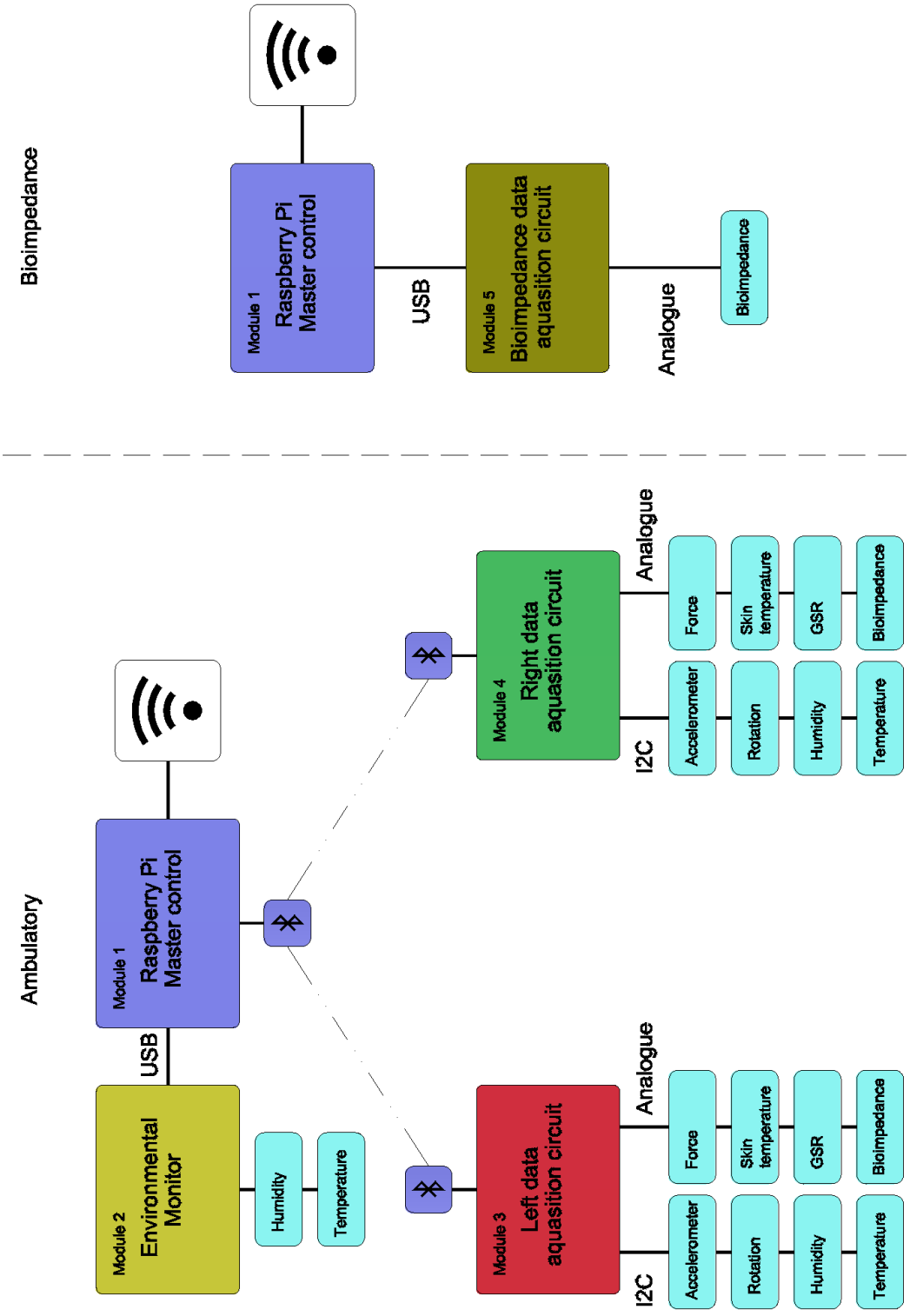

Figure 5.1: Ambulatory and bioimpedance data-capture schematic

control (PID) controlled oven in which sensors were compared to a calibrated Pico Technology PT104. An off the shelf PID controller was selected to provide stable temperature at the set points and gains where automatically set by the unit. Sensors

Sensing modality	Part #	Manufacturer	Interface	Range	Units	Calib. or valid.
Accelerometer	MPU6050	Invensense	I^2C	$\pm$ 16	g	Valid.
Rotation	MPU6050	Invensense	I^2C	$\pm$ 2000	°s	Valid.
Humidity	HYT271	Hygrochip	I^2C	0–99	% RH	Valid.
Temp. environ	HYT271	Hygrochip	I^2C	-40 – 125	°C	Valid.
GSR	—	Self built	Analogue	0 – 5000	kΩ	Valid.
Bioimpedance	AD9850	Analog –	Analogue	0 – 1023	AU	Valid.
	AD8302	Devices	Analogue	0 – 1023	AU	Valid.
Force	A401-25	Flexiforce	Analogue	0-140	N	Calib.
Temp. skin	104JT-25	ATC-Semitec	Analogue	20 – 40	°C	Calib.

Table 5.1: Sensor table

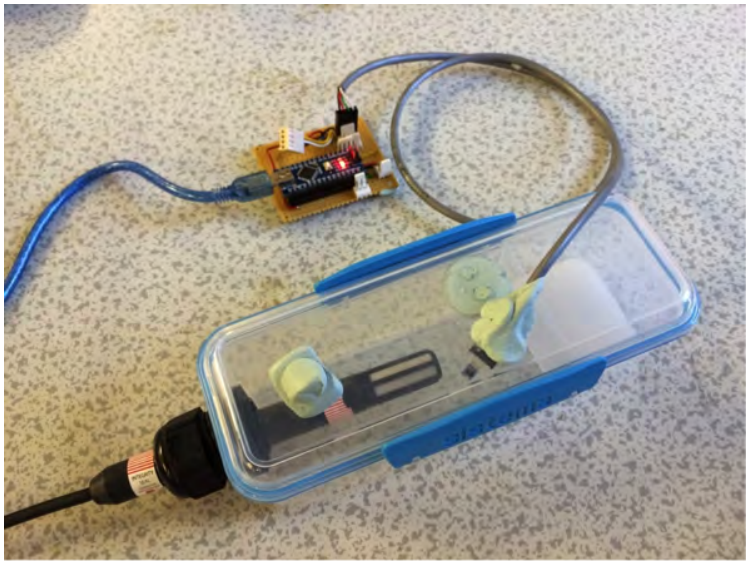

Figure 5.2: Humidity test cell. Calibrated Hygrowin temperature and hygrometer, HYT271 connected to the prototype board for output monitoring by P.C. Saturated aqueous NaCl solution producing 73.5% humidity.

were tested at ambient temperature, ≈ 30 and $\approx 38\,^{\circ}\mathrm{C}$ with a $\pm\ 0.5\,^{\circ}\mathrm{C}$ error being accepted.

Humidity validation was undertaken using a small humidity chamber in which sensor output was compared to a calibrated Rotronic HygroWin HC2-Win-USB humidity probe. Sensors were tested in ambient conditions, 2% and $73.5\%RH$ with a $\pm 2.0\%$ error being accepted. Desiccated colloidal silica gel and saturated NaCl water solution were used to generate the respective reference conditions as shown in Figure 5.2. A failure rate of 10% was experienced on parts supplied.

5.2.4 In shoe data acquisition circuit

The left and right data acquisition circuits, see Figure 5.1 – modules 3 and 4, – are controlled by dedicated Arduino Nano processors with blue tooth connection to the master controller. A custom PCB was designed to provide connectivity and signal conditioning for the sensors with the sensor modalities noted in Figure 5.1 and table 5.1. The I^2C sensors for temperature, humidity, acceleration and rotation were wired to a micro USB connector for robustness also allowing the flexibility to re-configure the sensors if required. The accelerometer and gyrometer unit was mounted adjacent to the lateral talocrural (ankle) joint so as to reduce the risk of being struck by the opposing foot.

Data acquisition, as previously stated, was controlled by the Raspberry Pi SBC that requested the environmental data from 'module 2' environmental monitor. The environmental monitor was configured to transmit data at $20Hz$ providing a data acquisition clock cycle of the same frequency. Once this was received the left, then right, in shoe data was requested in turn. Each in shoe data system (module 3 and 4) transmitted the data from the previous data collection cycle as a single concatenated data string prior, to gathering the subsequent data set. Each data set included time stamp, environmental monitor output, module time stamp and accelerometery data. To this either 5 seconds of bioimpedance data was added or $55s$ of skin temperature, force, GSR, in shoe humidity and temperature. This strategy maximised the data collection rate.

5.2.5 Foot mounted sensor array

The bioimpedance, force, skin temperature and GSR sensors were designed as a FPC as shown in Figure 5.4 with the circuit produced by electroless copper plating on Polyethylene Terephthalate (PET) film. This enabled the fitting of sensors inside the shoe maintaining comfort of fit and flexibility while minimising cost. The completed sensor assemblies where laminated to protect the sensors and tracks in proprietary polypropylene laminating pouches. The sensors for force, skin temperature and GSR were also built in a multi-strand wire configuration for flexibility of sensor positioning shown in Figure 5.5 alowing greater flexibility when positioning sensors and durability.

Early testing of the FPC devices revealed a lack of durability in the technology. Three methods of connecting the sensors to the FPC were attempted and all failed. The first method utilised low temperature solder *Nordson SOLDERSN42T3NC-D500A* as recommended by the FPC manufacturer (Conductive Inkjet Technology) and the second utilised *ITW Chemtronics CW2400* conductive epoxy. These systems caused the connection to fail as local stiffening of the FPC at the joint promoted track failure as shown in Figure 5.6. The third method utilised an anisotropic conductive tape *3M 9703-33X25* which failed when the bond pealed apart. This failure did

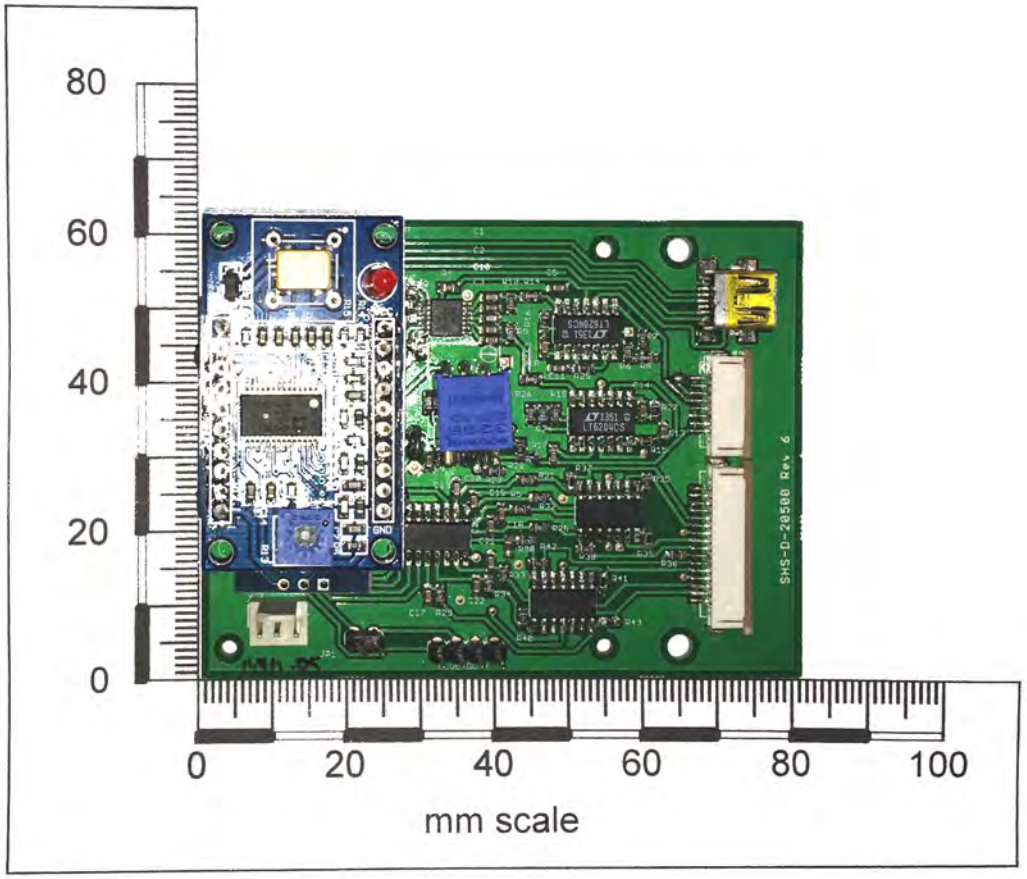

Figure 5.3: Sensor circuit

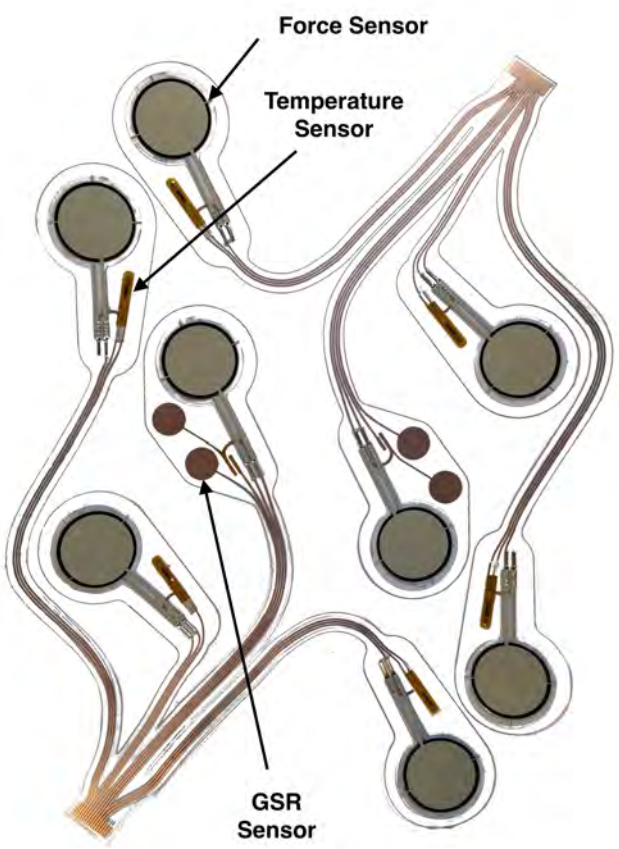

Figure 5.4: FPC populated

not cause track failure and would 'self heal' in use see Figure 5.7 enabling the sensor to regain a working state when the joint was re-compressed, though the sensors would always remain unreliable. The FPC circuits had a failure rate of 47.6% against a 21.9% for the wired sensors.

5.3 Sensor interface circuit design and assessment

Devices that were pre-calibrated at manufacture were validated to ensure conformance to expected performance criteria. Those that were not required calibration (see table 5.1) for further details. The following section provides an over view of the procedures used.

5.3.1 Acceleration

The acceleration sensing range was set at $\pm 16g$, utilising a 16 bit resolution a 0.000488g measurement resolution was achieved. The digital low pass filter was set at 10 Hz

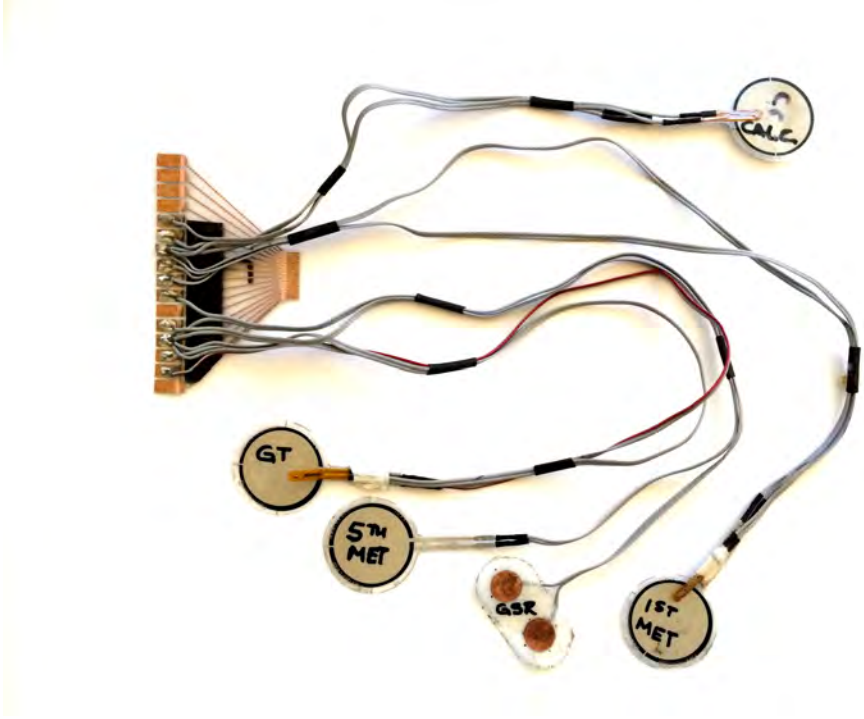

Figure 5.5: Wired sensor set

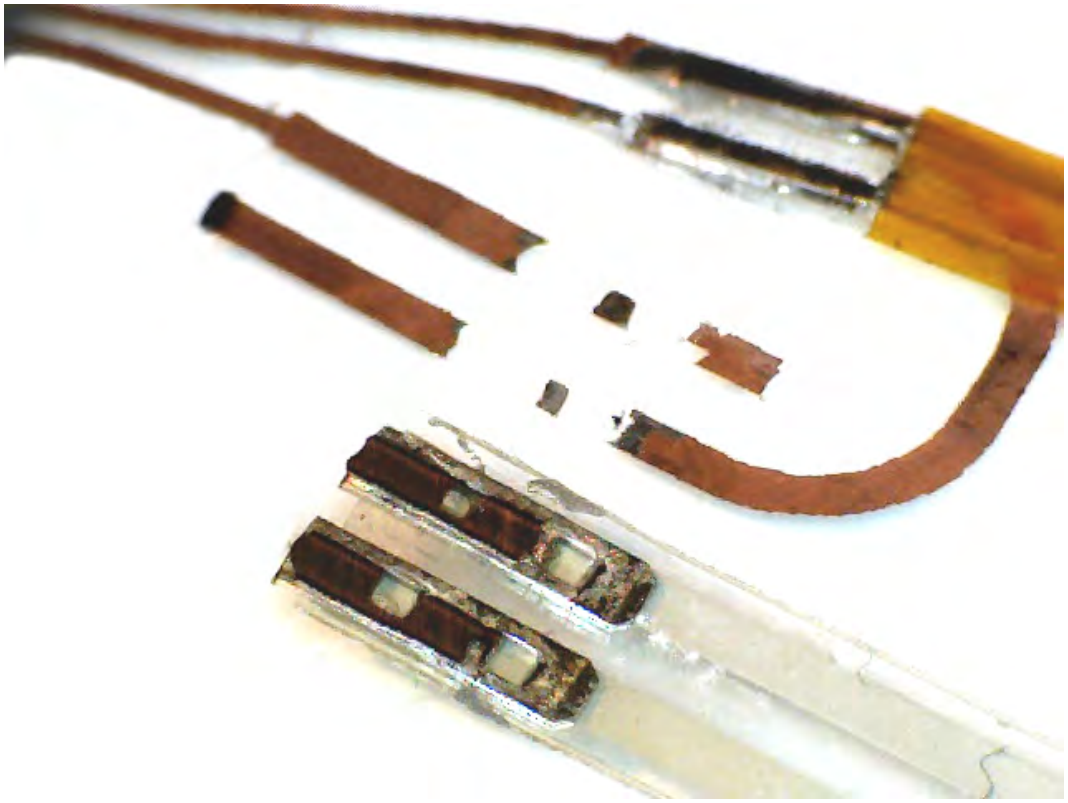

Figure 5.6: FPC track failure

utilising the libraries developed by Haq [141] .

Acceleration validation was performed by presenting each axis of the sensor to

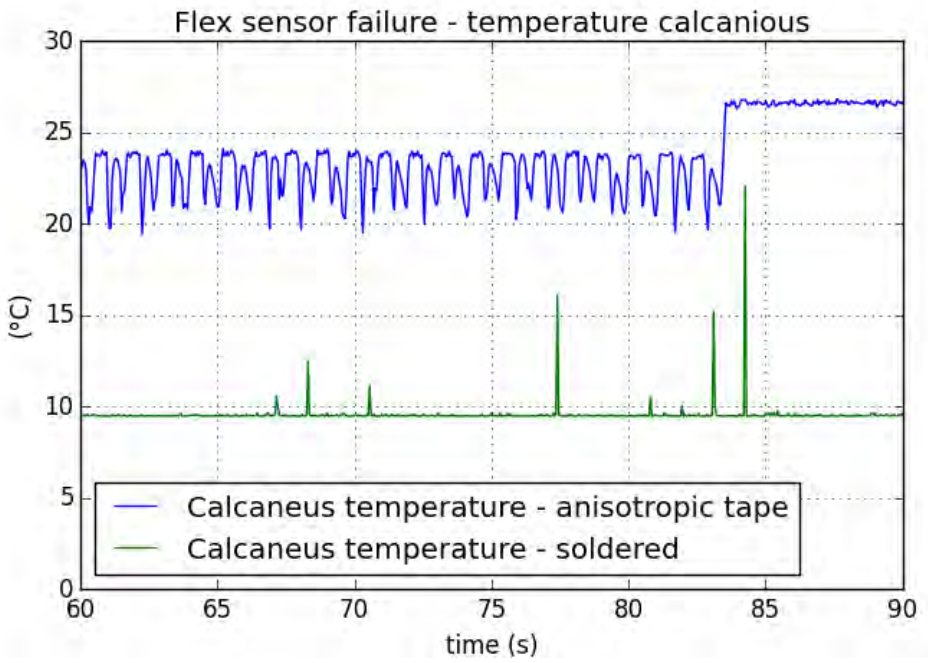

Figure 5.7: FPC failure - stiff sensor contacts cause delamination of the tracks from the substrate. The presented failure mode is typical of both conductive epoxy and soldered connection of the sensors to the substrate both sensors, were exposed to 27°C.

accelerations of $+1$g, 0g and -1g utilising the reference block shown in Figure 5.9 as demonstrated in section 3.5 errors of $\pm 0.05g$ were accepted. Th block provides reference angles through which to rotate the sensor device. Each axis should achieve +1g, 0g and -1g during this test cycle. However the investigator may need to allow for mounting errors on the accelerometer chip where the accelerometer axes has a fixed offset from the PCB on which it is mounted.

Validation of the on-board low pass filter was verified by changing the filter cut off frequency while exciting the accelerometer with a mechanically coupled 44 Hz input frequency and verifying that appropriate attenuation in signal was achieved see Figure 5.10 and Figure 5.11. Ideally a variable frequency vibration source would have been utilised and filter attenuation measured against a known input. As it was not possible to arrange the use of test equipment at short notice the method described above demonstrates that the filter was operational.

N.B. sample frequency was increased to $200Hz$ to ensure Nyquist limits where observed during this test.

5.3.2 Rotation rate

The rotation rate sensing range was set at $\pm 2000°$s, utilising a 16 bit resolution a $0.031°$s measurement resolution was achieved. The digital low pass filter was set at 10 Hz utilising the libraries developed by Haq [141].

Rotation validation was performed by rotating each axis of the sensor through

Figure 5.8: Sensors fitted directly to the foot

$90°$. Integrating the rotation data with respect to time and comparing this with the known rotation angle validated rotation with $\pm 2\,°$ error accepted as demonstrated in section 3.6. This was accomplished using the same device utilised in section 5.3.1. Precise timing of the rotations is not required and axes offsets can be ignored in this validation.

Validation of the on-board low pass filter was verified by changing the filter cut off frequency while exciting the accelerometer with a mechanically coupled 44 Hz input frequency and verifying that appropriate attenuation in signal was achieved in the same manner used for acceleration.

N.B. sample frequency was increased to $200Hz$ to ensure Nyquist limits where observed during this test.

5.3.3 Analogue sensor drive circuit

All analogue sensors were driven by the same constant voltage source set at $-0.25V$ as shown in Figure 5.12.

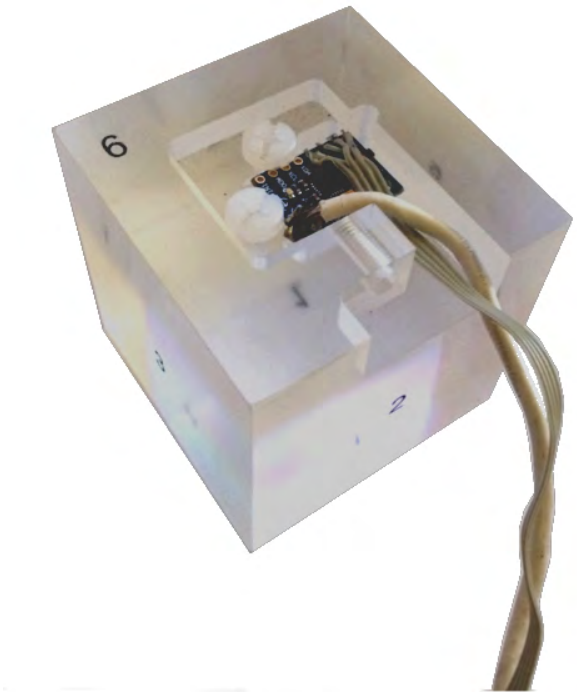

Figure 5.9: Accelerometer reference block

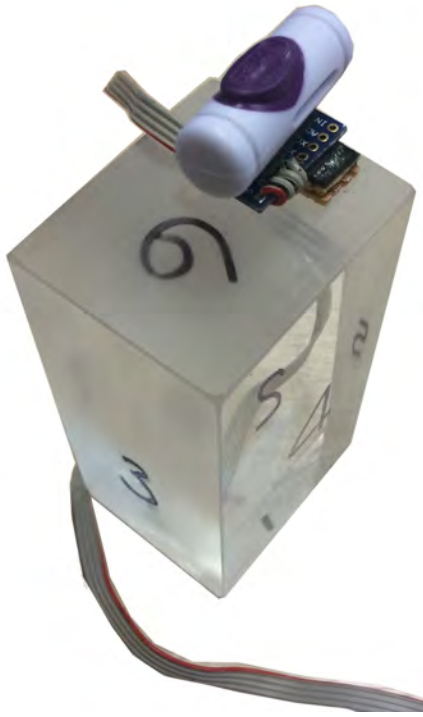

Figure 5.10: Low pass filter validation of the MPU 6050 accelerometer and gyrometer utilising a single frequency oscillator and MPU 6050 on a compliant mounting.

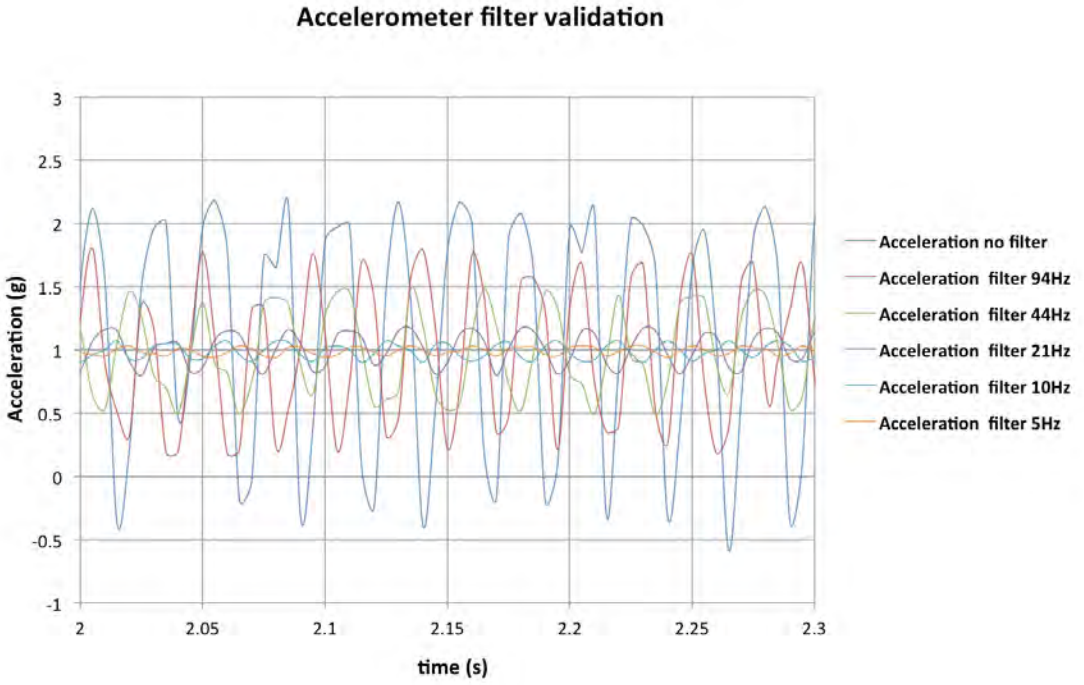

Figure 5.11: Accelerometer filter test. Excitation frequency $44Hz$, note increasing attenuation with decreasing filter cut off frequency.

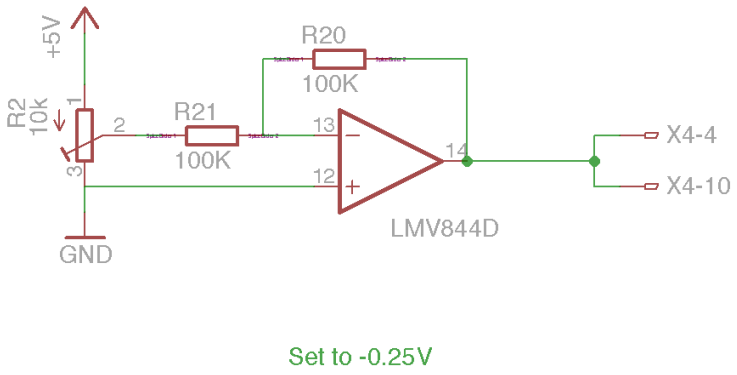

Figure 5.12: Analogue drive circuit. Force, skin temperature and GSR was driven by a $-0.25V$ source.

5.3.4 Force

Force sensing was undertaken with Flexiforce A401 sensors utilising the manufacturers suggested circuit with a $-0.25V$ sensor excitation voltage. Low pass filtering was implemented after amplification of signal as seen in Figure 5.13. A $5Hz$ low pass filter was implemented to remove noise from the signal. This enables the measurement of movement artefacts due to walking and biological signals to be visualised while removing higher frequency electrical noise.

Force trnsducers were calibrated utilising an Applied Measurements DBBSMM-

50kg-002-000 calibrated for output in Newtons. Sensors were first clamped at 170N for 5 minutes to precondition them in accordance with manufacturers instructions. Five cycles of loading with 0, 10, 20, 50, 90, 140, 90, 50, 20, 10, 0N were manually applied to the sensors. Sensor output was quadratically matched to the applied force as a means of calibration with R^2 values of higher than 0.995 obtained in all cases as seen in Figure 5.14.

Force low pass filter design

$$f_c = \frac{1}{2\pi RC} = \frac{1}{2\pi \cdot 32k\Omega \cdot 1\mu F} = 4.97Hz$$

Definitive force - resistance data is not provided for these devices. The quadratic equation from the calibration data is used to validate the resolution.

$$f(N) = -0.0003X^2 + 0.454X + 0.8005$$

Evaluating this at the lowest resolution, ADC $= 0$ to ADC $= 1$, results in a resolution of 0.45N increasing to 0.219N at ADC $= 400$. Resolution

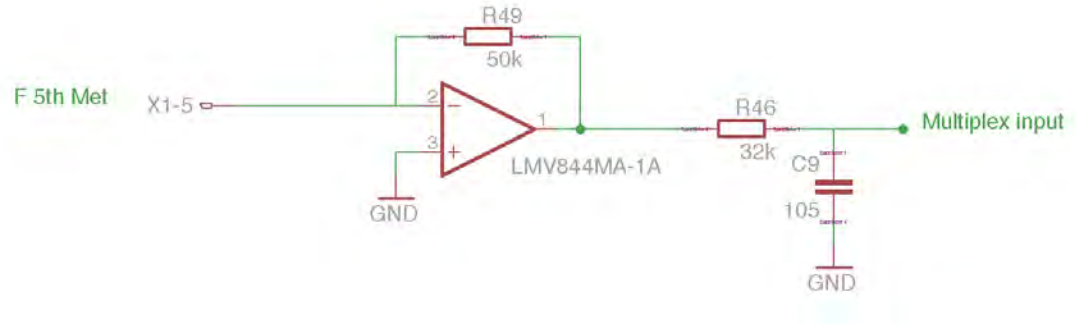

Figure 5.13: Force sensor circuit

From the data presented in Figure 5.14 it can be seen that the device as designed is using less than half the available ADC output. A typical plot of force is seen in Figure 5.28. Analysis of maximum force recorded for each sensor in the combined volunteer data reveals that the peak force recorded in over 30 data sets, 15 volunteers 4 walking exercises, was 163N with the 95^{th} percentile being 83.8N. This would indicate that the range of force sensing could be reduced to increase resolution at the cost of a small amount of out of range data.

5.3.5 Temperature - skin

The skin temperature monitoring circuit Figure 5.15 was designed to utilise 104 JT thermistors as sensors with a $-0.25V$ sensor excitation voltage and provide low pass filtering of the resultant signal. An inverting amplifier was used to invert

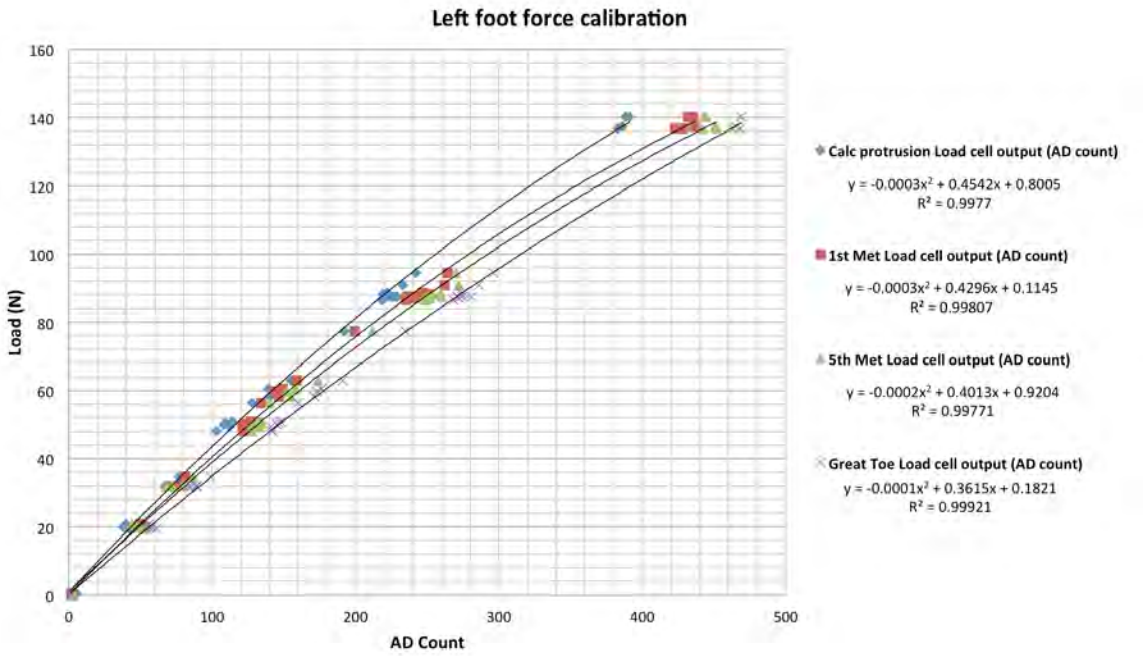

Figure 5.14: Force calibration

the negative input voltage. A $5Hz$ low pass filter was implemented to remove noise from the signal. This enables the measurement of movement artefacts due to walking and biological signals to be visualised while removing higher frequency electrical noise.

Temperature transducers were calibrated in a PID controlled oven, monitored by Pico Technology PT104 and probes calibrated by the supplier. Temperature was sequentially stabilised at room temperature(≈ 22) $and \approx 24, \approx 28, \approx 33, \approx 37\,^{\circ}\mathrm{C}$. Sensor output was quadratically matched to the test temperatures as a means of calibration with R^2 values of higher than 0.995 obtained in all cases see Figure 5.16.

Temperature low pass filter design

$$f_c = \frac{1}{2\pi RC} = \frac{1}{2\pi \cdot 32\mathrm{k}\Omega \cdot 1.0\mu\mathrm{F}} = 4.97Hz$$

The thermistor data sheet states the resistance at $30^{\circ}\mathrm{C}$ it is $78.88\mathrm{k}\Omega$ and at $40^{\circ}\mathrm{C}$ is $50.03\mathrm{k}\Omega$.

From:

$$Gain = \frac{V_{out}}{V_{in}} = -\frac{R_f}{R_T}$$

calculate the output voltages:

$$V_{out} = -V_{in} \times \frac{R_f}{R_T}$$

which results in $2.38V$ & $3.75V$ respectively. This equates to int 496 and int 782 as

the ADC output or a resolution of $\approx 0.035°C$

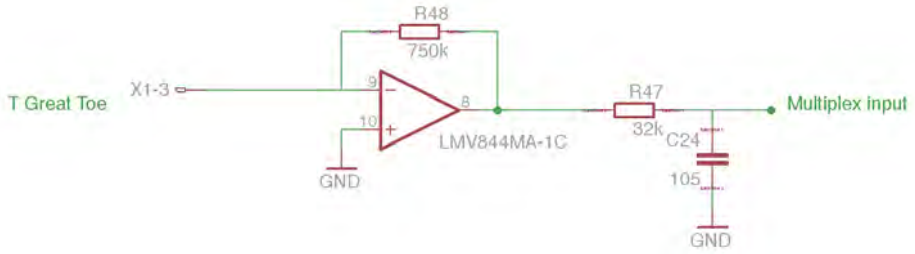

Figure 5.15: Temperature monitoring circuit inverting operational amplifier and filter.

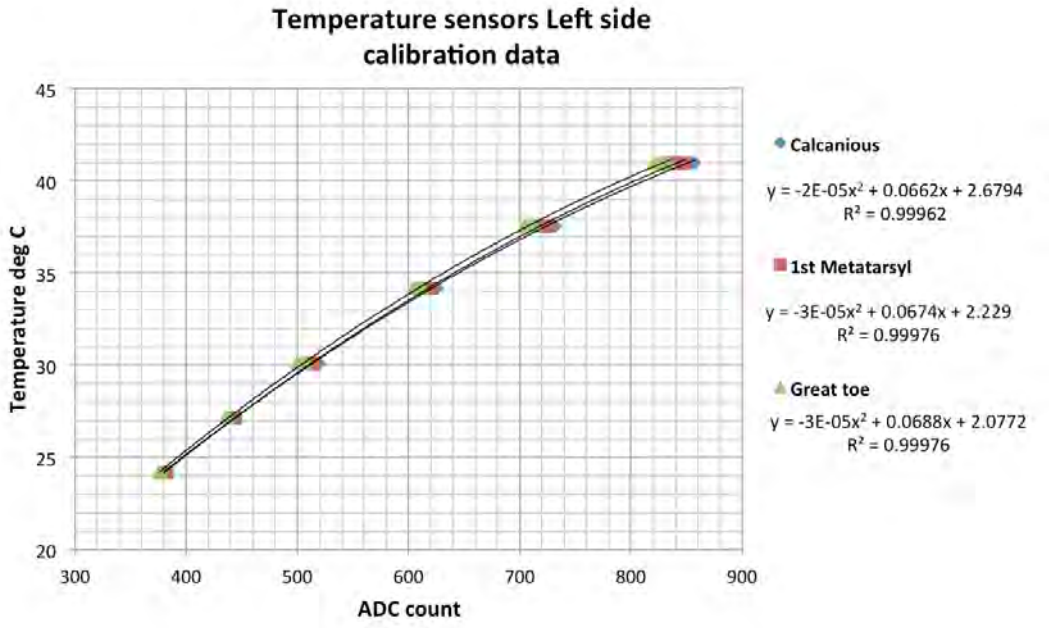

Figure 5.16: Temperature calibration data

5.3.6 GSR

The design of the GSR circuit Figure 5.17 was revised to enable the use of the reduced sensor drive voltage and provide low pass filtering of the resultant signal. An inverting amplifier was used to invert the negative input voltage. Though not ideal, as the output is non linear, this would provide adequate resolution to observe gross trends. A $2.0\,\mathrm{hertz}$ low pass filter was implemented to remove noise from the signal. This allows for elevated heart rate, with heart rate being the highest biological frequency of interest [133], while on the treadmill while reducing noise. This enables the measurement of movement artefacts due to walking and biological signals to be visualised while removing higher frequency electrical noise.

Filter design

$$f_T = \frac{1}{2\pi RC} = \frac{1}{2\pi \cdot 8.2\text{k}\Omega \cdot 10\mu\text{F}} = 1.9Hz$$

GSR was validated against reference resistances of 100 – 1000kΩ calibrated to $\pm 1\%$, a $\pm 10\%$ error was accepted. By convention electrical conductivity ($\mathrm{S/m}$) would be used for GSR but as the cell factor was unknowable due to the changing morphology of the skin as a response to exercise and/or disease state, resistance was utilised. Redesigning the electrodes for use in the combined sensor suit resulted in a reduction of contact area from $325.0\mathrm{mm}^2$ to $83.0\mathrm{mm}^2$. The cell resistance for a given resistivity is given by :

Cell resistance

$$R = \rho \cdot \frac{L}{A}$$

A = Area of electrode

L = distance between electrodes

As can be seen from the equation above a reduction in electrode area increases resistance. For the changes made during redesign measured resistance will increase by a factor of 3.87 compared to the reference data in chapter 4. This was discovered post hoc.

Defining an amplification constant to reduce processor load

$$Gain = \frac{V_{out}}{V_{in}} = -\frac{R_f}{R_{skin}}$$

$$R_{skin} + R_{Ilimit} = -\frac{V_{in}}{V_{out}} \times R_f$$

However V_{out} is measured as the product of the ADC measured input and the reference voltage.

$$V_{out} = \frac{\text{ADC}}{1023} \times V_{ref}$$

$$R_{skin} + R_{Ilimit} = \frac{\frac{-V_{in}}{V_{ref}} \times 1023 \times R_f}{\text{ADC}}$$

$$\text{GSR}_s = R_f \times 1023 \times \frac{-V_{in}}{V_{ref}}$$

Defining GSR_s in terms of the ADC output provides a computationally efficient means of calculating skin resistance.

$$R_{skin} = \frac{\text{GSR}_s}{\text{ADC}} - 51\text{k}\Omega$$

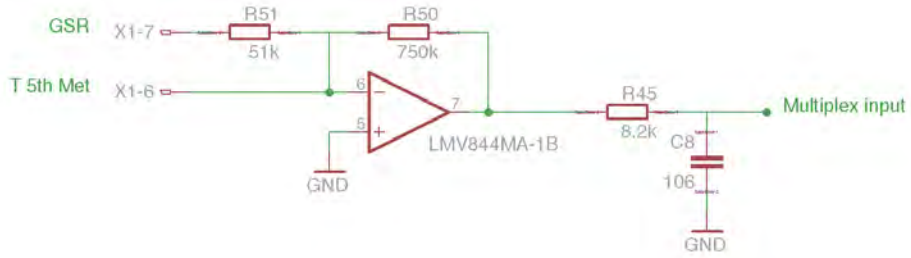

Figure 5.17: GSR circuit. This circuit can be configured for either GSR or temperature measurement by defining appropriate outputs from the sensor array.

5.3.7 Bioimpedance circuit and sensor

The bioimpedance, block diagram Figure 5.18 and circuit Figure 5.19 comprising a direct digital synthesis (DDS) device to generate the desired signal, signal conditioning circuit with bandpass filtering and signal amplification, a capacitive printed sensor and a phase/gain analyser was built into the in shoe monitoring circuit. The DDS was an AD9850 from analogue devices controlled by serial communication. The device was purchased ready mounted to a development board with a precision $125\text{M}Hz$ reference crystal with a stated output for the device of $0 - 40MHz$ with a resolution of $0.0291Hz$. An analogue devices AD8302 phase gain analyser was utilised to analyse the relationship between drive and signal. Gain of $\pm 30\text{dB}$ is output as $0 - 1.8V$ measured over 10bit ADC for a resolution of 0.059dB. Phase of $0°to180°$ is output as $0 - 1.8V$ measured over 10bit ADC for a resolution of $0.176°$. A phase of $180°to0°$ would be output over the same range, this is not distinguishable from a phase of $0to180\,\text{deg}$ as an output. As the device is measuring impedance comprising resistive and capacitive elements and in line with existing literature output is expected to lag rather than lead the input signal.

The output from the AD9850 DDS was amplified by a factor of 2 utilising a non inverting operational amplifier LMV844MA. Frequency response was tested at $100 - 1000\text{k}Hz$ at $100\text{k}Hz$ intervals. Figure 5.21 shows the AD9850 DDS output signal/ amplifier input was consistent over the frequency range tested. The output of the LMV844MA amplifier was not consistent over the frequency range. At frequencies over $300\text{k}Hz$ output tended towards a triangular wave form with an associated attenuation in output voltage to 0dB at $1000\text{k}Hz$. This is in variance to the datasheet for the LMV844MA which claims a gain of 10dB at $1000\text{k}Hz$ is possible.

Signal conditioning was implemented using an LT6204D operational amplifier for the phase gain detector, see Figure 5.19. Drive and return signal paths were

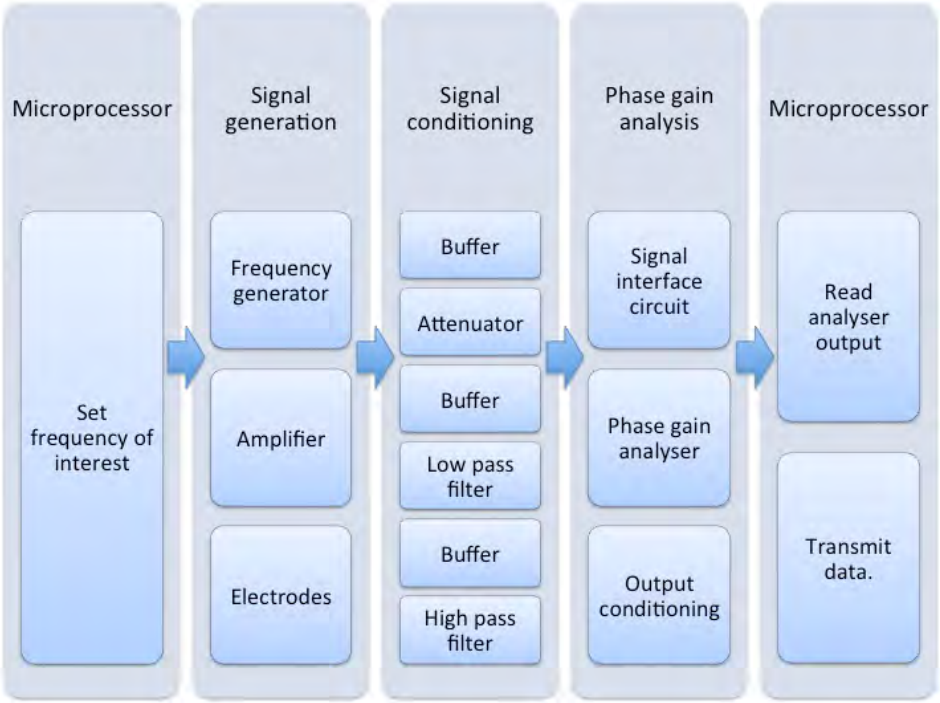

Figure 5.18: Bioimpedance block diagram defining major blocks and sub processes.

identical in design. All stages were configured as buffers. The first buffer acted as input to a 2:1 attenuator. This configuration was chosen allowing the possibility to remove attenuation in the return signal path to increase relative signal strength if required. The attenuated signal was fed into the second buffer before passing into the low pass filter with a cut off frequency of $1.9\mathrm{M}Hz$. The filtered signal passed through the third buffer prior to passing through the high pass filter set at $1.44\mathrm{k}Hz$. A final 2:1 attenuator was utilised after the final buffer to enable gain adjustment if necessary after further testing. Inputs to the phase gain analyser were capacitively coupled using $100\mathrm{pF}$ capacitors on all inputs.

The bioimpedance sensor was designed as a disposable unit, see Figure 5.20. The electrodes were printed on $125\mu\mathrm{m}$ Polyethylene Terephthalate (PET) film followed by electro-less copper plating of the final conductors. The sensor was then laminated between $75\mu\mathrm{m}$ polypropylene films prior to being trimmed to size. Physical size was reduced from the prototype to aid the fitting of other sensors.

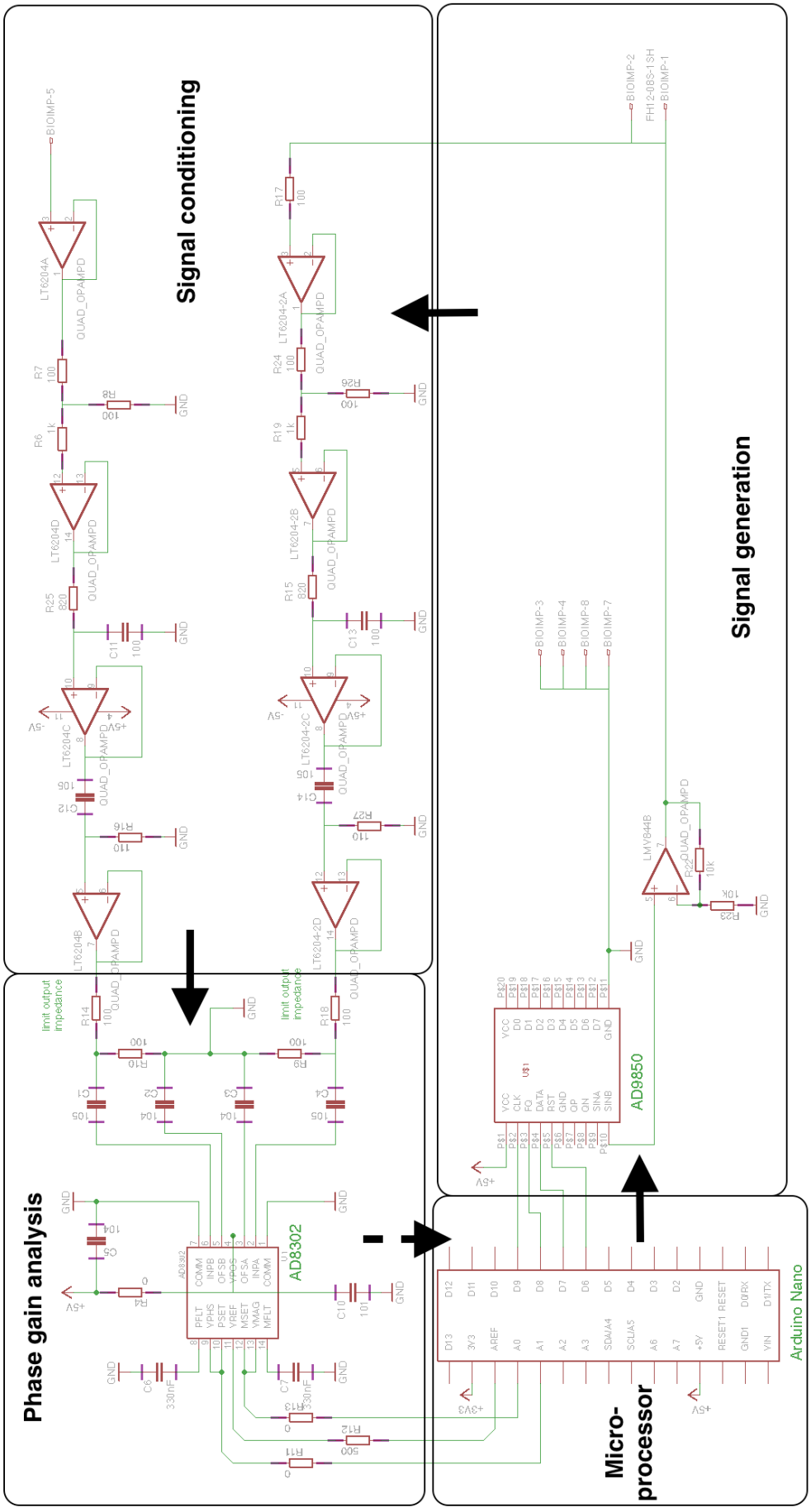

Figure 5.19: Bioimpedance circuit

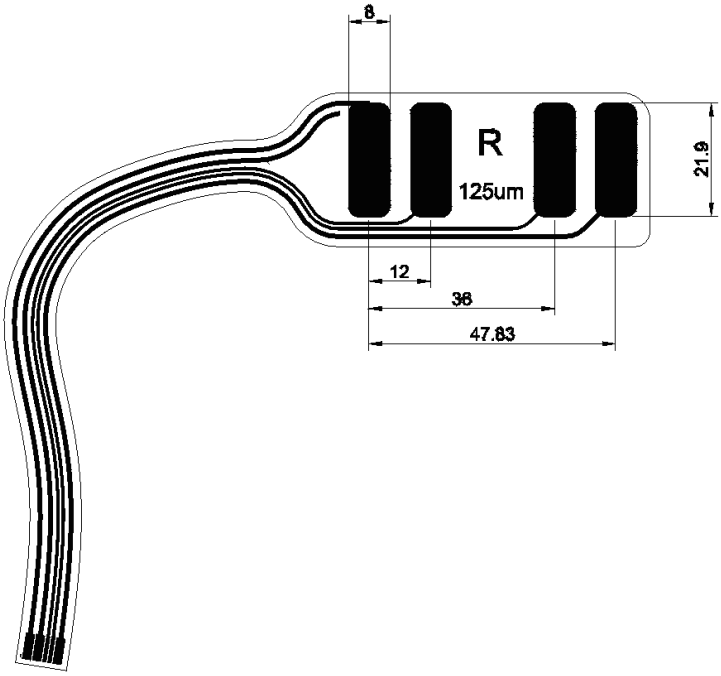

Figure 5.20: Bioimpedance sensor

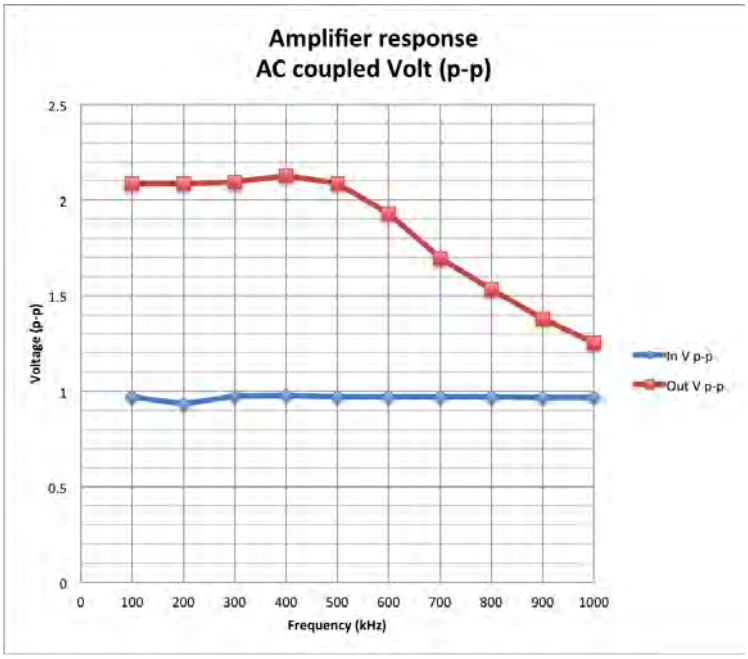

Figure 5.21: Test of bioimpedance frequency generation AD9850 and LMV844 amplifier circuit.

Capacitance

$$C = K \times E_o \times \frac{A}{D}$$

$$K = 2.26$$

$$E_o = 8.85419 \times 10^{-12} \frac{\mathrm{F}}{\mathrm{m}}$$

$$A = 175\mathrm{mm}^2$$

$$D = 0.075\mathrm{mm}$$

$$C = 47\mathrm{pF}$$

Current

As the circuit has changed from that used during early testing the applied current should be re-examined. The safe A.C. exogenic current limit of $100\mu A$ should not be exceeded. The analysis will ignore the bodies contribution to impedance and investigate the worst case. The circuit comprises two $107pF$ capacitors in series driven at $\pm 1.0V$ at frequencies given below.

$$X_c = \frac{1}{2\pi fC}$$

$$f = frequency Hz$$

$$f_{min} = 100\text{k}Hz$$

$$f_{max} = 1\text{M}Hz$$

$$X_{c(100\text{k}Hz)} = 33.9\text{k}\Omega$$

$$X_{c(1\text{M}Hz)} = 3.39\text{k}\Omega$$

Allowing for two capacitors in series

$$I_{100\text{k}Hz} = \frac{V}{R} = \frac{1.0V}{2 \times 33.9\text{k}\Omega} = 14.7\mu\text{A}$$

$$I_{1\text{M}Hz} = \frac{V}{R} = \frac{1.0V}{2 \times 3.39\text{k}\Omega} = 147\mu\text{A}$$

The capacitively coupled bioimpedance circuit integrated into the in shoe data acquisition circuit was utilised for stand alone bioimpedance testing. Capacitive coupling was chosen as it ensures that DC is eliminated and consequently no unresolved polarisation of the tissues occurs and removes the need for conductive gels or invasive contact mechanisms. The software was reconfigured to output only bioimpedance data and control the sample frequency to 20Hz. Sensitivity tests where undertaken to investigate the devices ability to differentiate between the states of no load, dead tissue and living tissue the results of which are presented in Figure 5.22 and the ability to detect changes in the concentration of capacitively coupled conductive solutions, presented in Figure 5.23.

Analysis of the spice model — Appendix B.3 revealed that the voltage attenuation between input and output circuits varies between -7.97 to -6.41 dB over the frequency range 100 - 1000kHz. The phase shift is 32.33 at 100kHz decreasing to 4.15 at 1000kHz according to the equation $\theta = 994016 f^{-0.896}(kHz)$. Spice analysis output — Appendix B.4

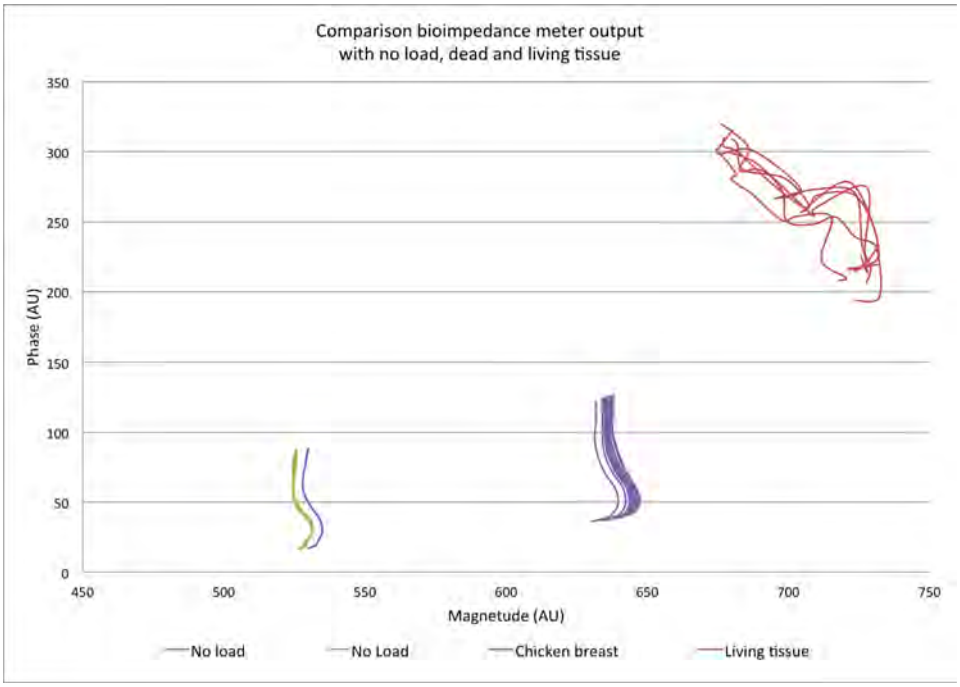

Figure 5.22: Bioimpedance comparison sensor tissue comparison. The impedance sensor on a glass surface signal was examined with no load on the sensor, with $250\,\mathrm{g}$ or raw (Tesco premium) chicken breast and finally the palm of the authors hand. Clear changes in output can be seen in the data presented with each state being clearly discernable form the next. Noise in the living tissue is likely to be the result of blood flow.

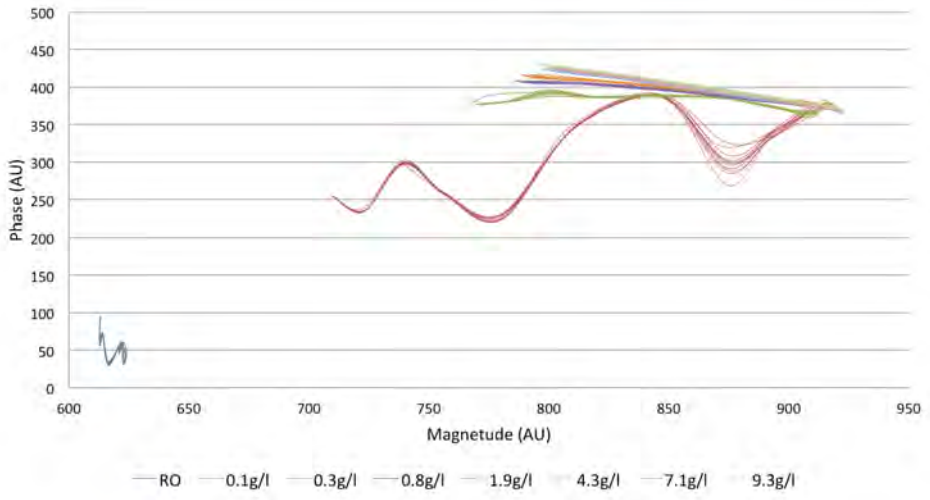

Figure 5.23: Bioimpedance saline sensitivity test. Varying the concentration of saline in RO water within a fixed cell polythene cell $95 \times 60 \times 30\mathrm{mm}$ deep $110\mu\mathrm{m}$ film. The device demonstrates high sensitivity at low NaCl concentrations becoming less sensitive with increased NaCl.

Bioimpedance calibration

Bioimpedance excitation signal was validated against a Picoscope 2206A oscilloscope over the frequencies of 5, 10, 20, 100, 400, 700, 1000 kHz at a voltage of ± 2.0 V (peak-peak). Signal analysis was validated against a dual channel direct digital synthesis (DDS) signal generator (UDB1300), providing artificial excitation and sensor signal, monitored with a Picoscope 2206A oscilloscope. The on board signal output amplifier was temporarily disconnected. The excitation signal was set at ± 1.73V(peak-peak) with a sensor signal of ± 0.09V(peak-peak). For each frequency of 5, 10, 20, 100, 400, 700, 1000 kHz the phase was changed through the range 0, 45, 90, 135, 180, 225, 270, 315, 360 degrees and output recorded. As can be seen in Figure 5.24 the gain response is linear over phase and frequency at approximately 1% of full scale deflection over the range 100 – 1000 kHz. For frequencies lower than 100 kHz the response is non linear in both phase and gain. This is a function of the phase gain analyser input capacitors which would need to be resized to investigate lower frequencies. A similar effect can be seen in phase Figure 5.25 which again occurs below 100 kHz. Output was left in 10bit format without calibration to enable the collection of data over a broad range of frequencies. This approach allows greater variation in measured frequency with frequency specific calibration applied post hoc where required.

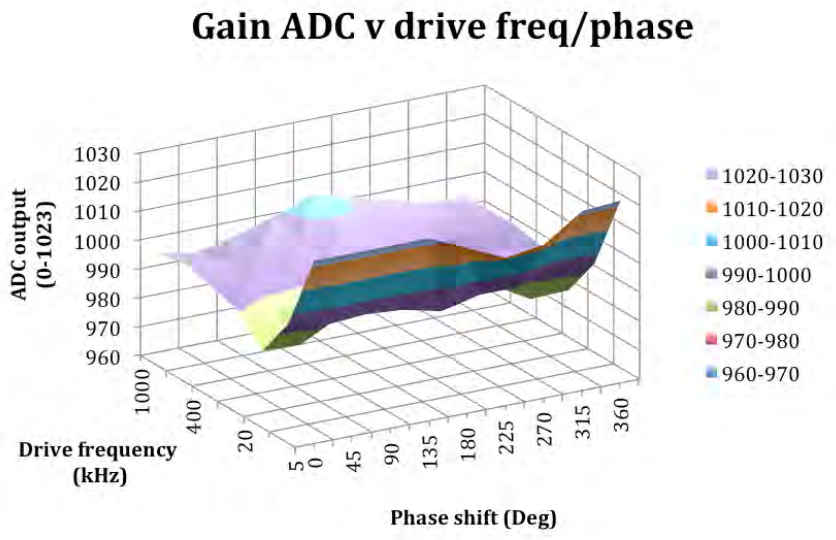

Figure 5.24: Bioimpedance calibration - effect of drive frequency and phase change on measured gain. Gain measurement is constant, 990 – 1010 from 100 – 1000kHz, though an inflection in the data is clearly visible showing the output to be non linear below this range.

The bioimpedance sensor was attached to the foot sensor map mounted on a toughened glass plate for stability. Batteries were fitted to the sensor circuit which was connected to the Master control via USB cable see Figure 5.1.

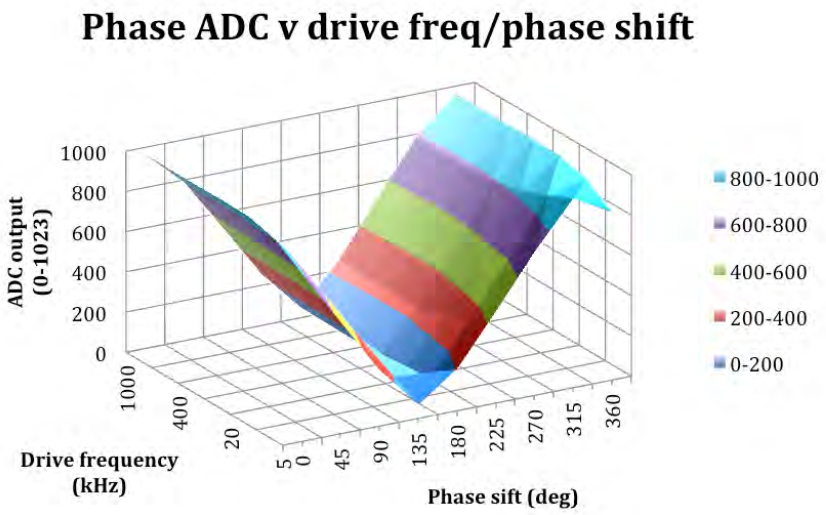

Figure 5.25: Bioimpedance calibration - effect of drive frequency and phase change on measured phase. Phase measurement is proportional to the phase from 100 – 1000kHz, below this range a perturbation is seen that increases with decreasing signal frequency.

5.4 Sensor evaluation

To fit the sensors in the correct anatomical positions a sensor map was generated for each of the volunteers feet on PET film. Sensor positions were established for the calcaneus, 1st metatarsal, 5th metatarsal and the pad of the great toe by palpation and transferred to the map using soft coloured wax. The calcaneus force sensor was positioned so as to detect heal strike while all other force sensors were positioned under the local load centre. Temperature was sensed adjacent to the force sensor on the calcaneus, 1st metatarsal and great toe while GSR was fitted behind the 5th metatarsal with bioimpedance sited between the 1st and 5th metatarsals over a sensed area 22mm wide x 55mm long. The sensors were mounted on zinc oxide tape as shown in Figure 5.26 prior to aligning the foot to the map and taping the sensors into position as seen in Figure 5.8. Shoes were then fitted to the volunteer and the appropriate (left/right) data acquisition circuit installed over the dorsal surface of the foot. The footwear chosen for the task were walking sandals which provide a secure fit while maintaining access to the insole for fitting sensors with multiple access points for wiring. Having fitted the footwear the system was allowed to stabilise for a period of 5 minutes, during which time the volunteer was seated and data was recorded to demonstrate that the system was operational.

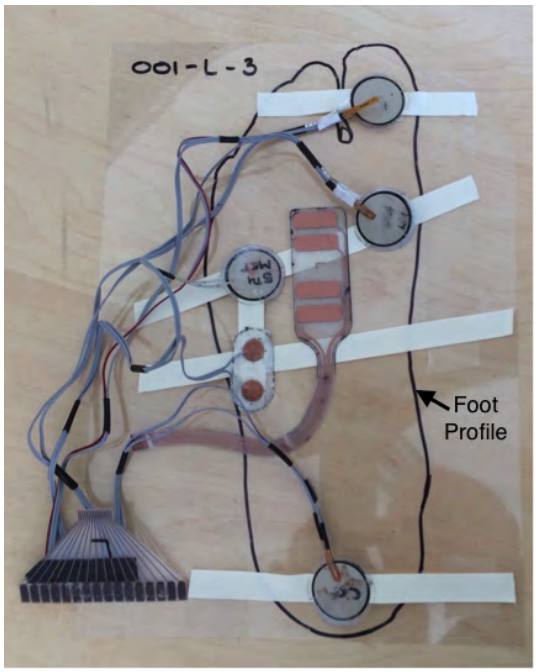

Figure 5.26: Sensor layout over the foot profile. Force and temperature sensors are positioned over the calcaneus (heal), great toe, 1st metatarsal (joint at the base of the great toe), 5th metatarsal (joint at the base of the small toe). GSR can be seen below the 5th metatarsal force sensor with bioimpedance placed mid foot

5.5 Test protocol

5.5.1 Laboratory setup

All testing was undertaken in the same laboratory setup in an office environment with temperature kept above 21 °C. No air conditioning or humidity control was available. A JLL S300 digital treadmill was used to control walking speed with the platform horizontal. A Tanita segmental body impedance scale BC-545N was used to characterise volunteers' body types. Resting blood pressure was obtained with a Kodea KD202F automatic blood pressure cuff with heart rate and SPO2 obtained using a Contec Pulse Oxymeter CMS50DL. Occlusion of blood supply to the leg was effected with an A&D Medical UM101 sphygmomanometer and Banmanometer V-Loc pressure cuff manually inflated by hand pump. The study protocol was approved by the University of Southampton ethics committee (ID: 8997) and conformed to the principles outlined in the Declaration of Helsinki. All participants gave their informed consent to participate in the study. All data were stored in an open format.

5.5.2 Test setup

Basic biometric data was gathered from each volunteer including: age, gender, blood pressure, height and weight. The volunteer then walked on the treadmill

Test	Exercise	Description
1	Stand 1	free standing
2	Sit 1	sitting in a rigid office chair
3	Walk 1	walk at 2.0k m/h on the treadmill
4	Walk 2	walk at 4.5 km/h on the treadmill
5	Stand 2	free standing
6	Walk 3	walk at a self-selected pace
7	Walk 4	walk at a self-selected pace
8	Stand 3	free standing
9	Sit 2	sitting in a rigid office chair

Table 5.2: Test table

in their own footwear for $4\mathrm{min}$ to acclimatise prior to fitting the sensors and sandals. After fitting, the sensors were allowed to stabilise for a period of $5\mathrm{min}$ with the volunteer seated prior to testing.

5.5.3 In shoe testing

A sequence of 9 tests were undertaken to characterise the in-shoe conditions for the events shown in Table 5.2. For each test 200 s of data was captured on the Raspberry Pi master controller to ensure 3 x 60s data cycles were acquired per test.

5.5.4 Bioimpedance testing

Two bioimpedance tests were undertaken on each foot utilising a range of 100 – 1000 kHz at 100kHz increments. The first investigated the sensors ability to differentiate between unloaded, lightly loaded and standing load on the sensor. For this each volunteer placed a foot on the sensor 10 s into the test while seated, then standing at 100 s with weight evenly distributed between both feet, the test concluding at 200 s. The second test investigated the difference between occluded and non occluded blood flow. We utilised this test to increase fluid load to the tissue hence creating a perturbation in the balance of resistive and capacitive conduction pathways. The volunteer was seated and a pressure cuff placed around the upper thigh of the leg to be tested, data recording was started, with the foot placed on the sensor after 10 s. The cuff was manually inflated to 20 mmHg above the volunteers systolic pressure 70s after the start of data recording and maintained for 60 s before rapid deflation. 500 s of data were collected during this test.

5.6 Results and Discussion

The following section presents illustrative results to demonstrate the system measurement capability. From this data it is possible to elucidate the relationship be-

tween events measured with different sensors or modalities for example vertical acceleration in opposing feet or force and acceleration on the same foot. We also investigate the use of our bioimpedance meter.

5.6.1 Vertical acceleration

Typical acceleration data is shown in Figure 5.27 asymmetry in the gate pattern. The accelerations in the left foot are rapidly followed by similar accelerations in the right foot with a lag before the accelerations repeat in the left foot. The accelerations indicate discrete components of foot motion, indeed the transition from one state to another. For a volunteer with even gait the timing and magnitude of any feature pairs in the data on the L-R foot stride should match the R-L stride . The lack of symmetry in the at presented indicates an irregular gait .

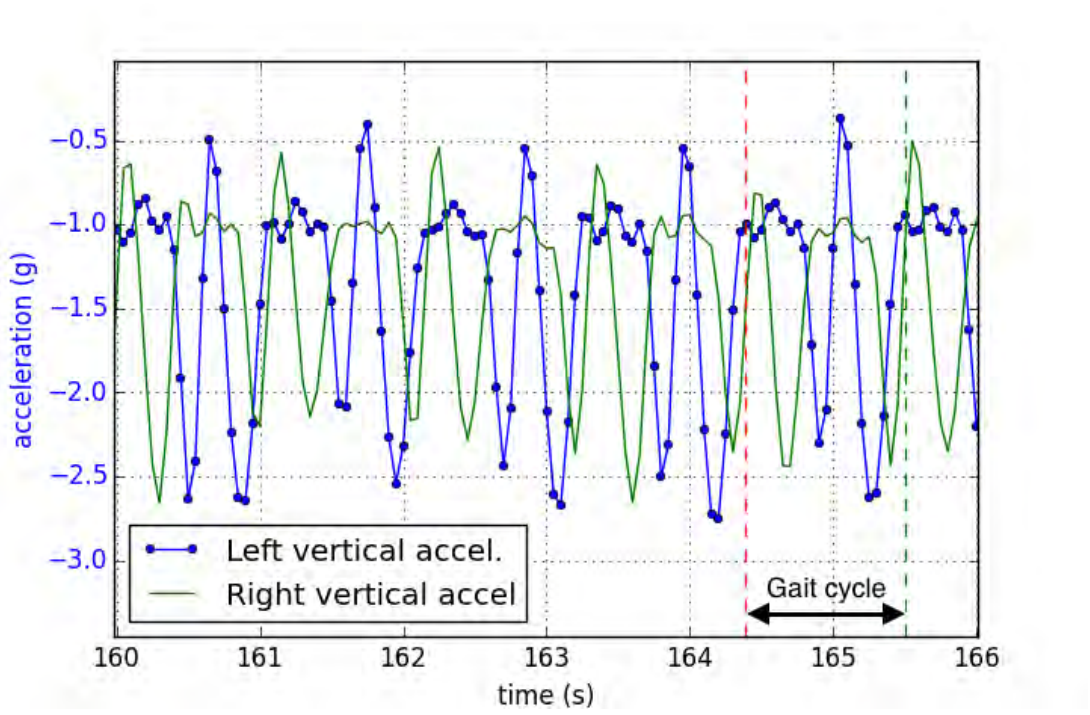

Figure 5.27: Comparison of vertical accelerations between the left and right feet while walking at 4.5 $\mathrm{km\,h^{-1}}$. Asymmetry in the gait cycle is shown.

5.6.2 Acceleration and force

The vertical acceleration and force data shown in Figure 5.28 clearly demonstrates the timing of the heal strike as being coincident with the deceleration from ≈ -2.5 to $-1.0g$ of the foot under test.

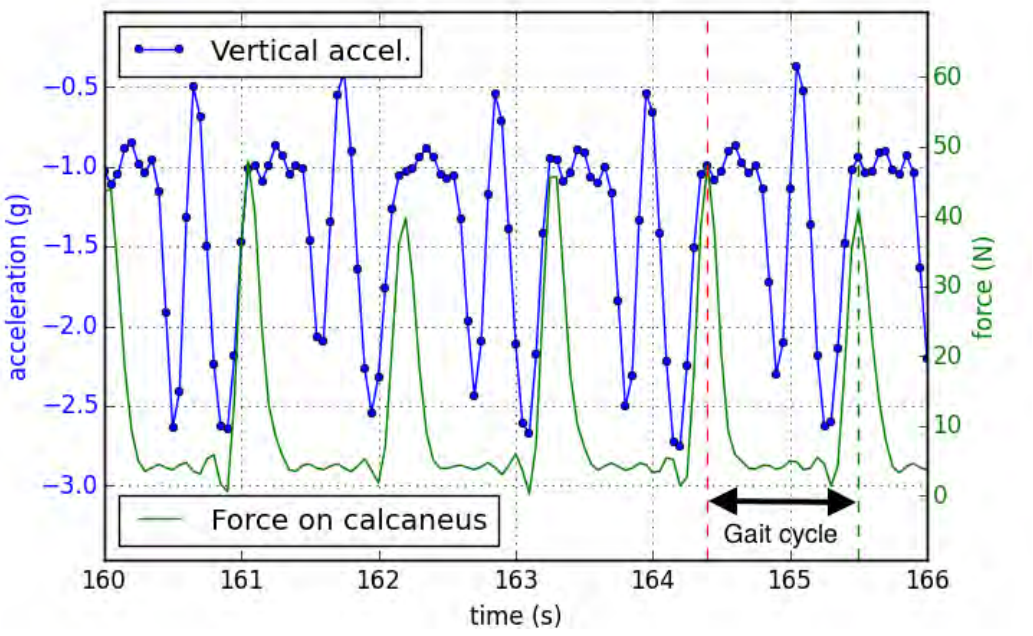

Figure 5.28: Comparison of changes in vertical acceleration to timing of peak force at the calcaneus (heal) while walking at $4.5\mathrm{m\,s^{-1}}$. Heal strike is indicated by the large spike in the calcaneus force data. The vertical acceleration has three small but distinct peaks. These are calcaneus strike, fifth metatarsal followed by first metatarsal-great toe. The large deceleration, acceleration, deceleration is due to the foot swing cycle.

5.6.3 Humidity and GSR

Sweat and in shoe humidity are useful factors for monitoring podiatric skin health, both dry and overly hydrated skin are prone to breakdown and infection. GSR is a useful metric for monitoring the moisture content of the skin and aids the prediction of future condition [142]. Humidity affects evaporation of sweat which may be significant in some environments. Gait frequency can be observed in both signals in Figure 5.29.

5.6.4 Bioimpedance

The data in Figure 5.30 shows the tissue response to 500 kHz capacitively coupled to the sole of the foot and is given for indication. This demonstrates that it is feasible to measure changes in output due to the no-load, light load and high load states with the capacitively coupled impedance measurement device presented.

5.6.5 Occluded blood flow

The occluded blood flow test was undertaken with a 1 minute occlusion which provided adequate change in the measurable signal to demonstrate measurement efficacy with minimal volunteer discomfort. As can be seen from Figure 5.31 the

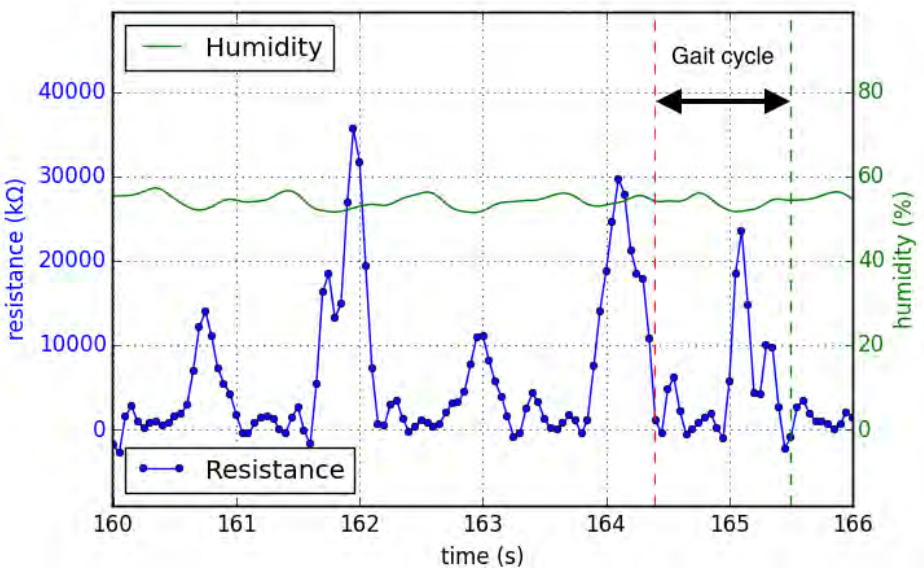

Figure 5.29: Comparison of GSR and humidity on the left foot while walking at $4.5\mathrm{m\,s^{-1}}$. The peaks in the resistance data are a function of reduced contact pressure on the electrodes when the foot is raised during walking.

frequency of the signal has increased from 0.16 Hz prior to the occlusion to - 0.26 Hz post occlusion in the example given, with some change in the magnitude of the phase measurement. From this and other testing we conclude that we are able to observe a measurable effect in tissue in vivo.

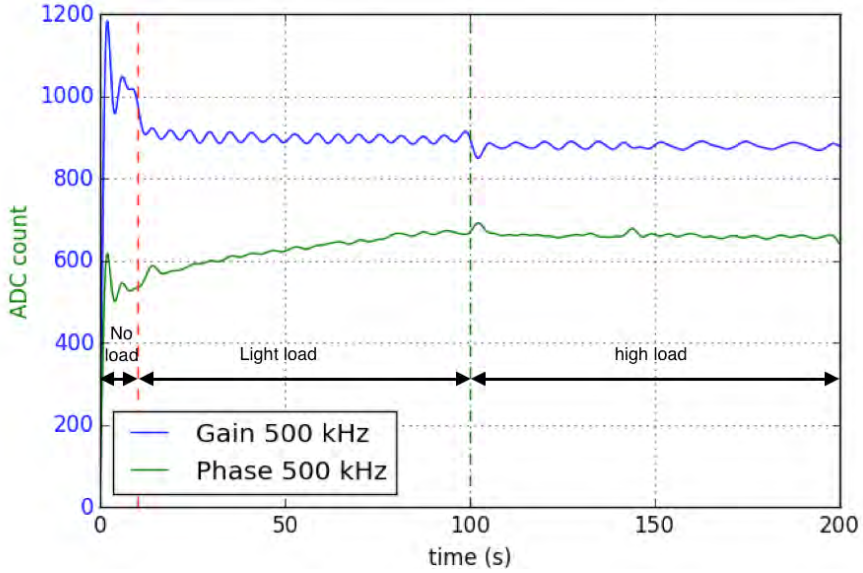

Figure 5.30: Bioimpedance sensor measuring unloaded – light load (foot resting on sensor, volunteer seated) – high load (volunteer standing). The data for gain show differences in the frequency and magnitude of signal for all three load conditions confirming the sensors ability to sense such changes.

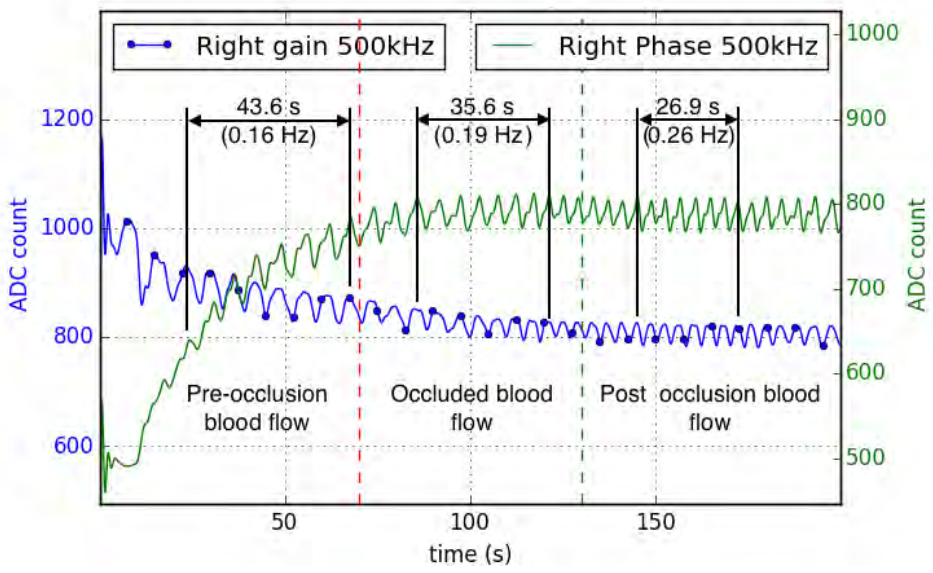

Figure 5.31: Bioimpedance sole of foot pre-occlusion, occluded and post occluded blood flow. The characteristic frequency for each condition was estimated by dividing the cycle count by the corresponding Δt.

5.7 Summary

Previous devices have combined up to three measurement modalities. The device presented measures eight bilaterally plus environmental temperature and humidity. This gives the opportunity to evaluate interdependencies in the metrics used and hence quantify the value of each measurement individually and in concert as multifactorial sensing algorithms. Evaluation of the interrelationship of some factors has historically been difficult due to the inability to measure multifactorial data in an unconstrained manner, this device alleviates that restriction.

With local force being measured in 4 locations and skin temperature in 3, alongside the 6 other metrics discussed it is now possible to gather comprehensive data from the in shoe environment. This development will give an enhanced understanding of the biomechanics and local environmental considerations that affect the well-being of the foot.

With an increasing understanding of the problems associated with the diabetic foot it will be necessary to modify the sensor arrays to suit specific investigations. This device is an extensible and adaptable measurement system which can be modified to optimise the sensor choices and location as required. The presented device demonstrated the measurement of multifactorial data utilising both analogue and I^2C interfaces in real time. These interfaces can be rapidly adapted to measure other sensors required by individual investigators enabling the customisation of the measurement array.

The presented system demonstrates the feasibility of measuring complex multifactorial data in the laboratory or gymnasium based on commodity hardware. Though the use of a battery pack and touch screen would allow the Raspberry Pi to be used in a mobile situation, further development could lead to either conversion to BTLe (BT4) with data logging on other mobile devices or peer to peer, in shoe, data logging for increased utility at a later date.

During testing it was noticed that the force sensor output was lower than the estimated loads. Although the loads of up to $110\mathrm{N}$ were observed the 75^{th} percentile reading was $16\mathrm{N}$ on the calcaneus and $10\mathrm{N}$ in the forefoot. Rescaling these outputs to a range of circa $0\,\mathrm{N} to 30\,\mathrm{N}$ would significantly increase the resolution for a small loss of observed data.

After testing the final sensor set comprised the following sensors:

1. Temperature - laboratory

2. Humidity - laboratory

3. Acceleration in 3 axis - in shoe. All sensors validated as meeting manufacturers specification.

4. Rotation in 3 axis - in shoe. All sensors except Roll validated as meeting manufacturers specification.

5. Humidity - in shoe. All sensors validated as meeting manufacturers specification with 1 failure in a batch of 20.

6. Temperature - in shoe. All sensors validated as meeting manufacturers specification with 1 failure in a batch of 20.

7. Temperature skin - in shoe. All sensors achieved a coefficient of variation (R^2) value greater than 0.9

8. Force - in shoe. All sensors achieved a coefficient of variation (R^2) value greater than 0.99

9. GSR - in shoe. All sensors achieved a coefficient of variation (R^2) value greater than 0.96.

10. Bioimpedance - in shoe

11. Bioimpedance - stand alone

Chapter 6 will examine data taken from a cohort of 10 volunteers utilising the sensor set defined here.

Chapter 6

Multifactorial analysis

6.1 Introduction

This chapter utilises the device and test protocol defined in chapter 5 to examine data from a cohort of 10 male non diabetic volunteers to form a baseline for testing diabetic volunteers against the same protocol.

Results derived from both the in shoe testing and the platform based bioimpedance tests will be analysed and the data examined. The in shoe test data will be cross correlated to investigate interdependencies and redundancy of measurement for data gathered in a perambulatory environment. This will help identify new sensor combinations with which to monitor diabetic foot health. To accommodate variability a fractional factorial experiment is utilised. This should be considered a pilot study due to the number of parameters to be measured and the small size of the testing cohort and time available.

6.2 Discontinuities in the in shoe data set

A novel device, by its nature, is prone to a range of known and unknown failure modes while being developed and this device has been no different. This has lead to some sensors such as 'Roll' and 'in shoe Bioimpedance' not providing usable data while others have failed sporadically requiring unreliable data to be removed prior to a correlation and significance analysis being performed across all available measurement channels. This chapter will describe the processes utilised to define good and bad data, the failure modes involved, methods of excluding this from the dataset alongside data processing techniques prior to the final inter metric correlations and significance tests. The challenges of managing data has been eloquently covered by Banaee et al [143].

As is normal with real world data there are a number of discontinuities which were needed to be addressed in the data analysis protocols for the data to be of use. The causes of these discontinuities will be discussed below and as there are a num-

ber of reasons for their existence, there are consequently a number of mitigations necessary to address them.

It is normal practice to filter data, ensuring only frequencies of interest are included. In this research both 'low' and 'band pass' filtering has been utilised to refine the data, both of which present challenges for non contiguous data sets. Filters are influenced by both their input and end conditions with data broken into multiple segments having particular challenges. In the data presented here, omitted data was set to zero before filtering. Post filtering the data was cropped to remove tail effects on the output data with cropped data replaced with place holders set at not a number (NAN). This prevents the unknown data becoming part of the correlation calculation.

6.2.1 Data collection structure and protocol

The first discontinuity to be discussed was introduced to address a limitation in the available data transition rate. Data was gathered from both in shoe sensors at a rate of 20Hz over Bluetooth at 115200 Baud. This presented a functional limit on the length of data strings that could be transmitted, which was less than the proposed data string length. To ameliorate this limitation data was gathered as two interlaced data sets totalling 60s. Firstly 5s of bioimpedance data was taken consisting of: test time, environmental sensor status, test cell temperature, test cell humidity, acceleration data, rotation data alongside phase and again data for each bioimpedance test frequency. As bioimpedance data has not been recorded in such a way previously, the decision was made to record $5\,\text{s}$ of data to give 100 data sets. This would give access to phenomena from $0.4 - 10Hz$. Secondly $55\,\text{s}$ of data was taken replacing the phase and gain data with force, skin temperatures, GSR, in shoe environmental temperature, humidity and status. This resulted in 5s and 55s interlaced blocks of data.

6.2.2 Systemic failure of sensor

Two sensors in each measurement circuit failed to record any usable data during testing, these being the 'roll' and 'in shoe bioimpedance' sensors. The former is due to a failure in the inertial measuring unit (IMU), where data was transmitted, though only a gradual drift was measured over time and is shown on the pitch axis in Figure 3.4. This was experienced over different rotational axis on different sensors. The IMU sensor location utilised the 'x' axis in the vertical, meaning that the sensor 'roll' axis measured 'yaw' of the foot. The decision was made that this was the axis to eliminate as the ankle and therefore the foot does not rotate in this axis. Ideally this choice would not be necessary as the data would be available. The in shoe bioimpedance sensor failed due to an inadequate length of connector lead disconnecting the sensor from the device during testing. This was not initially

obvious from the data recorded or with examination of the devices during testing. Consequently all in shoe bioimpedance data was discarded.

6.2.3 Connection failure

Connection failure was common to the analogue sensors which were prone to disconnection and damage to the FPC connector in use. Visual examination of the sensor interface and data was undertaken at the end of each test module to ensure effective connection. There was no discernible pattern to the failures. However every volunteers' data has at least a single sensor failure measuring either temperature, force or GSR. Sensor failure was detected during data analysis by setting functional limits to the sensor output with spurious data being automatically highlighted.

6.2.4 Data acquisition errors

The final failure mode is a function of error handling in the wireless data transmission. The data storage device requests each sequential string of data from each shoe via the Bluetooth link at predetermined intervals. If for any reason this fails, a blank row of data is recorded and the process carries on to the other shoe or environmental monitor. Data drop outs can be overcome/reduced in a production ready system with the inclusion of transmission control protocol (TCP) and cyclic redundancy check (CRC) technology to validate the data transfer in real time[144, 145].

Where any break in the data occurs the filter process assumes this data to be a zero, performs the filter functions and replaces the zero data and the filter transients with NAN. This process reduces the size of the dataset for later analysis and the analysis process must account for this variability in the data.

6.3 Interpretation of the data

The following sections describe how the data is interpreted using correlation, significance and statistical data analysis to remove spurious data due to the factors previously described. The data will be further sub divided by test and ethnic group.

6.3.1 Correlation, significance and frequency analysis

Having filtered the data, a factor analysis was performed across all sensor data streams to investigate correlation as a 'paired sample t test' with each correlation tested for significance with a single sided significance test. All correlations with a corresponding p value exceeding 0.05 were excluded from further analysis, see Table 6.1. The p value is a test of the significance of the data presented. Where a p value of 0.05 is used to indicate a significant result there is a small $(1:20)$ chance

Factor Analysis

Correlation Matrix

		Temperature - Lab - Low Pass 1.500 Hz	Humidity - Lab - Low Pass 1.500 Hz	Accl X - L - Low Pass 1.500 Hz	Accl Y - L - Low Pass 1.500 Hz	Accl Z - L - Low Pass 1.500 Hz	Pitch - L - Low Pass 1.500 Hz	Yaw - L - Low Pass 1.500 Hz	T calc - L - Low Pass 1.500 Hz	T1st met - L - Low Pass 1.500 Hz
Correlation	Temperature - Lab - Low Pass 1.500 Hz	1.000	-.870	-.026	.008	-.002	-.020	.023	.064	.287
	Humidity - Lab - Low Pass 1.500 Hz		1.000	.018	-.009	.003	.015	-.022	-.027	-.219
	Accl X - L - Low Pass 1.500 Hz			1.000	-.476	-.244	-.109	-.198	-.069	-.124
	Accl Y - L - Low Pass 1.500 Hz				1.000	.870	.473	.124	.465	.399
	Accl Z - L - Low Pass 1.500 Hz					1.000	.642	-.095	.398	.214
	Pitch - L - Low Pass 1.500 Hz						1.000	-.728	.275	.110
	Yaw - L - Low Pass 1.500 Hz							1.000	.009	.130
	T calc - L - Low Pass 1.500 Hz								1.000	.682
	T1st met - L - Low Pass 1.500 Hz									1.000
Sig. (1-tailed)	Temperature - Lab - Low Pass 1.500 Hz		.000	.066	.327	.463	.118	.093	.000	.000
	Humidity - Lab - Low Pass 1.500 Hz			.152	.298	.437	.196	.102	.058	.000
	Accl X - L - Low Pass 1.500 Hz				.000	.000	.000	.000	.000	.000
	Accl Y - L - Low Pass 1.500 Hz					.000	.000	.000	.000	.000
	Accl Z - L - Low Pass 1.500 Hz						.000	.000	.000	.000
	Pitch - L - Low Pass 1.500 Hz							.000	.000	.000
	Yaw - L - Low Pass 1.500 Hz								.305	.000
	T calc - L - Low Pass 1.500 Hz									.000
	T1st met - L - Low Pass 1.500 Hz									

Table 6.1: Sample correlation and significance analysis utilising a subset of data to demonstrate the analysis principles. Each data stream was compared against every other to investigate correlation as a paired sample t test. The same data was examined for significance with and sensor pairs with a significance greater than 0.05 being discarded.

that this result happened by chance. A p value of 0.05 or less is seen as a significant result. A frequency analysis was utilised to validate the data against boundary conditions, see Table 6.2. Each data stream in the frequency analysis was challenged against predefined functional limits for each data stream, including minima, maxima, a threshold variable and maximum number of missing data entries as a means of excluding spurious data.

6.4 Division of data by test and ethnicity

Only data from the ambulatory tests is presented here although data is also available for standing and seated tests. Testing was undertaken in two tranches, the first was undertaken with male Chinese volunteers (n=4) and utilising the FPC sensors mounted directly to the the sandal insole, while the second utilised male Caucasian volunteers (n=10) with sensors mounted directly to the foot. The change to protocol was due to early failures of the FPC sensors and difficulty maintaining consistent alignment of the sensors and feet during the first study as discussed in section 5.2.5. For these reasons only the Caucasian cohort data has been presented.

Frequencies

Statistics

		Temperature – Lab – Low Pass 1.500 Hz	Humidity – Lab – Low Pass 1.500 Hz	Accl X – L – Low Pass 1.500 Hz	Accl Y – L – Low Pass 1.500 Hz	Accl Z – L – Low Pass 1.500 Hz	Pitch – L – Low Pass 1.500 Hz
N	Valid	3748	3745	3745	3745	3745	3745
	Missing	1	4	4	4	4	4
Mean		24.9490045	40.4864107	-1.3108107	-.07890788	.170953217	-1.2592117
Std. Deviation		.120026117	.305634634	.242394618	.348025776	.235347134	25.8320774
Variance		.014	.093	.059	.121	.055	667.296
Skewness		-1.729	1.420	-.503	.676	-.160	1.061
Std. Error of Skewness		.040	.040	.040	.040	.040	.040
Kurtosis		2.649	.921	-.902	-.225	-.612	.387
Std. Error of Kurtosis		.080	.080	.080	.080	.080	.080
Range		.596430538	1.27580681	1.13532103	1.59139334	1.16679455	148.838393
Minimum		24.4800000	40.1728470	-1.9998364	-.68392428	-.43986504	-50.929581
Maximum		25.0764305	41.4486538	-.86451532	.907469060	.726929507	97.9088119
Percentiles	25	24.9161460	40.2840962	-1.5043737	-.34057225	-.02249796	-17.443449
	50	24.9897292	40.3798678	-1.2577385	-.11961069	.209183787	-9.1908218
	75	25.0256808	40.5623083	-1.0933393	.099299153	.316590947	10.9873263

Table 6.2: Sample frequency analysis utilising a subset of data to demonstrate the analysis principle. Frequency analysis enables the examination and validation of data against multiple statistical metrics including range, maxima, minima and the number of missing data.

6.5 Volunteer demographics

The volunteer demographics are described statistically in Table 6.3 and Figure 6.1. All volunteers were male, mean age 35.4 years $\pm SD$ 7.9 years and selected from a non diabetic population. It was not possible to test a diabetic cohort for direct comparison due to time and ethical constraints. The data presented here is intended to be used as a baseline for the same tests on a diabetic population. The testing developed here demonstrates a new paradigm in test capability.

6.6 In shoe data

Analysis of the in shoe data demonstrate coherence between a number of sensor pairs that are not reflected in the literature. This indicates that there is either a mechanistic relationship between the data, as a function of external influences such as design of shoe or measurement environment, or a systemic relationship, where proprioception and feedback are important components in the relationship. Where the latter is the case it is reasonable to suppose that this will be adversely affected by sensory and control neuropathy.

Statistical data for coherence of significant sensor pairs is presented in Figure 6.2. In this analysis the only opposing sensors to give a high correlation are the left and right in shoe environmental temperatures. This pairing is denoted with reference letter A. Other sensor pairs have unmatched complimentary pairings such as 'force in the 1st metatarsal left' and the 'acceleration Y right' being compared. These are denoted with reference numbers 1 – 12 with the sensor previously described being number 5. The number of cases included in each sensor pair

		Volunteer registration number	Time since last caffenated drink (Hrs)	Age (Years)	Blood pressure Systolic (mm/Hg)	Blood pressure Diastolic (mm/Hg)	Height (m)	Resting heart rate - from finger probe (bpm)	SO2 - from finger probe (%)	Bodywater (%)	Bodytype	bonemass (kg)	BMR (Kj)	Metabolic age (years)	Visceral fat level	Body weight (kg)
N	Valid	10	10	10	10	10	10	10	10	10	10	8	8	8	8	10
	Missing	0	0	0	0	0	0	0	0	0	2	2	2	2	2	0
Mean		0	9.6	35.4	126.4	79.4	20.228	69.7	97.4	56.32	3.5	3.35	8316.25	38.375	7.688	84.48
Std. Deviation		0	21.9859	7.919	8.6436	10.6479	58.246364	8.499	0.9661	5.1562	1.604	0.3251	920.9817	19.9495	4.5193	12.2422
Variance		0	483.378	62.711	74.711	113.378	3392.639	72.233	0.933	26.586	2.571	0.106	848207.36	397.982	20.424	149.871
Skewness		0	3.13	0.449	0.629	0.129	3.162	-0.423	-0.111	-0.095	0	-0.465	-0.428	-0.015	0.175	-0.499
Std. Error of Skewness		0	0.687	0.687	0.687	0.687	0.687	0.687	0.687	0.687	0.752	0.752	0.752	0.752	0.752	0.687
Kurtosis		0	9.848	-1.747	-0.227	-0.578	10	-0.629	-0.623	-1.499	-2.8	-0.444	-0.301	-2.573	-2.103	-0.957
Std. Error of Kurtosis		0	1.334	1.334	1.334	1.334	1.334	1.334	1.334	1.334	1.481	1.481	1.481	1.481	1.481	1.334
Range		0	71	19	27	33	184.255	27	3	15	3	1	2879	44	11.5	34.3
Minimum		0	1	27	116	63	1.745	55	96	49.1	2	2.8	6753	17	2.5	64.7
Maximum		0	72	46	143	96	1.9	82	99	64.1	5	3.8	9632	61	14	99
Percentiles	25	0	1	28	119.25	70.75	1.76625	63.5	96.75	51.2	2	3.1	7626.25	18.25	3.625	73.575
	50	0	2.5	33	125.5	79.5	1.815	71	97.5	57.7	3.5	3.45	8571	40	7.25	84.8
	75	0	4.5	45.25	132	87.25	1.8625	76.25	98	60.525	5	3.575	8898	57	11.75	96.7

		BMI (kg/m2)	Body fat whole (%)	Right arm (%)	Left arm (%)	Trunk (%)	Right Leg (%)	Left Leg (%)	Muscle mass whole (kg)	Right arm (kg)	Left arm (kg)	Trunk (kg)	Right Leg (kg)	Left Leg (kg)	Ambient Temp (°C)	Ambient Humidity (%RH)
N	Valid	10	10	10	10	10	10	10	10	10	10	10	10	10	10	10
	Missing	0	0	0	0	0	0	0	0	0	0	0	0	0	0	0
Mean		25.7	20.3	18.61	19.87	22.79	16.17	16.68	121.34	3.67	3.63	34.31	11.09	10.8	21.919	54.4219
Std. Deviation		3.0894	6.7594	4.893	4.4915	7.4994	6.5395	6.3152	183.4129	0.4668	0.5397	4.0545	0.8103	0.8327	1.44768	8.233813
Variance		9.544	45.689	23.941	20.173	56.241	42.765	39.882	33640.285	0.218	0.291	16.439	0.657	0.693	2.096	67.796
Skewness		0.162	0.23	0.813	0.724	0.213	0.269	0.182	3.155	-0.222	-0.317	-0.156	0.065	-0.163	0.392	-0.432
Std. Error of Skewness		0.687	0.687	0.687	0.687	0.687	0.687	0.687	0.687	0.687	0.687	0.687	0.687	0.687	0.687	0.687
Kurtosis		-0.716	-1.571	-0.546	-0.892	-1.515	-1.139	-1.259	9.964	-0.658	-0.698	-0.711	-0.426	-0.378	-1.2	-1.228
Std. Error of Kurtosis		1.334	1.334	1.334	1.334	1.334	1.334	1.334	1.334	1.334	1.334	1.334	1.334	1.334	1.334	1.334
Range		9.5	19.6	14.1	12.9	21.4	18.7	18.1	590.7	1.5	1.7	13.2	2.7	2.8	4.3	23.35
Minimum		21.1	10.7	13.9	15.2	12	7	7.7	52.3	2.9	2.7	27.5	9.8	9.4	19.9	40.95
Maximum		30.6	30.3	28	28.1	33.4	25.7	25.8	74.2	4.4	4.4	40.7	12.5	12.2	24.2	64.3
Percentiles	25	23.625	14.8	14.375	16.4	16.775	11.075	12.375	58.3	3.325	3.225	30.9	10.375	10	20.8575	47.91275
	50	25.4	18.15	16.5	17.75	20.45	14.45	14.75	66.15	3.75	3.65	34.65	11.25	11.05	21.515	55.7565
	75	28.55	27.175	22.4	23.525	29.825	21.975	22.75	70	4.025	4.05	37.4	11.65	11.3	23.5	61.95

Table 6.3: Volunteer demographic statistics

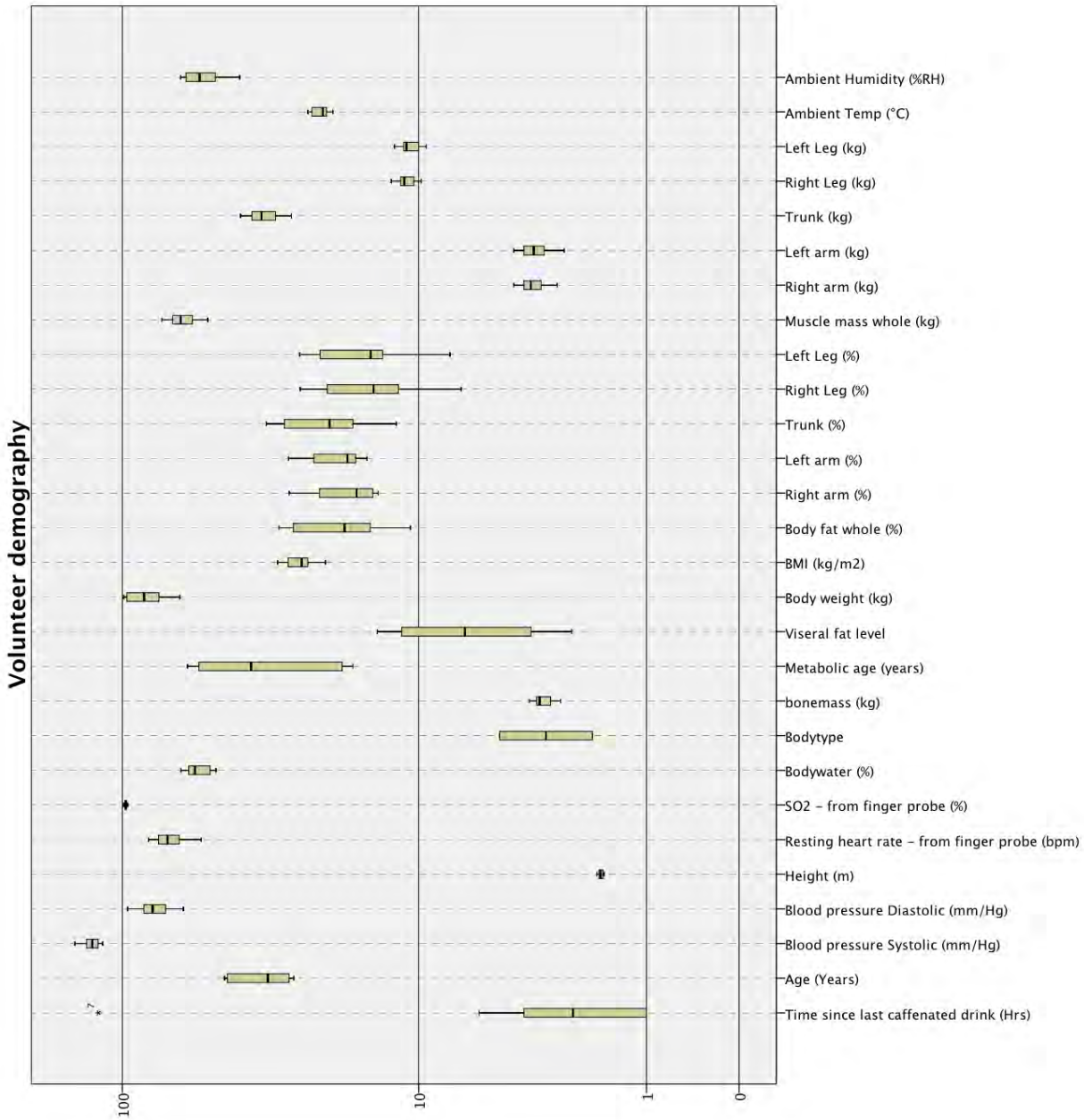

Figure 6.1: Volunteer demography. The units for each measured category are shown in brackets after the category name.

is summarised in table 6.5.

6.6.1 Environmental temperature

Environmental temperature in opposing feet (reference A) is configured to sample temperature without contacting the foot, providing an accessible measurement of the in shoe environmental temperature at the ball of the foot. This sensor configuration exhibited the highest median correlation of all sensor pairs at 0.969 with 40/40 sets of test data being valid. Although Maluf et al [146] have built a device for measuring in shoe temperature there is a paucity of data for this metric. Currently in shoe environmental temperature is not mentioned in the literature, though skin temperature is extensively examined. This is less challenging than skin surface measurement as physical isolation from the skin is required allowing the use of socks within the shoe. With such high correlation, small changes in the Δ temperature and correlation factor are likely to be easily observable, making this a useful metric for monitoring foot pathology. Changes in temperature are a known analogue of both microvasculature degradation and infection.

6.6.2 In shoe skin temperatures

In shoe monitoring of skin temperature has revealed four intra site correlations, items 1 – 4 in Figure 6.2 which are of interest, with the caveat that although the median correlations are high, with two exceptions, the ranges are also high. The open sandal test platform is believed to have exacerbated the variability and it is expected that variability would be lower in an enclosed shoe. Items 1 & 2 show a wide variation in results indicating that some volunteers were negatively correlated while others were positive. This is likely to be due to movement induced flushing of the in shoe environmental sensor with air. Manual observation indicated that the gait of some volunteers promoted more foot to shoe motion than others. This aside, the median temperature correlations were high in the calcaneus, great toe and first metatarsal when compared to environmental temperature. This is of interest as a change in these correlation ratios is likely to be an indicator of localised cooling or heating in an unmonitored site. It is worth noting that the temperatures of the great toe and first metatarsal, item 3 correlate with a slightly lower range than the other metrics. Despite the broad body of knowledge concerning the value of monitoring skin temperature in the diabetic foot there is as of yet nothing published regarding in shoe temperatures for either diabetic or non diabetic cohorts.

		Temp - L AN	Humidity - La	Humidity - La	Accy Y - R and	Accy Y - L and	T calc - R AN	T calc L AND	T 1st met - R	T 1st met - L	GSR - R lp AN	GSR - L lp AN	T GT - R AND	T GT - L AND	F 1st met - R	F 1st met - L
N	Valid	40	40	40	40	39	31	27	32	26	27	13	32	29	32	28
	Missing	0	0	0	0	1	9	13	8	14	13	27	8	11	8	12
Mean		0.8378	-0.59585	-0.5054	-0.73743	0.63592	0.28845	0.18844	0.43591	0.44146	0.83044	0.89946	0.26875	0.29303	0.778	0.52561
Std. Deviation		0.391636	0.485307	0.541007	0.137367	0.207031	0.68956	0.670488	0.539993	0.563113	0.195577	0.088444	0.735584	0.717228	0.152486	0.362552
Variance		0.153	0.236	0.293	0.019	0.043	0.475	0.45	0.292	0.317	0.038	0.008	0.541	0.514	0.023	0.131
Skewness		-3.792	2.026	1.583	1.194	-1.132	-0.675	-0.571	-1.202	-0.959	-1.49	-1.425	-0.793	-0.594	-3.773	-0.431
Std. Error of Skewness		0.374	0.374	0.374	0.374	0.378	0.421	0.448	0.414	0.456	0.448	0.616	0.414	0.434	0.414	0.441
Kurtosis		14.118	3.142	1.234	0.995	0.939	-1.14	-1.293	0.49	-0.443	1.031	1.731	-1.186	-1.415	18.24	-1.468
Std. Error of Kurtosis		0.733	0.733	0.733	0.733	0.741	0.821	0.872	0.809	0.887	0.872	1.191	0.809	0.845	0.809	0.858
Range		1.798	1.756	1.816	0.56	0.816	1.908	1.876	1.862	1.714	0.651	0.301	1.894	1.879	0.9	1.099
Minimum		-0.807	-0.969	-0.957	-0.891	0.053	-0.948	-0.947	-0.894	-0.73	0.342	0.683	-0.93	-0.912	0.041	-0.15
Maximum		0.991	0.787	0.859	-0.331	0.869	0.96	0.929	0.968	0.984	0.993	0.984	0.964	0.967	0.941	0.949
Percentiles	25	0.8885	-0.86225	-0.85775	-0.84375	0.517	-0.403	-0.486	0.185	-0.0635	0.767	0.8475	-0.7495	-0.462	0.74025	0.131
	50	0.968	-0.7965	-0.727	-0.777	0.677	0.589	0.459	0.5325	0.6345	0.928	0.915	0.584	0.615	0.793	0.6945
	75	0.9825	-0.5365	-0.376	-0.6555	0.816	0.881	0.801	0.87875	0.86925	0.957	0.963	0.8795	0.9305	0.8415	0.8415

		Temp - R AN	Temp - L AN	Humidity - R	Humidity - L	Temp 1 st R AN	Temp 1 st L AN	F 1st met R AN	F 1st met L AN	T 1st met - L	T 1st met - R	T 1st met - L	T 1st met - R	T GT - L AND	T GT - R AND
N	Valid	38	39	37	39	39	35	36	37	31	27	36	37	30	32
	Missing	2	1	3	1	1	5	4	3	9	13	4	3	10	8
Mean		-0.46208	-0.49303	-0.37243	-0.61772	0.44823	0.44774	0.64614	-0.45635	0.40003	0.36919	0.47028	0.38738	0.25957	0.34731
Std. Deviation		0.485302	0.513801	0.547402	0.397697	0.538557	0.633777	0.117588	0.274779	0.528349	0.512896	0.612327	0.592349	0.739173	0.680102
Variance		0.236	0.264	0.3	0.158	0.29	0.402	0.014	0.076	0.279	0.263	0.375	0.351	0.546	0.463
Skewness		1.035	1.445	0.989	1.636	-0.886	-1.07	-0.696	0.92	-1.173	-0.396	-1.265	-0.892	-0.563	-1.001
Std. Error of Skewness		0.383	0.378	0.388	0.378	0.378	0.398	0.393	0.388	0.421	0.448	0.393	0.388	0.427	0.414
Kurtosis		0.229	1.266	-0.002	2.103	-0.079	-0.484	-0.315	-0.119	0.219	-1.035	0.219	-0.257	-1.452	-0.664
Std. Error of Kurtosis		0.75	0.741	0.759	0.741	0.741	0.778	0.768	0.759	0.821	0.872	0.768	0.759	0.833	0.809
Range		1.79	1.869	1.852	1.61	1.841	1.89	0.445	1.052	1.72	1.596	1.93	1.867	1.92	1.92
Minimum		-0.988	-0.987	-0.986	-0.981	-0.857	-0.914	0.359	-0.821	-0.775	-0.628	-0.951	-0.885	-0.943	-0.95
Maximum		0.802	0.882	0.866	0.629	0.984	0.976	0.804	0.231	0.945	0.968	0.979	0.982	0.977	0.97
Percentiles	25	-0.88925	-0.878	-0.8145	-0.896	0.056	0.063	0.58475	-0.6455	0.277	0.051	0.18175	0.0575	-0.59475	-0.18
	50	-0.651	-0.669	-0.598	-0.788	0.494	0.76	0.6405	-0.557	0.533	0.302	0.704	0.449	0.621	0.694
	75	-0.123	-0.306	-0.091	-0.522	0.945	0.927	0.7475	-0.3175	0.777	0.872	0.93375	0.9315	0.9305	0.85325

Table 6.4: In shoe data statistics. The table shows the statistical metrics utilised to quantify the individual sensor data sets for each test. These metrics enable the researcher to identify and eliminate invalid data prior to analysis.

Case Processing Summary						
	Cases					
	Valid		Missing		Total	
	N	Percent	N	Percent	N	Percent
Temp - L AND Temp - R	40	100.00%	0	0.00%	40	100.00%
T calc - L AND Temp - L	27	67.50%	13	32.50%	40	100.00%
T calc - R AND Temp - R	31	77.50%	9	22.50%	40	100.00%
T GT - L AND Temp - L	29	72.50%	11	27.50%	40	100.00%
T GT - R AND Temp - R	32	80.00%	8	20.00%	40	100.00%
T 1st met - L AND T GT - L	26	65.00%	14	35.00%	40	100.00%
T 1st met - R AND T GT - R	32	80.00%	8	20.00%	40	100.00%
T 1st met - L AND Temp - L	35	87.50%	5	12.50%	40	100.00%
T 1st met - R AND Temp - R	39	97.50%	1	2.50%	40	100.00%
T 1st met - L AND T GT - R	31	77.50%	9	22.50%	40	100.00%
T 1st met - R AND T GT - L	27	67.50%	13	32.50%	40	100.00%
T 1st met - L AND Temp - R	36	90.00%	4	10.00%	40	100.00%
T 1st met - R AND Temp - L	37	92.50%	3	7.50%	40	100.00%
T GT - L AND Temp - R	30	75.00%	10	25.00%	40	100.00%
T GT - R AND Temp - L	32	80.00%	8	20.00%	40	100.00%
Temp - L AND Humidity - L	39	97.50%	1	2.50%	40	100.00%
Temp - R AND Humidity - R	38	95.00%	2	5.00%	40	100.00%
Humidity - Lab AND Temp - L	40	100.00%	0	0.00%	40	100.00%
Humidity - Lab AND Temp - R	40	100.00%	0	0.00%	40	100.00%
Humidity - L AND Temp - R	39	97.50%	1	2.50%	40	100.00%
Humidity - R AND Temp - L	37	92.50%	3	7.50%	40	100.00%
F 1st met - L AND F GT - L	28	70.00%	12	30.00%	40	100.00%
F 1st met - R AND F GT - R	32	80.00%	8	20.00%	40	100.00%
Accy Y - R AND Accy Z - R	40	100.00%	0	0.00%	40	100.00%
Accy Y - L AND Accl Z - L	39	97.50%	1	2.50%	40	100.00%
F 1st met - L AND Accy Y - R	37	92.50%	3	7.50%	40	100.00%
F 1st met - R AND Accy Y - L	36	90.00%	4	10.00%	40	100.00%
GSR - R lp AND GSR - R bp	27	67.50%	13	32.50%	40	100.00%
GSR - L lp AND GSR - L bp	13	32.50%	27	67.50%	40	100.00%

Table 6.5: In shoe test case processing summary

6.6.3 Intra shoe temperatures

The use of an integrated measuring system has allowed the examination of intra foot perambulatory temperatures to be measured for the first time, items 5, 6 & 7 in Figure 6.2. It is interesting to note that the highest correlations did not occur between the same sites on the opposing feet but between the first metatarsal and opposing great toe, the first metatarsal and the in shoe ambient temperature and the great toe and ambient temperature of opposing feet. This may have merit for monitoring diabetic foot disorder as a metric if closer correlations are achieved with a non diabetic cohort in enclosed shoes.

6.6.4 Humidity and temperatures in shoe

High correlations were seen between the in shoe environmental temperature and humidity, though again the ranges were large, items 8, 9 &10 in Figure 6.2. Humidity measurement was shown to have a considerably faster response than the temperature measurement during testing. This is important where rapid changes in the ambient conditions are experienced, such as with cool dry air being drawn into the shoe, past a warm moist foot while walking. As with temperature testing above, tighter correlation ranges are expected in a closed shoe environment, though this may happen due to the humidity sensor reaching saturation, so caution is advised in drawing conclusions. Saturation was noted in the data presented here with an open sandal arrangement and this would be expected to be a bigger concern in a closed shoe environment. However, that is not to say it should not be measured in a neuropathic population, where a reduction in sweating is expected. This may be an important metric as it is very sensitive. There is a paucity of literature dedicated to in shoe environmental temperature and humidity with little other than Maluf et al [146].

An interesting correlation exists between the laboratory humidity and the in shoe environmental temperature, item 9. This is likely to be stronger in a sandal than a closed shoe as the latter will restrict airflow and the ability of external air to cool the foots' local environment. Mounting a discrete external environmental sensor on shoes for use outside the lab that would not be affected by the proximity of the wearer, would be challenging, so it is not envisaged that this would be worth pursuing.

6.6.5 Motion of the foot and inter/intra foot monitoring

Foot motion has been investigated by Leardini [147] amongst others. The utilisation of high resolution solid-state inertial measuring units is a logical progression of this and can easily be incorporated into footwear for long term monitoring of gait. The correlation of forward and lateral motion reference 12, Accy Y being for-

ward acceleration and Z being lateral in this implementation, indicates a consistent well defined gait pattern. In the event that neuropathy develops in the sensory or control nerves, changes to both the magnitude and strength of correlation are likely and further investigation would be recommended.

The correlation between force exerted by the great toe and the first metatarsal of the same foot is expected as both are involved in the generation of forward propulsion during the 'toe off' phase of the gait cycle, item 11 in Figure 6.2. What is surprising is the difference between left and right feet correlations. The right foot shows a low spread of coherence while the left shows a significantly wider spread. This appears to indicate that the right leg is dominant in the volunteers tested. It is not felt that this is likely to be beneficial for monitoring the diabetic foot but may have some utility in sport science.

The high correlation between force of the first metatarsal and acceleration along the longitudinal axis of the opposing foot is of interest. This shows one foot rolling forward onto the forefoot while the opposing foot accelerates forward. This cycle is repeatable with a low spread of coherence but this cycle would be expected to deteriorate with the onset of sensory or control neuropathy.

6.6.6 GSR

Item 12 in Figure 6.2 shows a relationship between the low pass ($1.5Hz$) and band pass ($0.1Hz - -1.5Hz$) filtered GSR data. GSR is usually a highly dynamic response but ANS pathology restricts the skins ability to sweat, causing an increase in the overall resistance and a reduction in the dynamic response. From the data presented here it would be advisable to further investigate coherence between these two metrics in diabetic and non diabetic volunteers.

It is important to note that there are safety concerns where utilising this metric in the diabetic volunteer. Polarisation of the tissue is especially dangerous in compromised tissue, where changes to the milieu could compromise the tissue viability. Hence the measurement device must be designed to eliminate polarisation of the tissue (fully reverse the current flow) and minimise the measurement time when a volunteer is connected.

6.7 Bioimpedance measurement

A number of tests were undertaken to estimate the efficacy of using bioimpedance for investigating soft tissue status in the foot. It was not possible to test this on diabetic patients, though a number of tests were undertaken that indicate that it is a suitably sensitive instrument to determine changes in tissue. Whether this is sensitive enough to measure skin degradation with sufficient granularity to sense early tissue degradation will require further work.

The first investigation utilised an early prototype sensor to look at the changes in phase and gain due to the orientation of anisotropic living tissue, the palm of a hand. As shown previously in Figure 3.18, measuring impedance in the palmer distal proximal axis gave a 15° phase shift and a 20% greater attenuation, hence demonstrating good sensitivity.

The second investigation utilised the sensor described in Section 5.3.7, investigating the sensitivity to no load, dead tissue (chicken breast) and living tissue (palm of a hand). As demonstrated in Figure 5.22 clear differentiation can be seen between the different states.It is expected that for ulcerated tissue phase and magnitude of the signal will tend towards that of the dead tissue used, though this was not tested in this body of work. It is also noted that the living tissue returns a much less regular signal and this is to be expected where living tissues and processes cause changes in the balance of resistive and capacitive pathways.

The third investigation again utilised the sensor from 5.3.7, to measure changes increasing salinity in an electrically isolated cell. This investigates the sensors ability to measure changing resistance in a fluid under test. Though the response was non linear it was possible to measure the change in salinity using the device presented between RO water and physiological saline solution see Figure 5.23.In volunteer testing the device differentiated between foot not on sensor, unloaded and loaded foot contact together with gross changes in blood flow in the foot.

The device is capacitively coupled ensuring only AC voltages can be transmitted to the tissue, consequently the device can not cause polarisation of the tissue. Further investigation is required to examine tissue changes in the diabetic foot and consequent changes in the bioimpedance against which this device could be validated.

6.8 Summary

Two main contributions are presented here, the first being a new set of metrics with which to investigate the external influences on the diabetic foot. These are summarised in Table 6.6. The high coherence sensor pairings will be the most powerful. However, the low effort and technical difficulty of adding a temperature sensor for the first metatarsal and great toe giving access to the remaining sensor pairings make it advisable to include these sensors as well.

The second contribution is the bioimpedance sensor. Though this requires further characterisation and investigation into the expected impedance ranges for investigating the diabetic foot, it is an entirely new method of investigating the condition. It is expected that this device will measure the deep tissues giving early warning of deep tissue inflammation.

The above are the subject of a paper in the peer reviewed journal *electronics* [5].

The internal environmental temperature and humidity sensor is the most challenging device to site as it needs to be mounted so as to measure only the internal conditions without being influenced by the mounting arrangement or foot contact. It must also be mounted so as not to present a hazard to the user and remain clean. The primary consideration for temperature and force sensors is maintaining consistent alignment with the target areas of the foot. GSR simply needs to be kept in contact with the foot ideally with direct contact. If used for more than short term testing as conducted here measures should be taken to minimise the risk of tissue polarisation.

Acceleration and rotation can be measured in a single high resolution 6 degree of freedom device as used here and therefore the data is readily available and forms a useful reference metric.

Coherence variation in GSR has been demonstrated for the first time.

All the above has been achieved with a novel extensible multimodal sensing system.

Optimal in shoe measurement metrics			
Primary metric	Complimentary metric	sites to measure	Utility
In shoe environmental temperature	**In shoe environmental temperature**	Opposing feet	High coherence
GSR Low pass	**GSR Band pass**	Single foot	High coherence
Force at first metatarsal	**Acceleration - longitudinal axis of the foot**	Opposing feet	High coherence
Acceleration - longitudinal axis of the foot	**Acceleration along coronal axis**	Single foot	High coherence
Force at first metatarsal	**Force at great toe**	Single foot	High coherence
In shoe humidity	**In shoe environmental temperature**	Opposing feet	High coherence
In shoe humidity	**In shoe environmental temperature**	Single foot	Medium Coherence
Temperature great toe	**In shoe environmental temperature**	Opposing feet	Medium Coherence
Temperature first metatarsal	**In shoe environmental temperature**	Opposing feet	Medium Coherence
Temperature first metatarsal	**Temperature of great toe**	Opposing feet	Medium Coherence
Temperature first metatarsal	**In shoe environmental temperature**	Single foot	Medium Coherence
Temperature first metatarsal	**Temperature of great toe**	Single foot	Medium Coherence
Acceleration 3 axis		Both feet	Well represented in literature
Rotation 3 axis		Both feet	Well represented in literature

Table 6.6: Recomended sensor suit

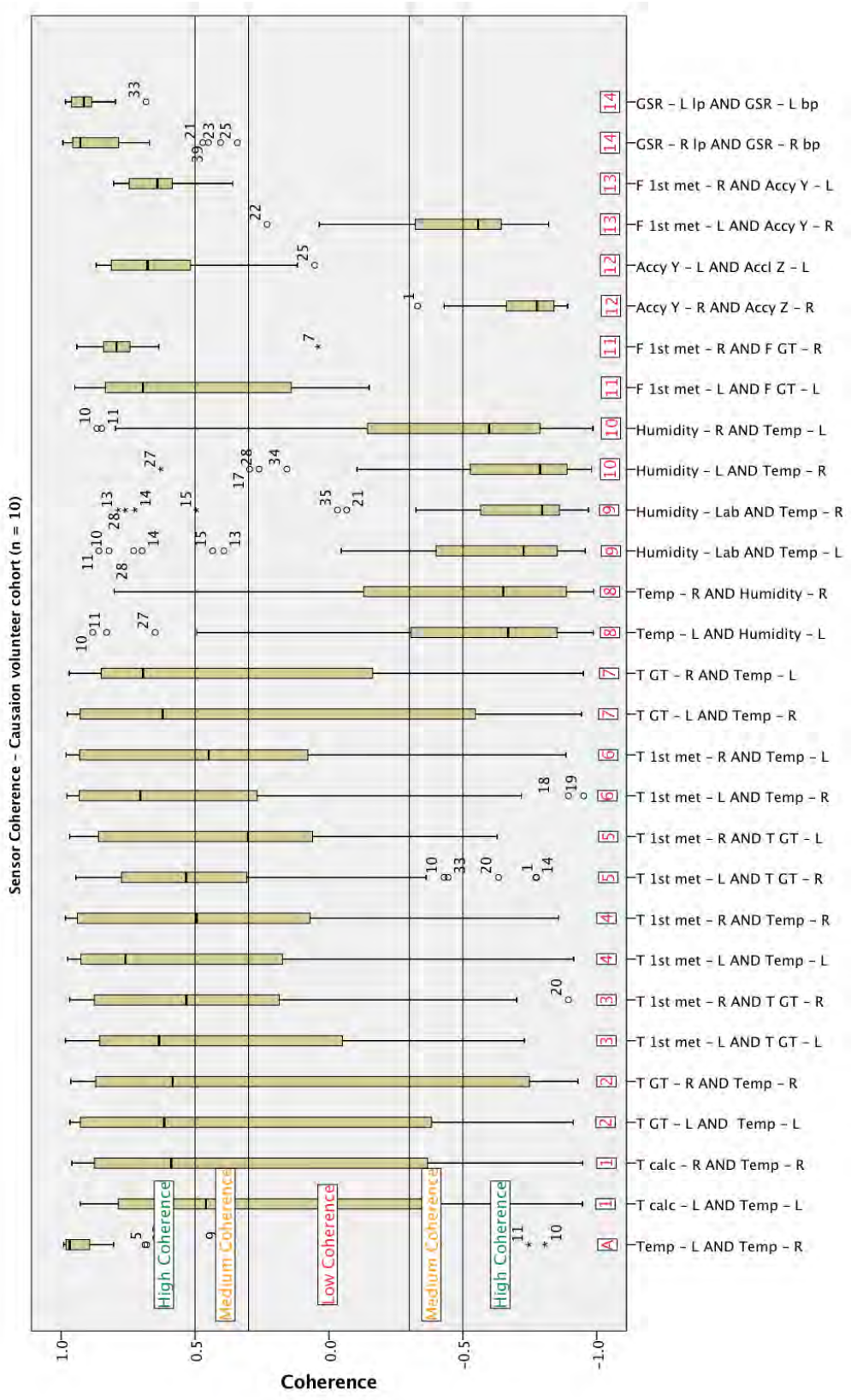

Figure 6.2: Sensor coherence for ambulatory data set pairs. Sensor pairings with medium or high coherence included and significance of $p \leq 0.05$. Pairing data sets in such a way enables the identification of novel interdependencies.

Chapter 7

Conclusions and further work

As stated in 'motivation for research', section 1.1, this project has expanded the scope for monitoring multiple sensing modalities concurrently that are suitable for the DF as there is strong evidence that suggests monitoring environmental factors applied to the plantar tissue, the tissues' reaction, together with known diagnostic parameters will enable an enhanced level of understanding and a practical method of predicting and detecting the early signs of tissue breakdown. Though excellent work is being done to improve the management of diabetes through better understanding of the pathological processes, with improvements being made in the clinical management of the disease, it is not currently possible to prevent ulceration and therefore ameliorate the associated health risks. Many studies link applied pressure, shear, skin stiffness, dermal hydration, temperature, blood flow, pulse strength, humidity and prior scar tissue to be some of the predictive indicators in the development of new or recurrent diabetic foot ulcers. However, none have yet provided reliable threshold levels of any individual parameter that can be utilised to predict tissue breakdown, and even if available, would be difficult to apply in the free-living environment, due to the lack of suitable continuously wearable monitoring devices.

The GSR study in chapter 4 has demonstrated a technique that shows sensitivity in the measurement of ANS activity between feet, which should be expanded. The technique of using the variability of coherence as a metric of ANS variability currently shows some promise, though remains to be proven. The formal analysis of the lead – lag phenomena still needs to be addressed but again this shows some level of sensitivity that may be exploitable. .

The device shown in this research is a prototype multi sensor insole technology which will need further development to be usable in the worn in shoe environment on a daily basis. However this research has shown that novel data can be gathered using this technology.

The investigation into using sensors printed or assembled on flexible printed circuits has shown that there is further work required to develop a valid solution to

flexible circuitry in the worn environment. Currently the circuitry and particularly the interface to the sensors is prone to early failure. This is particularly problematic in the harsh environment of the shoe where large stresses and strains are imparted on the circuit.

It is not currently viable to use the sensor set in a daily worn device as the sensor assembly/printing to a flexible circuit is still in an immature state. There are a number of commercial and research bodies trying to address this at present. however there is currently no robust solution.

With regard to the use of a multimodal approach to sensing in a wearable device outlined in chapter 1 developed in chapter 5, and the analysis of the resultant data in chapter 6 has yielded novel approaches to monitoring and understanding the podiatric data. With the development of an ensemble device to measure data in the free-living environment it will become possible to measure the fatigue cycles, temperature, sweat, bioimpedance etc. of the diabetic foot offering new insight into how differing levels of applied stress affect the plantar tissues.

The aim to investigate novel associations of sensing modalities is addressed in data presented in Figure 6.2. It has been shown that there is correlation between sensor pairings in the data that we examined. That is not to say that it is possible to infer there is a causal relationship at this stage.

The examination of bioimpedance has shown there is a sensitivity to a number of factors relating to skin health. It has been demonstrated that living tissue has a markedly different signature to dead tissue or a no load state and all three states can be differentiated under the testing undertaken. The device was also able to differentiate different states in living tissue. These being low load on the foot when seated — load on the foot while standing and with blood flow — without blood flow. As blood flow in the extremities is known to be compromised in the DF it is likely that the device as shown will be useful in the monitoring of DF. That said further research is necessary using a diabetic cohort is necessary to validate this.

The investigation of GSR has demonstrated that this technology is capable of monitoring perspiration in the soles of the feet. It has been demonstrate that intra site perturbations are indeed measurable with the device as shown though extra investigation will be necessary to validate this with a diabetic cohort.

A novel set of sensing modalities have been identified and investigated in this work together with a new system architecture. These have been demonstrated as a concept and a provisional implementation showing that useful data can be gathered. Data has been gathered and appraised from a cohort of 10 volunteers from which the final sensor set has been identified.

7.1 Contribution to the body of knowledge

Prior to this thesis little was known about the use of multifactorial sensing in the foot. This thesis starts to elucidate how multivariate data can be utilised to investigate the podiatric health and suggests new metrics for doing so. This will be especially useful in the field of diabetic foot health. A new extensible device specifically designed for the purpose is also offered that significantly reduces the challenges in making the measurements.

1. Novel associations of sensors for monitoring the diabetic foot see Table 6.6.
2. The development of a novel bioimpedance measuring device.
3. The development of a novel wearable extensible multimodal sensing platform as published in *electronics* [5].
4. Demonstrate DC through textile GSR measurement.
5. Demonstrate the effect of caffeine on GSR coherence for the first time.

The sensing system demonstrates sensing of environmental factors such as temperature, humidity and time of day, alongside linear/rotational accelerations, skin temperature, contact force, galvanic skin response and bio-impedance in a single device. This toolset will give access to new data from the free-living environment that will enable the investigation of the interplay of factors that cause tissue breakdown in the diabetic foot. This has not been possible before as the technology to measure these parameters has been too bulky, until recently.

The use of Bio-Impedance for monitoring tissue state is novel in the diabetic foot, though it has been used as a diagnostic tool for various forms of cancer, fluid load in the body, dental carries, muscle percentage of body mass and fat percentage. This is expected to reveal many changes in the tissue state, both in healthy and pathologically compromised tissue. This, coupled with the use of capacitive coupling of the electrodes to the body to be tested, will be new to the field.

7.2 Further work

1. Investigate the influence of fatigue and recovery of tissue with a possible design of a no-decompression model. There is currently no guidance available for how much work can be undertaken by tissues of the diabetic foot or how long they need to recover after work. This is a complex issue as the input state of the tissue needs to be established and a model for how much stress this can tolerate is required, but a predictor of over exertion would be a useful. There is evidence [148] that exercise improves the outcomes for those living with

diabetes however this presents a small risk of damage the tissues of the foot [149]. Any metric that can minimise this risk while empowering those living with diabetes to engage in exercise will improve quality of life.

2. Investigate a surrogate haptic feedback system to overcome sensory DPN. Where sensory neuropathy exists, developing a sensory feedback mechanism to a surrogate site such as the buttocks or backs of the thighs could enable those living with neuropathy to regain lost feedback signals in an intuative manner. Morley suggested this in 2001 [110] and there is no evidence of further work in this area. This is likely due to the historic difficulty in devising discrete circuitry with which to implement this. There are now many cost effective technologies with which to address this problem.

3. Investigate the viability of stimulating the ANS, and/or induce sweating to better maintain desired moisture level in the foot. Wilkins [41] demonstrated that Faradically coupled AC could induce sweating to the healthy tissue under test. It is possible that this mechanism could be pressed into service to increase skin hydration in the event that the sweat glands are still physically functional but lacking neuronal control.

4. Develop a robust method of connecting sensors to FPC that is tolerant of the in shoe environment. The in shoe environment is challenging for sensor design due to the high flex, strain, shear and humidity/moisture. Technologies are available to manufacture thin film high flex circuits that are could be deployed in wearable devices. However as noted by Park et al [150] there are currently no suitable methods of connecting these new technologies to devices that are robust for worn sensing devices. For a system such as this to be viable as a worn device in a community care environment the sensor must be simple, poka-yoke and reliable.

5. Increase the resolution of the Bioimpedance device circuit with a gain of 20 on the return signal and optimise the phase - range to $\pm 30^{\circ}$. Figures 5.22 and 5.23 demonstrate that only part of the $0 - 1023AU$ senosr range is being utilised. Removing the resistor R8 in Figure 5.19 will reduce the return signal attenuation by a factor of 2. Meanwhile changing R4 to $400\,\mathrm{w}$ill increase the drive signal attenuation to $4:1$ from $2:1$ thus a $4:1$ overall increase in the magnitude signal can be produced. To reduce the range and increase the resolution of the measured phase, amplification of the phase output on the phase gain analyser will be necessary..

6. Redesign the GSR to be a voltage divider with non inverting amplification and active filter to reduce drive current and increase accuracy. Reducing the exposure to applied current reduces the risks of polarisation in. Both reducing

drive current and duration of exposure are valid means of achieving this aim.

7. Define GSR routine as a momentary excitation rather than permanently energised and reverse electrode polarity for each cycle to ensure minimal tissue polarisation.

8. Adjust GSR range to suit electrode size or adjust electrode size to suit current circuit. Rossel et al. reported impedances in the range of $10\mathrm{k}-3.5\mathrm{M}\Omega\mathrm{cm}^2$. The electrodes in the final design were undersized resulting in reduced resolution at high resistances.

9. Replace sensor connector system to improve robustness. The FPC connector system utilised in testing has proven to be inadequate as alignment is critical and sensor retention force inadequate. This was exacerbated by the sensor cable being too short for use while walking causing the cable to be pulled out of the socket.

10. Rescaling these outputs to a range of circa $0 - 30\mathrm{N}$ would significantly increase the resolution for a small loss of observed data. Though the force sensors provided usable output the range chosen was greater than required for the task undertaken. Reducing the range would allow greater resolution of measurement.

The use of the technology and techniques discussed in this thesis is not unique to the task in hand as there are a number of obvious alternate applications. Monitoring of motion, flexure, temperature, accelerations, and environment could easily be utilised in the fields of podiatry, sporting performance optimisation, monitoring at risk populations such as military personnel, labourers and the elderly to name a few.

With increased knowledge and development the device and analysis system could prove to be a valuable aid to monitoring the effects of physical therapy and rehabilitation in a wide range of fields [151]. It is often difficult to quantify the benefit of rehabilitation, particularly towards the culmination of therapy, as improvements are often subtle, with therapy often finishing where minimal improvement is observable. Wearable technology offers the opportunity to gather finer resolution long-term data that pertains to the users living environment rather than the abstract setting of the clinic.

This technology has potential as a means of monitoring both able and handicapped athletes. Where small enhancements in performance are hard to measure with traditional metrics, a wearable configurable device can measure multiple factors specifically selected for a particular sport or athlete. The same applies to monitoring personnel working in hostile environments.

With minor adaptation the motion sensing could be utilised in veterinary medicine for gait analysis on quadrupeds enabling the quantification of gait change that can be subjective [152] in the way it is currently observed. Similarly the measurement of flexure is an important metric that is difficult to measure/quantify but can be inferred from accelerometery. Though measurements of gait have been of the attempted in horses over many years the devices used in this study would allow a greater number of metrics to be utilised over a longer time-scale enabling a finer granularity of measurement.

Appendix A

Appendix - Ethics approval

Assesor: Jim Coates	Date: 29.01.2014	Task assesed	Skin health sensing sensor characterisation				
Validated by:	Date:						
Forseable hazard	Probability	Severity	**RISK**	Controls	Probability	Severity	**RISK**
Electric shock - from Bioimpedance	Possible	Moderate	1	Limit current to less than micro shock allowable limits	Possible	Minor	0.1
Electric Shock - GSR	Almost never	Minor	0.0001		Almost never	Minor	0.0001
Electric shock - ground lead USB lead act as ground lead for externally applied current source	Possible	Moderate	1	Only allow wireless connection to computer unless computer working from batery.	Almost never	Minor	0.0001
Electric shock - Device +/- 5V	Unlikely	Moderate	0.1		Unlikely	Moderate	0.1
Heating of tissue - acoustic impedance	Possible	Moderate	1	Limit power output/ duration	Unlikely	Moderate	0.1
Skin irritation - Polorisation of tissue - GSR	Almost certain	Minor	10	Limit duration of current source	Possible	Minor	0.1
Skin irritation - Polorisation of tissue - Bioimpedance	Unlikely	Minor	0.01		Unlikely	Minor	0.01
Trip hazard - coms wire to sensor	Possible	Moderate	1	Only allow wireless connection to computer unless computer working from batery.	Rare	Moderate	0.01
Trip hazard - mounting/ dismount treadmill	Possible	Moderate	1	Warn participant	Unlikely	Moderate	0.1
Trip hazard - cables (treadmill, computers etc.)	Possible	Moderate	1	Tidy cable placement or cable covers if nevessary	Unlikely	Moderate	0.1
Loss of balance - disorientation dueto treadmill	Possible	Moderate	1	Aclimatisation to tradmill. Remind Test subject of risk after stopping treadmill	Unlikely	Moderate	0.1
Tripping - on moving treadmill	Possible	Moderate	1	Urilise appropriate failsafe/ auto stop	Unlikely	Moderate	0.1
Over exertion - on treadmill	Possible	Moderate	1	Monitor heart rate ensure no more than moderate exercise is taken (<80% maximal heart rate).	Unlikely	Moderate	0.1
lifting injury - instaltion	Possible	Moderate	1	Use existing instalation or get apropriate help	Unlikely	Moderate	0.1
Fire	Rare	Critical	1	Advise nearest exit and rondevous point	Almost never	Critical	0.1
			#N/A				#N/A

Severity	**Definition**
Minor	Superficial injury or slight or temporary health effect, trivial damage to a building, minor disruption to work
Moderate	Significant injury or illness or temporary minor disability, minor damage to equipment or building, slight disruption to work
Major	Serious injury or illness or significant or permanent disability, or significant damage to equipment/ building, or significant disruption
Critical	fatal injury or ilness, or substantial and permanent disability, or severe damage to equipment/ building, or extensive disruption to
Catastrophic	Multiple fatal injuries or illness, or enormous damage to equipment/ building, or disaterous disruption to work

SHS-G-30030 Risk Assesment- Skin health sensing sensor characterisation.xlsx

Figure A.1: Risk assesment

UNIVERSITY OF Southampton

ERGO application form – Ethics form

All mandatory fields are marked (M*). Applications without mandatory fields completed are likely to be rejected by reviewers. Other fields are marked "if applicable". Help text is provided, where appropriate, in italics after each question.

1. APPLICANT DETAILS

1.1 (M*) Applicant name:	James Martin Coates
1.2 Supervisor (if applicable):	Dr. Andrew Chipperfield
1.3 Other researchers/collaborators (if applicable): *Name, address, email, telephone*	**Professor Geraldine F. Clough** G.F.Clough@soton.ac.uk

2. STUDY DETAILS

2.1 (M*) Title of study:	Multimodal sensing of the skin
2.2 (M*) Type of study (*e.g. Undergraduate, Doctorate, Masters, Staff*):	Doctorate
2.3 i) (M*) Proposed start date:	01/04/2014
2.3 ii) (M*) Proposed end date:	30/10/2014

2.4 (M*) What are the aims and objectives of this study?
To assess the suitability of a number of different sensing devices, both individually and in combination, for use in determining skin health at the foot and to provide baseline data from healthy individuals to inform later planned studies on those in disease states, e.g. minor wounds and ulceration.

2.5 (M*) Background to study (*a **brief** rationale for conducting the study*):
Tissue breakdown in the diabetic foot is a leading casue of ulceration and consequently amputation in people with diabetic diabetes. It is estimated that 15-25% of all daibetics will experience ulceration in the lower limb druing their lives. People with diabetes are 23 times more likely to suffer amputaion than non-diabetics, however 85% of these are reportedly preventable if appropriately treated in a timely manner. There is no known single test that is able to predict the state of the skin health. In this study, a range of standard sensing techniques will be used to measure parameters attributed to skin health (e.g. Galvanic skin response, impedance, temperature and pressure distribution) in order to a) evaluate the feasibility of these devices/techniques for use in measuring foot skin health; b) evaluate the feasibility of using these devices in combination; and c) to acquire baseline measurement data from healthy individuals.

Figure A.2: Ethics application

UNIVERSITY OF Southampton

Participant Information Sheet

Study Title: Multimodal sensing of the skin

Researcher: James Coates **Ethics number**:

Please read this information carefully before deciding to take part in this research. If you are happy to participate you will be asked to sign a consent form.

What is the research about?
This study aims to improve our understanding of sensing parameters associated with measuring the health status of the foot. This involves testing existing individual and multiple sensing devices simultaneously at multiple sites on the sole of the foot under rest and active conditions. This will help us understand the properties of these devices, their efficacy and provide sensor data that can later be compared to that from individuals affected by ulceration or other foot tissue disease conditions. The research will be conducted by PhD student James Coates, as part of his doctoral work.
The University of Southampton is the research sponsor and will be funding the study.

Why have I been chosen?
You have been chosen because you are a healthy person between 18 and 70 years old who has no known health issues that would exclude you from this study.

What will happen to me if I take part?
The testing will approximately take 1.5 hours. Your suitability for the study will be assessed via a verbal questionnaire and you will be asked to complete a health questionnaire and sign a consent form. You will be weighed with body composition scales, your height and waist measured, your blood pressure may be taken and measures of skin blood flow and/or oxygenation recorded.

You will be asked to wear an instrumented insole and may have sensors directly placed on the skin of your foot. Readings will then be taken from these devices over a period of time during which you may be asked to stand or walk. Individual sensor recording tests will not normally take more than five minutes each and there will be breaks between these recordings. The insole sensing parameters to be measured will include one or more of: applied pressure to the sole of the foot; temperature; humidity; acceleration; sweat; bioimpedance; and pulse rate. The data will be securely and anonymously recorded directly onto a computer.

Are there any benefits in my taking part?
There will be no direct benefit to taking part in the research. However, your results will be beneficial to this study and potentially to our increased understanding of skin degradation in the foot.

Are there any risks involved?
Low-level electrical signals (±5v) may be applied to the skin. However, the voltage levels used in this study are well within safe limits. The procedure will be stopped at the first indication of any discomfort or at the participant's request.

Will my participation be confidential?
Yes, your data will be stored on a password protected computer in an anonymised form and will be kept confidential in accordance with the University's policy.

What happens if I change my mind?
You have the right to withdraw from the study at any time without having to state reason.

What happens if something goes wrong?
Contact Dr Martina Prude, Head of Research Governance (02380 595058, mad4@soton.ac.uk)

Where can I get more information?
James Coates (PhD student, Bioengineering Science Research Group) – jmc1g12@soton.ac.uk
Dr Andrew Chipperfield (Research Project Supervisor) – a.j.chipperfield@soton.ac.uk

Figure A.3: Participant information sheet

UNIVERSITY OF Southampton

Contra-indication list

Please confirm (initial point 5) that you do not have any of the contra-indicators shown below. If you have any contra-indicators please inform the researcher that it is not possible to sign this clause.

1) Currently or within the last month been on any long or short-term medication, you do not need to declare the contraceptive pill or sub-dermal contraceptive implant if used.
2) Have any form of cardiovascular disease.
3) Have abnormally high or low blood pressure.
4) Have had any form of surgery in the past 6 months.
5) Suffer from epilepsy.
6) Suffer from vertigo.
7) Are not capable of walking 3 miles in an hour.
8) Suffer from diabetes type 1 or 2.

Figure A.4: Contra-indication list

UNIVERSITY OF Southampton

CONSENT FORM (*Version 1*)

Study title: Multimodal skin sensing
Researchers: James Martin Coates
Study reference: **Ethics reference**:
Participant reference:

Please initial the box(s) if you agree with the statement(s):

1. I have read and understood the participant information sheet and have had the opportunity to ask questions about the study. ☐
2. I understand that my participation in this study is completely voluntary and that I may withdraw at any point, without reason and without my legal rights being affected. ☐
3. I understand that this is a PhD research project. ☐
4. I understand that all the data gathered from this research project will be retained by the University of Southampton for ten years in line with University policy. ☐
5. I confirm that I have read the contra-indication list (page 2) and that I am not contra-indicated for this test. ☐
6. I agree to take part in this research project and agree for my data to be used for the purpose of this study. ☐

Data Protection
I understand that information collected about me during my participation in this study will be stored on a password protected computer and that this information will only be used for the purpose of this study. All files containing any personal data will be made anonymous.

Name of participant: **(Please print in capitals)**
.....
Signature of participant:
..... Date: .....
Name of researcher: **James Martin Coates**
.....
Signature of researcher:
..... Date: .....

SHS-G-30031_Consent Form.doc 21/07/2014 - Version 1

Figure A.5: Consent form

UNIVERSITY OF Southampton

Study questionnaire

Study title: Multimodal skin sensing
Researcher: James Martin Coates
Study reference:

Participant Ref:

1) Has no health conditions excluding participant from the study:
2) Height:
3) Weight:
4) Age:
5) Gender:
6) Resting blood pressure prior to test:
7) Resting heart rate prior to test:
8) Heart rate at end of test:
9) How much if any caffeine have you consumed in the last 12 hours and when?

10) Did you feel any unusual discomfort during the test? If so please indicate on the diagram below where this occurred.

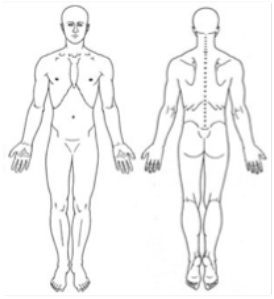

11) Did you have any unusual discomfort after testing? If so please indicate the diagram below where this is.

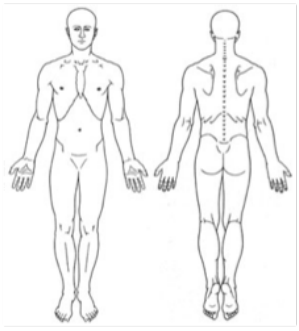

SHS-G-30035_Questionnaire.doc 21/07/2014 - Version 1

Figure A.6: Study questionare

Appendix B

Appendix - Circuit design

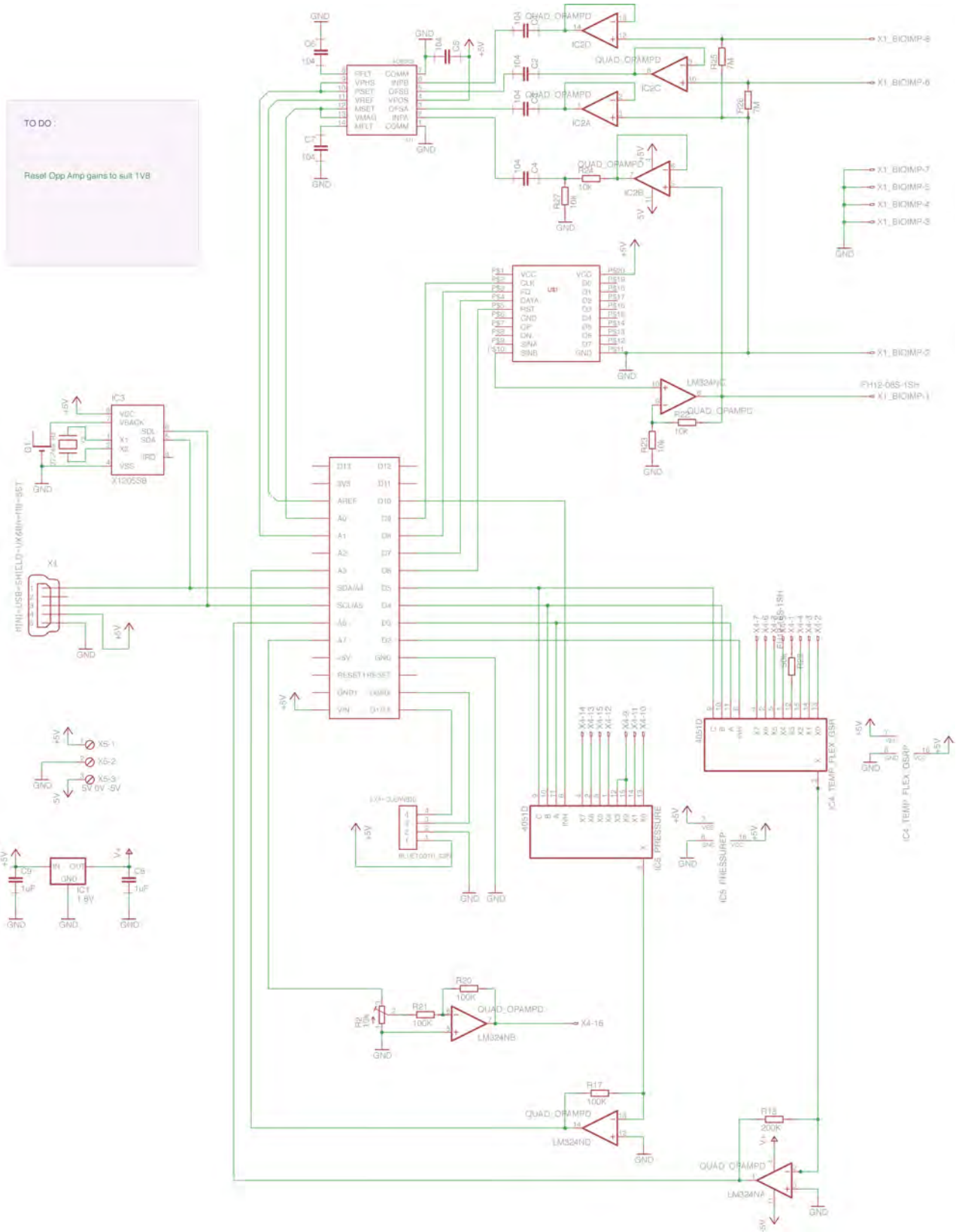

Figure B.1: Circuit V2 development system

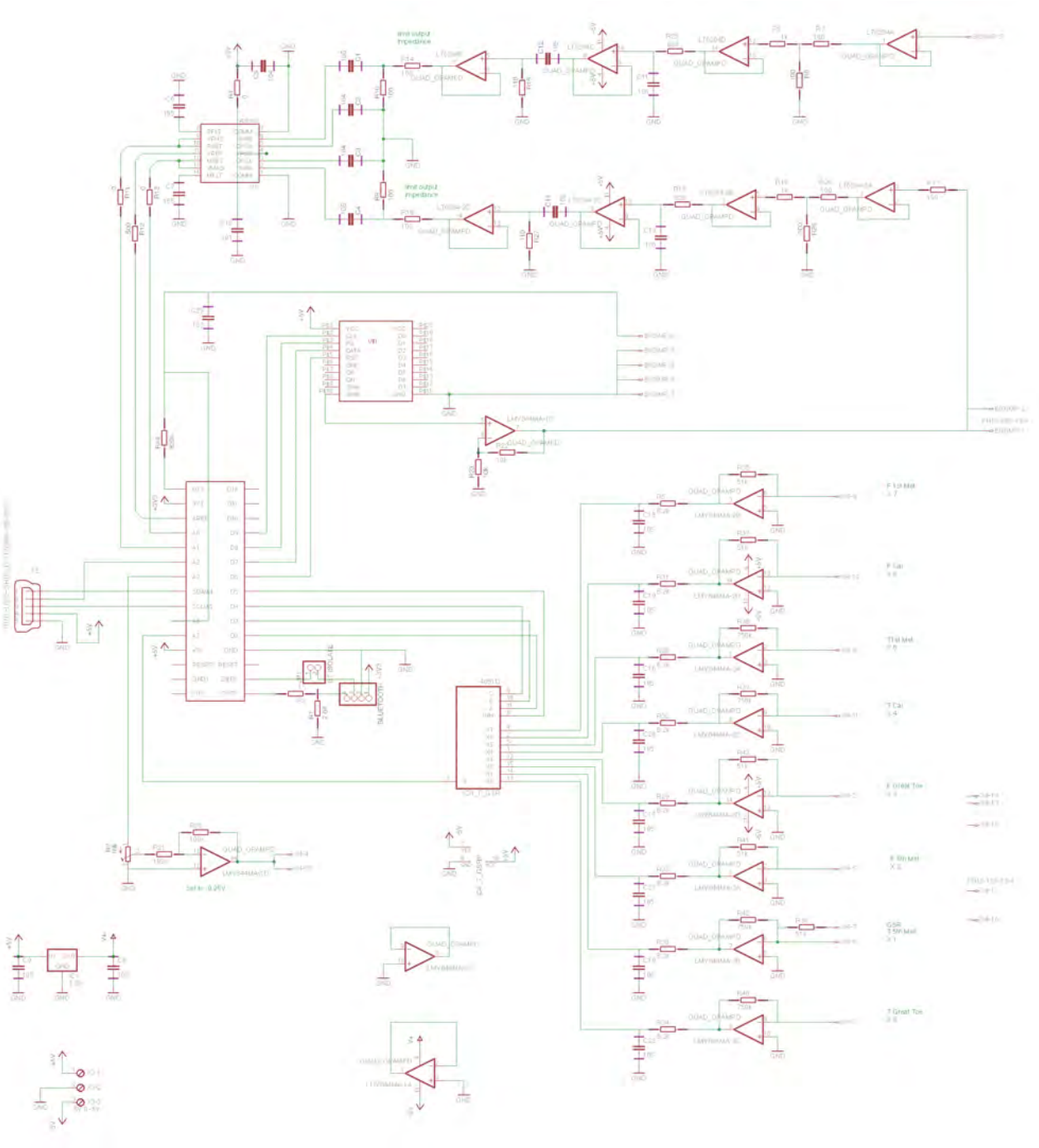

Figure B.2: Circuit V6 test system

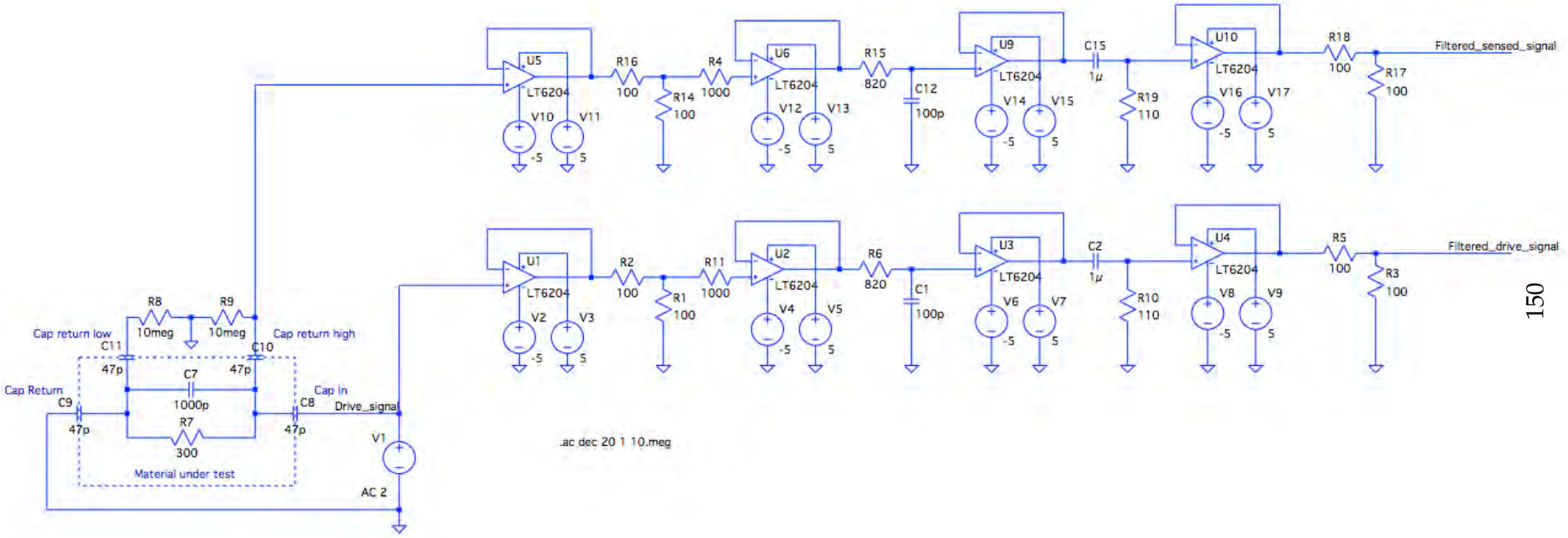

Figure B.3: Bioimpedance spice model

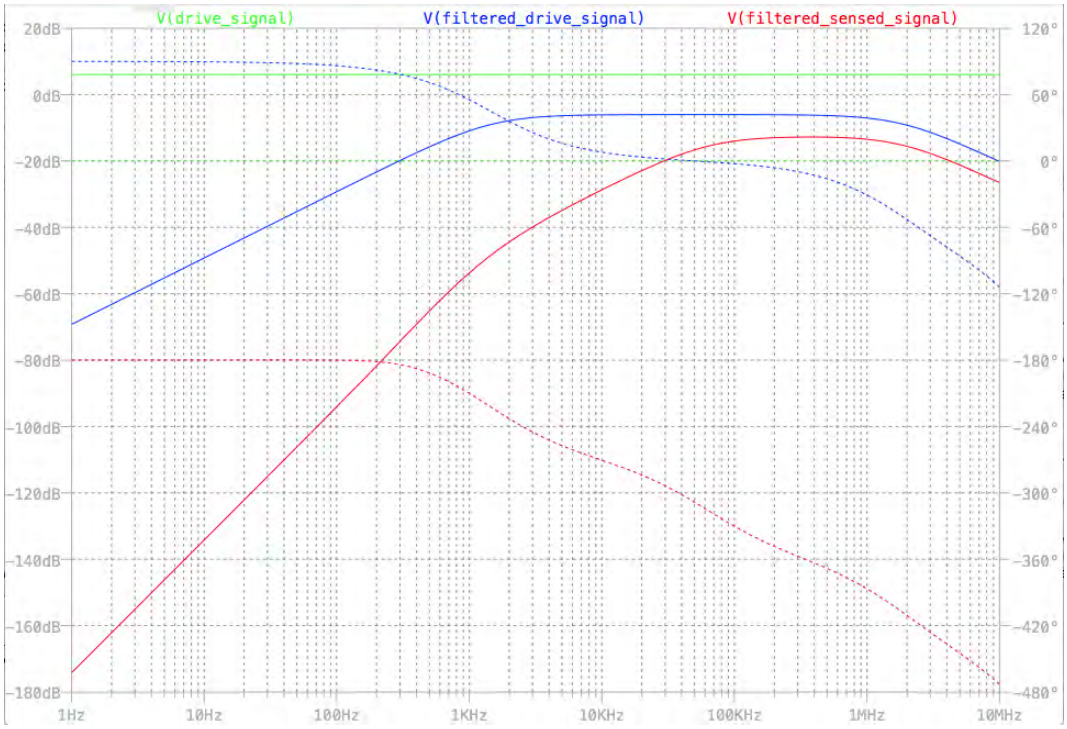

Figure B.4: Bioimpedance spice plot

Bibliography

[1] M. Hall and A. Felton, "The st vincent declaration, 20 years on–defeating diabetes in the 21 st century," *Diabetes Voice*, vol. 54, no. 2, pp. 42–44, 2009.

[2] A. J. Boulton, L. Vileikyte, G. Ragnarson-Tennvall, and J. Apelqvist, "The global burden of diabetic foot disease," *The Lancet*, vol. 366, no. 9498, pp. 1719–1724, 2005.

[3] D. E. Bild, J. V. Selby, P. Sinnock, W. S. Browner, P. Braveman, and J. A. Showstack, "Lower-extremity amputation in people with diabetes: epidemiology and prevention," *Diabetes care*, vol. 12, no. 1, pp. 24–31, 1989.

[4] G. E. Reiber, E. J. Boyko, and D. G. Smith, "Lower extremity foot ulcers and amputations in diabetes," *Diabetes in America*, vol. 2, pp. 409–27, 1995.

[5] J. Coates, A. J. Chipperfield, and G. F. Clough, "Wearable multimodal skin sensing for the diabetic foot," *Electronics - Raspberry Pi Technology*, vol. 5, no. 3, p. 45, 2016.

[6] NICE, "diabetes-footcare cg10. nice, london, 2004," January 2004.

[7] S. Ewings, "Sensing skin health: Literature review," July 2011, internal literature review comisioned by Andy Chipperfield.

[8] Diabetes-info, "What is diabetes?" January 2014. [Online]. Available: http://www.diabetes-info.co.uk/what-is-diabetes.html

[9] M. Laakso and K. Pyörälä, "Age of onset and type of diabetes," *Diabetes care*, vol. 8, no. 2, pp. 114–117, 1985.

[10] J.-L. Besse, T. Leemrijse, and P.-A. Deleu, "Diabetic foot: the orthopedic surgery angle," *Orthopaedics & Traumatology: Surgery & Research*, vol. 97, no. 3, pp. 314–329, 2011.

[11] G. Alberti, P. Zimmet, J. Shaw, Z. Bloomgarden, F. Kaufman, and M. Silink, "Type 2 diabetes in the young: The evolving epidemic the international diabetes federation consensus workshop," *Diabetes care*, vol. 27, no. 7, pp. 1798–1811, 2004.

[12] D. co uk, "Glycaemic control," January 2016. [Online]. Available: http://www.diabetes.co.uk/what-is-hba1c.html

[13] NICE, "Clinical guidelines for type 2 diabetes blood glucose management," Clinical guidlines, March 2002.

[14] G. E. Reiber, L. Vileikyte, E. d. Boyko, M. Del Aguila, D. G. Smith, L. A. Lavery, and A. Boulton, "Causal pathways for incident lower-extremity ulcers in patients with diabetes from two settings." *Diabetes care*, vol. 22, no. 1, pp. 157–162, 1999.

[15] W. J. Jeffcoate and K. G. Harding, "Diabetic foot ulcers," *The Lancet*, vol. 361, no. 9368, pp. 1545–1551, 2003.

[16] C. Quattrini, M. Jeziorska, M. Tavakoli, P. Begum, A. Boulton, and R. Malik, "The neuropad test: a visual indicator test for human diabetic neuropathy," *Diabetologia*, vol. 51, no. 6, pp. 1046–1050, 2008.

[17] J. S. Wrobel, J. A. Mayfield, and G. E. Reiber, "Geographic variation of lower-extremity major amputation in individuals with and without diabetes in the medicare population," *Diabetes Care*, vol. 24, no. 5, pp. 860–864, 2001.

[18] NICE, "Diabetic foot problems: prevention and management (ng19)," 2015.

[19] D. G. Armstrong, K. Holtz-Neiderer, C. Wendel, M. J. Mohler, H. R. Kimbriel, and L. A. Lavery, "Skin temperature monitoring reduces the risk for diabetic foot ulceration in high-risk patients," *The American Journal of Medicine*, vol. 120, no. 12, pp. 1042–1046, 2007.

[20] D. G. Armstrong, L. A. Lavery, P. J. Liswood, W. F. Todd, and J. A. Tredwell, "Infrared dermal thermometry for the high-risk diabetic foot," *Physical Therapy*, vol. 77, no. 2, pp. 169–175, 1997.

[21] L. A. Lavery, K. R. Higgins, D. R. Lanctot, G. P. Constantinides, R. G. Zamorano, D. G. Armstrong, K. A. Athanasiou, and C. M. Agrawal, "Home monitoring of foot skin temperatures to prevent ulceration," *Diabetes Care*, vol. 27, no. 11, pp. 2642–2647, 2004.

[22] WHO, "St. vincent declaration," October 1989. [Online]. Available: https://www.idf.org/sites/default/files/St%20Vincent%20Declaration%201989_WHO%20Euro%20and%20IDF%20Europe.pdf

[23] CDC, "Healthy people 2010," Book, January 2000.

[24] S. L. Norris, J. Lau, S. J. Smith, C. H. Schmid, and M. M. Engelgau, "Self-management education for adults with type 2 diabetes a meta-analysis of the effect on glycemic control," *Diabetes care*, vol. 25, no. 7, pp. 1159–1171, 2002.

[25] NICE, "Costing statement: 'diabetic foot problems: inpatient management of diabetic foot problems'," *NICE*, vol. 1, no. 1, p. 7, March 2011.

[26] A. Gordois, P. Scuffham, A. Shearer, A. Oglesby, and J. A. Tobian, "The health care costs of diabetic peripheral neuropathy in the us," *Diabetes care*, vol. 26, no. 6, pp. 1790–1795, 2003.

[27] A. D. McInnes, "Diabetic foot disease in the united kingdom: about time to put feet first," *Journal of foot and ankle research*, vol. 5, no. 1, pp. 26–32, 2012.

[28] K. Bakker, W. H. van Houtum, and P. C. Riley, "The international diabetes federation focuses on the diabetic foot," *Current diabetes reports*, vol. 5, no. 6, pp. 436–440, 2005.

[29] J. New, D. McDowell, E. Burns, and R. Young, "Problem of amputations in patients with newly diagnosed diabetes mellitus," *Diabetic medicine*, vol. 15, no. 9, pp. 760–764, 1998.

[30] R. S. Most and P. Sinnock, "The epidemiology of lower extremity amputations in diabetic individuals," *Diabetes care*, vol. 6, no. 1, pp. 87–91, 1983.

[31] G. Ragnarson Tennvall, *The Diabetic Foot. Costs, health economic aspects, prevention and quality of life.* Lund University, 2000.

[32] L. Uccioli, L. Mancini, A. Giordano, A. Solini, P. Magnani, A. Manto, P. Cotroneo, A. Greco, and G. Ghirlanda, "Lower limb arterio-venous shunts, autonomic neuropathy and diabetic foot," *Diabetes research and clinical practice*, vol. 16, no. 2, pp. 123–130, 1992.

[33] Y.-Z. Lam and J. K. Atkinson, "Biomedical sensor using thick film technology for transcutaneous oxygen measurement," *Medical engineering & physics*, vol. 29, no. 3, pp. 291–297, 2007.

[34] J. Cobb and D. Claremont, "Noninvasive measurement techniques for monitoring of microvascular function in the diabetic foot," *The international journal of lower extremity wounds*, vol. 1, no. 3, pp. 161–169, 2002.

[35] S. Tesfaye and D. Selvarajah, "Advances in the epidemiology, pathogenesis and management of diabetic peripheral neuropathy," *Diabetes/metabolism research and reviews*, vol. 28, no. S1, pp. 8–14, 2012.

[36] K. Prabhu, K. Patil, and S. Srinivasan, "Diabetic feet at risk: a new method of analysis of walking foot pressure images at different levels of neuropathy for early detection of plantar ulcers," *Medical and Biological Engineering and Computing*, vol. 39, no. 3, pp. 288–293, 2001.

[37] H. Chen, B. Nigg, M. Hulliger, and J. De Koning, "Influence of sensory input on plantar pressure distribution," *Clinical Biomechanics*, vol. 10, no. 5, pp. 271–274, 1995.

[38] A. Caselli, H. Pham, J. M. Giurini, D. G. Armstrong, and A. Veves, "The forefoot-to-rearfoot plantar pressure ratio is increased in severe diabetic neuropathy and can predict foot ulceration," *Diabetes care*, vol. 25, no. 6, pp. 1066–1071, 2002.

[39] Ezscan. (2014, January) Ezsacn screnning of diabetes risk. [Online]. Available: http://www.impeto-medical.com/about-ezscan/immediate-findings-with-ezscan-the-ezsc/

[40] K. Sun, Y. Liu, M. Dai, M. Li, Z. Yang, M. Xu, Y. Xu, J. Lu, Y. Chen, J. Liu *et al.*, "Accessing autonomic function can early screen metabolic syndrome," *PLoS One*, vol. 7, no. 8, p. e43449, 2012.

[41] R. Wilkins, H. Newman, and J. Doupe, "The local sweat response to faradic stimulation," *Brain*, vol. 61, no. 3, pp. 290–297, 1938.

[42] J. W. Klaesner, M. K. Hastings, D. Zou, C. Lewis, and M. J. Mueller, "Plantar tissue stiffness in patients with diabetes mellitus and peripheral neuropathy," *Archives of physical medicine and rehabilitation*, vol. 83, no. 12, pp. 1796–1801, 2002.

[43] S. Pai and W. R. Ledoux, "The compressive mechanical properties of diabetic and non-diabetic plantar soft tissue," *Journal of biomechanics*, vol. 43, no. 9, pp. 1754–1760, 2010.

[44] A. Vexler, I. Polyansky, and R. Gorodetsky, "Evaluation of skin viscoelasticity and anisotropy by measurement of speed of shear wave propagation with viscoelasticity skin analyzer1," *Journal of investigative dermatology*, vol. 113, no. 5, pp. 732–739, 1999.

[45] W. R. Ledoux and J. J. Blevins, "The compressive material properties of the plantar soft tissue," *Journal of biomechanics*, vol. 40, no. 13, pp. 2975–2981, 2007.

[46] D. D. Robertson, M. J. Mueller, K. E. Smith, P. K. Commean, T. Pilgram, and J. E. Johnson, "Structural changes in the forefoot of individuals with diabetes and a prior plantar ulcer," *J Bone Joint Surg Am*, vol. 84, no. 8, pp. 1395–1404, 2002.

[47] V. Thomas, K. Patil, and S. Radhakrishnan, "Three-dimensional stress analysis for the mechanics of plantar ulcers in diabetic neuropathy," *Medical and Biological Engineering and Computing*, vol. 42, no. 2, pp. 230–235, 2004.

[48] S. Rajbhandari, R. Jenkins, C. Davies, and S. Tesfaye, "Charcot neuroarthropathy in diabetes mellitus," *Diabetologia*, vol. 45, no. 8, pp. 1085–1096, 2002.

[49] A. Nardone, M. Grasso, and M. Schieppati, "Balance control in peripheral neuropathy: are patients equally unstable under static and dynamic conditions?" *Gait & Posture*, vol. 23, no. 3, pp. 364–373, 2006.

[50] A. J. Boulton, A. I. Vinik, J. C. Arezzo, V. Bril, E. L. Feldman, R. Freeman, R. A. Malik, R. E. Maser, J. M. Sosenko, and D. Ziegler, "Diabetic neuropathies a statement by the american diabetes association," *Diabetes care*, vol. 28, no. 4, pp. 956–962, 2005.

[51] N. Nikkels-Tassoudji, F. Henry, C. Letawe, C. Pierard-Franchimont, P. Lefebvre, and G. Pierard, "Mechanical properties of the diabetic waxy skin," *Dermatology*, vol. 192, no. 1, pp. 19–22, 1996.

[52] H. S. Yoon, S. H. Baik, and C. H. Oh, "Quantitative measurement of desquamation and skin elasticity in diabetic patients," *Skin Research and Technology*, vol. 8, no. 4, pp. 250–254, 2002.

[53] W. B. Mendes, "Assessing autonomic nervous system activity," *Methods in social neuroscience*, pp. 118–147, 2009.

[54] W.-M. Chen, T. Lee, P. V.-S. Lee, J. W. Lee, and S.-J. Lee, "Effects of internal stress concentrations in plantar soft-tissue—a preliminary three-dimensional finite element analysis," *Medical engineering & physics*, vol. 32, no. 4, pp. 324–331, 2010.

[55] A. Gefen, "Plantar soft tissue loading under the medial metatarsals in the standing diabetic foot," *Medical Engineering & Physics*, vol. 25, no. 6, pp. 491–499, 2003.

[56] M. J. Mueller, L. J. Tuttle, J. W. LeMaster, M. J. Strube, J. B. McGill, M. K. Hastings, and D. R. Sinacore, "Weight-bearing versus nonweight-bearing exercise for persons with diabetes and peripheral neuropathy: a randomized controlled trial," *Archives of physical medicine and rehabilitation*, vol. 94, no. 5, pp. 829–838, 2013.

[57] K. M. Shah and M. J. Mueller, "Effect of selected exercises on in-shoe plantar pressures in people with diabetes and peripheral neuropathy," *The Foot*, vol. 22, no. 3, pp. 130–134, 2012.

[58] K. Maluf and M. Mueller, "Comparison of physical activity and cumulative plantar tissue stress among subjects with and without diabetes mellitus and

a history of recurrent plantar ulcers," *Clinical Biomechanics*, vol. 18, no. 7, pp. 567–575, 2003.

[59] B. Holt, A. Tripathi, and J. Morgan, "Viscoelastic response of human skin to low magnitude physiologically relevant shear," *Journal of biomechanics*, vol. 41, no. 12, pp. 2689–2695, 2008.

[60] M. Yavuz, A. Erdemir, G. Botek, G. B. Hirschman, L. Bardsley, and B. L. Davis, "Peak plantar pressure and shear locations relevance to diabetic patients," *Diabetes Care*, vol. 30, no. 10, pp. 2643–2645, 2007.

[61] A. J. Boulton, "Diabetic foot–what can we learn from leprosy? legacy of dr paul w. brand," *Diabetes/metabolism research and reviews*, vol. 28, no. S1, pp. 3–7, 2012.

[62] M. Yavuz, A. Tajaddini, G. Botek, and B. L. Davis, "Temporal characteristics of plantar shear distribution: relevance to diabetic patients," *Journal of biomechanics*, vol. 41, no. 3, pp. 556–559, 2008.

[63] L. A. Lavery, D. G. Armstrong, R. P. Wunderlich, J. Tredwell, and A. J. Boulton, "Predictive value of foot pressure assessment as part of a population-based diabetes disease management program," *Diabetes care*, vol. 26, no. 4, pp. 1069–1073, 2003.

[64] D. J. Lott, D. Zou, and M. J. Mueller, "Pressure gradient and subsurface shear stress on the neuropathic forefoot," *Clinical Biomechanics*, vol. 23, no. 3, pp. 342–348, 2007.

[65] [Online]. Available: https://www.tekscan.com

[66] M. Lord, R. Hosein, and R. Williams, "Method for in-shoe shear stress measurement," *Journal of biomedical engineering*, vol. 14, no. 3, pp. 181–186, 1992.

[67] P. Laszczak, L. Jiang, D. L. Bader, D. Moser, and S. Zahedi, "Development and validation of a 3d-printed interfacial stress sensor for prosthetic applications," *Medical engineering & physics*, vol. 37, no. 1, pp. 132–137, 2015.

[68] J. E. Perry, J. O. Hall, and B. L. Davis, "Simultaneous measurement of plantar pressure and shear forces in diabetic individuals," *Gait & posture*, vol. 15, no. 1, pp. 101–107, 2002.

[69] M. Lord and R. Hosein, "A study of in-shoe plantar shear in patients with diabetic neuropathy," *Clinical Biomechanics*, vol. 15, no. 4, pp. 278–283, 2000.

[70] (2012-2013, January). [Online]. Available: http://www.learnengineering.org/2012/12/what-is-von-mises-stress.html

[71] (2012-2013, January). [Online]. Available: http://www.efunda.com/formulae/solid_mechanics/failure_criteria/failure_criteria_ductile.cfm

[72] G. Yarnitzky, Z. Yizhar, and A. Gefen, "Real-time subject-specific monitoring of internal deformations and stresses in the soft tissues of the foot: a new approach in gait analysis," *Journal of biomechanics*, vol. 39, no. 14, pp. 2673–2689, 2006.

[73] M. Yavuz, G. Botek, and B. L. Davis, "Plantar shear stress distributions: comparing actual and predicted frictional forces at the foot–ground interface," *Journal of biomechanics*, vol. 40, no. 13, pp. 3045–3049, 2007.

[74] M. Petre, A. Erdemir, and P. R. Cavanagh, "An mri-compatible foot-loading device for assessment of internal tissue deformation," *Journal of biomechanics*, vol. 41, no. 2, pp. 470–474, 2008.

[75] Y. Gu, J. Li, X. Ren, M. J. Lake, and Y. Zeng, "Heel skin stiffness effect on the hind foot biomechanics during heel strike," *Skin Research and Technology*, vol. 16, no. 3, pp. 291–296, 2010.

[76] O. Hall and P. Brand, "The etiology of the neuropathic plantar ulcer: a review of the literature and a presentation of current concepts." *Journal of the American Podiatry Association*, vol. 69, no. 3, pp. 173–177, 1979.

[77] M. Flynn, M. Edmonds, J. Tooke, and P. Watkins, "Direct measurement of capillary blood flow in the diabetic neuropathic foot," *Diabetologia*, vol. 31, no. 9, pp. 652–656, 1988.

[78] M. Edmonds, "The neuropathic foot in diabetes part i: Blood flow," *Diabetic medicine*, vol. 3, no. 2, pp. 111–115, 1986.

[79] M. Bharara, V. Viswanathan, and J. E. Cobb, "Cold immersion recovery responses in the diabetic foot with neuropathy," *International wound journal*, vol. 5, no. 4, pp. 562–569, 2008.

[80] ——, "Warm immersion recovery test in assessment of diabetic neuropathy–a proof of concept study," *International wound journal*, vol. 5, no. 4, pp. 570–576, 2008.

[81] J. J. Valletta, A. Chipperfield, G. Clough, and C. D. Byrne, "Metabolic regulation during constant moderate physical exertion in extreme conditions in type 1 diabetes," *Diabetic Medicine*, vol. 29, no. 6, pp. 822–826, 2012.

[82] J. J. Valletta, A. J. Chipperfield, G. F. Clough, and C. D. Byrne, "Daily energy expenditure, cardiorespiratory fitness and glycaemic control in people with type 1 diabetes," *PloS one*, vol. 9, no. 5, p. e97534, 2014.

[83] M. J. Mathie, A. C. Coster, N. H. Lovell, and B. G. Celler, "Accelerometry: providing an integrated, practical method for long-term, ambulatory monitoring of human movement," *Physiological measurement*, vol. 25, no. 2, p. R1, 2004.

[84] H. Lau and K. Tong, "The reliability of using accelerometer and gyroscope for gait event identification on persons with dropped foot," *Gait & posture*, vol. 27, no. 2, pp. 248–257, 2008.

[85] S. Brave and A. Dahley, "intouch: a medium for haptic interpersonal communication," in *CHI'97 Extended Abstracts on Human Factors in Computing Systems*. ACM, 1997, pp. 363–364.

[86] S. Czernichow, J. R. Greenfield, P. Galan, F. Jellouli, M. E. Safar, J. Blacher, S. Hercberg, and B. I. Levy, "Macrovascular and microvascular dysfunction in the metabolic syndrome," *Hypertension Research*, vol. 33, no. 4, pp. 293–297, 2010.

[87] D. Yudovsky, A. Nouvong, K. Schomacker, and L. Pilon, "Monitoring temporal development and healing of diabetic foot ulceration using hyperspectral imaging," *Journal of biophotonics*, vol. 4, no. 7-8, pp. 565–576, 2011.

[88] M. Nitzan, A. Babchenko, B. Khanokh, and D. Landau, "The variability of the photoplethysmographic signal-a potential method for the evaluation of the autonomic nervous system," *Physiological measurement*, vol. 19, no. 1, p. 93, 1998.

[89] A. Humeau-Heurtier, E. Guerreschi, P. Abraham, and G. Mahé, "Relevance of laser doppler and laser speckle techniques for assessing vascular function: State of the art and future trends," *IEEE*, 2013.

[90] J. Cobb and D. Claremont, "In-shoe measurement of plantar blood flow in diabetic subjects: results of a preliminary clinical evaluation," *Physiological measurement*, vol. 23, no. 2, p. 287, 2002.

[91] P. Mohr, U. Birgersson, C. Berking, C. Henderson, U. Trefzer, L. Kemeny, C. Sunderkötter, T. Dirschka, R. Motley, M. Frohm-Nilsson *et al.*, "Electrical impedance spectroscopy as a potential adjunct diagnostic tool for cutaneous melanoma," *Skin Research and Technology*, vol. 19, no. 2, pp. 75–83, 2013.

[92] P. Åberg, *Skin cancer as seen by electrical impedance*. Institutionen för laboratoriemedicin/Department of Laboratory Medicine, 2004.

[93] S. Stall, N. Ginsberg, R. Lynn, and P. Zabetakis, "Bioelectrical impedance analysis and dual energy x-ray absorptiometry to monitor nutritional status," *Peritoneal dialysis international*, vol. 15, no. Suppl 5, pp. S59–S62, 1995.

[94] A. Hinton, B. Sayers, and V. R. Solartron, "Advanced instrumentation for bioimpedance measurements," *Gen*, vol. 1260, no. 1255, pp. 1250–1253, 1998.

[95] H. Seirafi, K. Farsinejad, A. Firooz, S. Davoudi, R. Robati, M. Hoseini, A. Ehsani, and B. Sadr, "Biophysical characteristics of skin in diabetes: a controlled study," *Journal of the European Academy of Dermatology and Venereology*, vol. 23, no. 2, pp. 146–149, 2009.

[96] A. E. Helfand, *A Protocol for Primary Podogeriatric Assessment for Older Patients with Diabetes Mellitus*. INTECH Open Access Publisher, 2011.

[97] F. F. De Mul, F. Morales, A. J. Smit, and R. Graaff, "A model for post-occlusive reactive hyperemia as measured with laser-doppler perfusion monitoring," *Biomedical Engineering, IEEE Transactions on*, vol. 52, no. 2, pp. 184–190, 2005.

[98] D. Jennings, A. Flint, B. Turton, and L. Noke, *Introduction to Medical Electronics Applications*, E. Arnold, Ed. Edward Arnold, 1995, no. 8.1.1.

[99] B. ISO. (2012) Bs en 60601-1 inc a11 2011. [Online]. Available: https://webstore.iec.ch/publication/2612

[100] H. Goadby and C. Downman, "Peripheral vascular and sweat-gland reflexes in diabetic neuropathy," *Clinical Science*, vol. 45, no. 3, pp. 281–289, 1973.

[101] B. T. Shahani, J. Halperin, P. Boulu, and J. Cohen, "Sympathetic skin response–a method of assessing unmyelinated axon dysfunction in peripheral neuropathies." *Journal of Neurology, Neurosurgery & Psychiatry*, vol. 47, no. 5, pp. 536–542, 1984.

[102] M. Dashboard and T. Picks, "Galvanic skin response."

[103] J. J. Valletta, A. J. Chipperfield, and C. D. Byrne, "Gaussian process modelling of blood glucose response to free-living physical activity data in people with type 1 diabetes," in *Engineering in Medicine and Biology Society, 2009. EMBC 2009. Annual International Conference of the IEEE*. IEEE, 2009, pp. 4913–4916.

[104] W. Boucsein, D. C. Fowles, S. Grimnes, G. Ben-Shakhar, W. T. roth, M. E. Dawson, D. L. Filion, and M. Society for Psychophysiological Research Ad Hoc Committee on Electrodermal, "Publication recommendations for electrodermal measurements," *Psychophysiology*, vol. 49, no. 8, pp. 1017–34, 2012, boucsein, Wolfram Fowles, Don C Grimnes, Sverre Ben-Shakhar, Gershon roth, Walton T Dawson, Michael E Filion, Diane L eng Guideline 2012/06/12 06:00 Psychophysiology. 2012 Aug;49(8):1017-34. doi: 10.1111/j.1469-8986.2012.01384.x. Epub 2012 Jun 8. [Online]. Available: http://www.ncbi.nlm.nih.gov/pubmed/22680988

[105] K. Wilke, A. Martin, L. Terstegen, and S. Biel, "A short history of sweat gland biology," *International journal of cosmetic science*, vol. 29, no. 3, pp. 169–179, 2007.

[106] P. R. Quintavalle, C. H. Lyder, P. J. Mertz, C. Phillips-Jones, and M. Dyson, "Use of high-resolution, high-frequency diagnostic ultrasound to investigate the pathogenesis of pressure ulcer development," *Advances in skin & wound care*, vol. 19, no. 9, pp. 498–505, 2006.

[107] J.-F. Deprez, G. Cloutier, C. Schmitt, C. Gehin, A. Dittmar, O. Basset, and E. Brusseau, "3d ultrasound elastography for early detection of lesions. evaluation on a pressure ulcer mimicking phantom," in *Engineering in Medicine and Biology Society, 2007. EMBS 2007. 29th Annual International Conference of the IEEE*. IEEE, 2007, pp. 79–82.

[108] C. Y. Chao, Y.-P. Zheng, and G. L. Cheing, "Epidermal thickness and biomechanical properties of plantar tissues in diabetic foot," *Ultrasound in medicine & biology*, vol. 37, no. 7, pp. 1029–1038, 2011.

[109] (2014, December). [Online]. Available: http://www.fda.gov/Radiation-EmittingProducts/RadiationEmittingProductsandProcedures/MedicalImaging/ucm115357.htm

[110] R. E. Morley Jr, E. J. Richter, J. W. Klaesner, K. S. Maluf, and A. J. Mueller, "In-shoe multisensory data acquisition system," *IEEE Transactions on Biomedical Engineering*, vol. 48, no. 7, pp. 815–820, 2001.

[111] P. Bach-y Rita and S. W. Kercel, "Sensory substitution and the human–machine interface," *Trends in cognitive sciences*, vol. 7, no. 12, pp. 541–546, 2003.

[112] (2010, January). [Online]. Available: http://www.tekscan.com/medical/system-fscan1.html

[113] N. Murphy *et al.*, "Foot pressure measurement in a clinical setting," *Tekscan, Inc*, pp. 1–17, 2012.

[114] (2010, January). [Online]. Available: http://www.amti.biz/fps-guide.aspx

[115] (2005, December). [Online]. Available: http://www.arduino.cc/;http://en.wikipedia.org/wiki/Arduino

[116] (2012, Feb). [Online]. Available: http://www.raspberrypi.org/;http://en.wikipedia.org/wiki/Raspberry_Pi

[117] (2008, July). [Online]. Available: http://beagleboard.org

[118] G. Grewal, M. Bharara, J. Cobb, V. Dubey, and D. Claremont, "A novel approach to thermochromic liquid crystal calibration using neural networks," *Measurement Science and Technology*, vol. 17, no. 7, p. 1918, 2006.

[119] M. Segev-Bar, A. Landman, M. Nir-Shapira, G. Shuster, and H. Haick, "Tunable touch sensor and combined sensing platform: Toward nanoparticle-based electronic skin," *ACS applied materials & interfaces*, vol. 5, no. 12, pp. 5531–5541, 2013.

[120] A. Nahapetian, F. Dabiri, and M. Sarrafzadeh, "Energy minimization and reliability for wearable medical applications," in *Parallel Processing Workshops, 2006. ICPP 2006 Workshops. 2006 International Conference on*. IEEE, 2006, pp. 8–pp.

[121] F. Dabiri, A. Vahdatpour, H. Noshadi, H. Hagopian, and M. Sarrafzadeh, "Electronic orthotics shoe: Preventing ulceration in diabetic patients," in *Engineering in Medicine and Biology Society, 2008. EMBS 2008. 30th Annual International Conference of the IEEE*. IEEE, 2008, pp. 771–774.

[122] M. Chan, D. Estève, J.-Y. Fourniols, C. Escriba, and E. Campo, "Smart wearable systems: Current status and future challenges," *Artificial intelligence in medicine*, vol. 56, no. 3, pp. 137–156, 2012.

[123] [Online]. Available: http://nw3weather.co.uk/wx10.php

[124] M. Hanlon and R. Anderson, "Real-time gait event detection using wearable sensors," *Gait Posture*, vol. 30, no. 4, pp. 523–7, 2009, hanlon, Michael Anderson, Ross eng Research Support, Non-U.S. Gov't England 2009/09/05 06:00 Gait Posture. 2009 Nov;30(4):523-7. doi: 10.1016/j.gaitpost.2009.07.128. Epub 2009 Sep 3. [Online]. Available: http://www.ncbi.nlm.nih.gov/pubmed/19729307

[125] C. Morio, M. J. Lake, N. Gueguen, G. Rao, and L. Baly, "The influence of footwear on foot motion during walking and running," *Journal of biomechanics*, vol. 42, no. 13, pp. 2081–2088, 2009.

[126] M. S. Cowley, E. J. Boyko, J. B. Shofer, J. H. Ahroni, and W. R. Ledoux, "Foot ulcer risk and location in relation to prospective clinical assessment of foot shape and mobility among persons with diabetes," *Diabetes research and clinical practice*, vol. 82, no. 2, pp. 226–232, 2008.

[127] "Flexiforce force sensors — single button force sensing resistor — tekscan.pdf."

[128] D. Covill, Z. Guan, M. Bailey, and D. Pope, "Effects of varying the environmental conditions on in-shoe temperature," 2003.

[129] C. Martin, J.-P. Auffray, C. Badetti, G. Perrin, L. Papazian, and F. Gouin, "Monitoring of central venous oxygen saturation versus mixed venous oxygen saturation in critically ill patients," *Intensive care medicine*, vol. 18, no. 2, pp. 101–104, 1992.

[130] S. Grimnes and O. G. Matrinsen, *Bioimpedance and Bioelectricity*, 2nd ed. Academic Press, 2008.

[131] (2004, January). [Online]. Available: http://www.analog.com/static/imported-files/data_sheets/AD9850.pdf

[132] S. Prună, "Improved technique for testing autonomic dysfunction: evaluation of transient behaviour of the autonomic response," *Medical and Biological Engineering and Computing*, vol. 28, no. 2, pp. 119–126, 1990.

[133] A. Stefanovska, M. Bračič, and H. D. Kvernmo, "Wavelet analysis of oscillations in the peripheral blood circulation measured by laser doppler technique," *Biomedical Engineering, IEEE Transactions on*, vol. 46, no. 10, pp. 1230–1239, 1999.

[134] M. Bračič and A. Stefanovska, "Wavelet-based analysis of human blood-flow dynamics," *Bulletin of mathematical biology*, vol. 60, no. 5, pp. 919–935, 1998.

[135] K. H. Hong, S. M. Lee, Y. G. Lim, and K. S. Park, "Measuring skin conductance over clothes," *Medical & biological engineering & computing*, vol. 50, no. 11, pp. 1155–1161, 2012.

[136] S. Shapkin, "Influence of caffeine on physiological and cognitive functions of humans," *Human Physiology*, vol. 28, no. 1, pp. 128–133, 2002.

[137] J. R. J. C. P. R. R. P.-A. J. G. Webster, "Skin impedance from 1 hz to 1 mhz," *IEEE Transactions on Biomedical Engineering*, vol. 35, no. 8, pp. 649–651, August 1988.

[138] S. Prună and C. Ionescu-TîrgoviˆCste, "Dual-channel self-balancing electrodermal impedance reactometer for autonomic response studies," *Medical and Biological Engineering and Computing*, vol. 25, no. 6, pp. 613–619, 1987.

[139] M. Handler, R. Nelson, D. Krapohl, and C. R. Honts, "An eda primer for polygraph examiners," *Polygraph*, vol. 39, no. 2, pp. 68–108, 2010.

[140] Z. Sawacha, G. Gabriella, G. Cristoferi, A. Guiotto, A. Avogaro, and C. Cobelli, "Diabetic gait and posture abnormalities: A biomechanical investigation through three dimensional gait analysis," *Clinical Biomechanics*, vol. 24, no. 9, pp. 722–728, 2009.

[141] (2014, 05). [Online]. Available: http://hobbylogs.me.pn/?p=47

[142] J. S. Petrofsky and K. McLellan, "Galvanic skin resistance—a marker for endothelial damage in diabetes," *Diabetes technology & therapeutics*, vol. 11, no. 7, pp. 461–467, 2009.

[143] H. Banaee, M. U. Ahmed, and A. Loutfi, "Data mining for wearable sensors in health monitoring systems: a review of recent trends and challenges," *Sensors*, vol. 13, no. 12, pp. 17 472–17 500, 2013.

[144] K. R. Fall and W. R. Stevens, *TCP/IP illustrated, volume 1: The protocols*. addison-Wesley, 2011.

[145] D. R. Irvin and K.-B. Sy, "Preservation of crc integrity upon intentional data alteration during message transmission," Jun. 9 1992, uS Patent 5,121,396.

[146] K. S. Maluf, R. E. Morley, E. J. Richter, J. W. Klaesner, and M. J. Mueller, "Monitoring in-shoe plantar pressures, temperature, and humidity: reliability and validity of measures from a portable device," *Archives of physical medicine and rehabilitation*, vol. 82, no. 8, pp. 1119–1127, 2001.

[147] A. Leardini, M. Benedetti, F. Catani, L. Simoncini, and S. Giannini, "An anatomically based protocol for the description of foot segment kinematics during gait," *Clinical Biomechanics*, vol. 14, no. 8, pp. 528–536, 1999.

[148] N. G. Boulé, E. Haddad, G. P. Kenny, G. A. Wells, and R. J. Sigal, "Effects of exercise on glycemic control and body mass in type 2 diabetes mellitus: a meta-analysis of controlled clinical trials," *Jama*, vol. 286, no. 10, pp. 1218–1227, 2001.

[149] J. W. LeMaster, M. J. Mueller, G. E. Reiber, D. R. Mehr, R. W. Madsen, and V. S. Conn, "Effect of weight-bearing activity on foot ulcer incidence in people with diabetic peripheral neuropathy: Feet first randomized controlled trial," *Physical Therapy*, vol. 88, no. 11, p. 14, 2008.

[150] S. Park and S. Jayaraman, "Wearable sensor systems: opportunities and challenges," in *Engineering in Medicine and Biology Society, 2005. IEEE-EMBS 2005. 27th Annual International Conference of the*. IEEE, 2005, pp. 4153–4155.

[151] K. D. Cicerone, "Evidence-based practice and the limits of rational rehabilitation," *Archives of physical medicine and rehabilitation*, vol. 86, no. 6, pp. 1073–1074, 2005.

[152] K. Keegan, D. Wilson, D. Wilson, B. Smith, E. Gaughan, R. Pleasant, J. Lillich, J. Kramer, R. Howard, C. Bacon-Miller *et al.*, "Evaluation of mild lameness in horses trotting on a treadmill by clinicians and interns or residents and correlation of their assessments with kinematic gait analysis." *American journal of veterinary research*, vol. 59, no. 11, pp. 1370–1377, 1998.